

Copyright is owned by the Author of the thesis. Permission is given for a copy to be downloaded by an individual for the purpose of research and private study only. The thesis may not be reproduced elsewhere without the permission of the Author.

# **Complexation between Whey Protein and Octenyl Succinic Anhydride Modified Starch: A Novel Approach for Encapsulation of Lipophilic Bioactive Compounds**

A thesis presented in partial fulfilment of the requirements for the degree of

**Master of Food Technology**

at Massey University, Manawatū, New Zealand

**Dan Wu**

2018



## Abstract

Proteins and polysaccharides are frequently used in food industry, and their interactions in food systems could affect the properties of food products such as the texture and stability. Therefore, the knowledge of the interactions between these two macromolecules is of great significance for food manufacturers.

The aim of this study was to investigate the complexation process between whey protein isolate (WPI) and octenyl succinic anhydride (OSA)-modified starch and explore the application of their interactions in the encapsulation of lipophilic bioactive compounds.

The formation of complexes between WPI and OSA-modified starch was investigated as a function of pH (7-3), the heat treatment of WPI, and the concentration ratio of WPI and OSA-modified starch (1:1, 1:10 and 1:20). The complexation process was evaluated by the determinations of the absorbance, particle size and  $\zeta$ -potential of the mixtures, which were determined by spectrophotometer and dynamic light scattering. It was found that the OSA-modified starch was more likely to interact with heated WPI (HWPI, 90°C for 20 min) rather than non-heated WPI (NWPI). The optimum condition for the formation of insoluble coacervates was at ratio of 1:10 and pH 4.5, which was driven by both electrostatic and hydrophobic interactions. The structure of the complexes formed under the optimum condition could be affected by different molecular characteristics of OSA-modified starch including molecular weight (Mw) and degrees of substitution (DS) value. It was found that OSA-modified starch with higher Mw was difficult to form a dense precipitation phase with HWPI due to its higher viscosity restricting the movement of any particles present. Stable soluble complexes could be formed between HWPI and OSA-modified starch with higher DS value under the same condition, which may be attributed

to the stronger steric hindrance of OSA-modified starch with higher DS values. It seems that the complexation between HWPI and OSA-modified starch was induced by electrostatic interactions, while the structural properties of the complexes were determined by hydrophobic interactions.

The soluble complexes between HWPI and OSA-modified starch with a DS value of  $4.29 \pm 0.11\%$  formed at ratio of 1:10 and pH 4.5 were applied to encapsulate  $\beta$ -carotene, which was used as a model of lipophilic bioactive compounds in this study. The apparent aqueous solubility of  $\beta$ -carotene was enormously improved ( $264.05 \pm 72.53 \mu\text{g/g}$ ) after encapsulation in the soluble complexes. No significant differences were observed under transmission electron microscopy (TEM) and scanning electron microscope (SEM) between the soluble complexes before and after encapsulation of  $\beta$ -carotene whether in a liquid or a powdered form. Results of Fourier transform infrared spectroscopy (FT-IR), X-ray diffraction (XRD) and differential scanning calorimetry (DSC) indicated that the  $\beta$ -carotene was in an amorphous form loaded inside the soluble complexes, which suggested that the molecules of  $\beta$ -carotene evenly distribute within the complex particles by hydrophobic force. In addition, the  $\beta$ -carotene-loaded freeze-dried soluble complexes showed good redispersion behaviour and a high retention rate of the loaded  $\beta$ -carotene (89.75%), which indicated that the  $\beta$ -carotene-loaded soluble complexes could be successfully converted into a powdered form. The accelerated stability study showed that these soluble complexes could effectively protect the loaded  $\beta$ -carotene at pH 4.5 during storage, especially after 7 days of storage. This indicated the potential of using the soluble complexes between HWPI and OSA-modified starch to protect lipophilic bioactive compounds for long-term storage under low pH conditions.

This study may be beneficial for the potential using the soluble complexes between HWPI and OSA-modified starch as delivery systems for lipophilic bioactive compounds in commercial applications.



## Acknowledgments

I would like to express my special thanks of gratitude to my supervisor, Associate Professor Aiqian Ye, who gave me continuous support throughout the project. His patience, profound knowledge and attitude to research inspire me all the time. The door to his office was always open whenever I had a question or met troubles about my research or writing. The completion of this research and writing of this thesis was inseparable from his help.

My most sincere gratitude goes to Professor Harjinder Singh for providing me the opportunity to complete my Master's research project at Riddet Institute.

I would also like to express my endless thanks to Dr. Quanquan Lin, for her insightful guidance and encouragement whether in the experiments of the project or writing of this thesis. I am grateful for her very valuable comments on this thesis and her patient guidance throughout the project. Apart from the interactions with her about work, we have also built a deep friendship. I have been inspired and encouraged by her positive and enthusiastic attitudes in both professional and personal life.

I am also grateful to Ms. Maggie Zou and Mr. Steve Glasgow, who gave me the access to the laboratory and training of the required instruments. My sincere thank also goes to Dr. Matthew Savoian, Ms. Jordan Taylor and Ms. Niki Minards, the staff of Manawatu Microscopy and Imaging Centre, for their professional help on the microscopy work in this project.



Furthermore, I am thankful to all the postgraduate students and researchers at Riddet Institute for their help and encouragement whether on my thesis or life. I would also like to thank my dearest friends and flatmates for their comfort and encouragement whenever I encountered difficulties during this project.

I am also grateful to Mr. John Henley King, Ms Ansley Te Hiwi, Ms Terri Palmer, Ms Hannah Hutchinson and Dr. Michael Parker for their administrative assistances, and I would like to express my thanks to Mr. Matt Levin for his assistance in computer systems.

A special thank also goes to my family for their encouragement, support and funding, which gave me the opportunity to pursue advanced studies at Massey University.

Last but foremost, I really appreciate my husband, Sihan Ma, for his love, help, encouragement, support, care in the passed eight years. I would also like to gratitude his tolerance to my tantrums when I felt depressed during the master programme.

## Table of Contents

<b>Abstract</b> .....	i
<b>Acknowledgments</b> .....	v
<b>Table of Contents</b> .....	vii
<b>List of Figures</b> .....	xi
<b>List of Tables</b> .....	xv
<b>List of Abbreviations</b> .....	xvii
<b>Chapter 1 Introduction</b> .....	1
1.1. Background .....	1
1.2. Aim and objectives .....	4
<b>Chapter 2 Literature review</b> .....	5
2.1. Milk protein.....	5
2.1.1. Whey protein.....	5
2.2. Modified starch.....	7
2.2.1. OSA-modified starch .....	8
2.3. Interactions between proteins and polysaccharides.....	9
2.3.1. Nature of complexation between protein and polysaccharide .....	12
2.4. Factors affecting the interactions between proteins and polysaccharides .....	13
2.4.1. pH.....	14
2.4.2. Ionic strength .....	16
2.4.3. Ratio and concentration of biopolymers .....	17

2.4.4. Charge density .....	19
2.4.5. Conformation and molecular weight of biopolymers .....	20
2.4.6. Processing factors .....	21
2.5. Applications in encapsulation of lipophilic bioactive compounds .....	22
2.5.1. Encapsulation of $\beta$ -carotene .....	28
2.6. Conclusion.....	31
<b>Chapter 3 Formation of insoluble and soluble complexes between WPI and OSA-</b> <b>modified starch .....</b>	<b>33</b>
3.1. Abstract .....	33
3.2. Introduction .....	34
3.3. Materials.....	36
3.4. Methods .....	37
3.4.1. Preparation of OSA-modified starch .....	37
3.4.2. Determination of DS of OSA-modified starch .....	38
3.4.3. Determination of Mw of OSA-modified starch.....	39
3.4.4. Preparation of mixtures of WPI and OSA-modified starch.....	39
3.4.5. Absorbance measurement.....	40
3.4.6. Particle size and $\zeta$ -potential measurement.....	41
3.4.7. Statistical analysis.....	41
3.5. Results and discussion.....	41
3.5.1. Effect of the characteristics of WPI.....	41
3.5.2. Effect of the characteristics of OSA-modified starch.....	58

3.5.3. Proposed mechanism of the interactions between HWPI and OSA-modified starch.....	63
3.6. Conclusion.....	66
<b>Chapter 4 Encapsulation of <math>\beta</math>-carotene in soluble complexes between HWPI and OSA-modified starch .....</b>	<b>69</b>
4.1. Abstract .....	69
4.2. Introduction .....	70
4.3. Materials .....	72
4.4. Methods .....	73
4.4.1. Preparation of soluble complexes between HWPI and OSA-modified starch (HWPI-OSA SC) .....	73
4.4.2. Encapsulation of $\beta$ -carotene .....	74
4.4.3. Determination of $\beta$ -carotene .....	74
4.4.4. Particle size measurement.....	75
4.4.5. Transmission electron microscopy .....	75
4.4.6. Scanning electron microscope .....	75
4.4.7. Fourier-transform infrared spectroscopy .....	76
4.4.8. X-ray diffraction .....	76
4.4.9. Differential scanning calorimetry .....	76
4.4.10. Accelerated stability study.....	77
4.4.11. Statistical analysis.....	77
4.5. Results and discussion.....	78

4.5.1. Concentration of $\beta$ -carotene bound with soluble complexes.....	78
4.5.2. Changes in particle size of soluble complexes after encapsulation of $\beta$ -carotene .....	81
4.5.3. TEM observation .....	82
4.5.4. Properties of $\beta$ -carotene bound with soluble complexes in a powdered form .....	86
4.5.5. FT-IR spectroscopy .....	96
4.5.6. X-ray diffraction .....	99
4.5.7. DSC.....	101
4.5.8. Accelerated stability study.....	103
4.5.9. Proposed encapsulation mechanism for $\beta$ -carotene of soluble complexes..	107
4.6. Conclusion.....	109
<b>Chapter 5 Summary and Recommendations.....</b>	<b>111</b>
5.1. Summary .....	111
5.2. Recommendations for future work.....	113
<b>References .....</b>	<b>115</b>
<b>Appendices.....</b>	<b>129</b>

## List of Figures

Figure 2. 1. Structure of native and denatured whey protein. ....	6
Figure 2. 2. Structure of OSA-modified starch. ....	8
Figure 2. 3. Main trends in the behaviour of mixed systems of protein and polysaccharide. .....	10
Figure 2. 4. Picture of the whey protein-Gum Arabic coacervates (de Kruif et al., 2004). .....	12
Figure 2. 5. Factors influencing the complex formation in protein-polysaccharide mixed systems. ....	14
Figure 2. 6. TEM micrographs of complexes observed in the mixed system of 0.5% (w/w) sodium caseinate and 0.5% (w/w) Gum Arabic at pH 4.2. The scale bar represents 500 nm (Ye et al., 2006).....	18
Figure 2. 7. Two preparation methods for encapsulation of lipophilic bioactive compounds by protein-polysaccharide complex coacervates. ....	24
Figure 2. 8. Curcumin and folic acid nano-encapsulation at pH 4.25: curcumin dissolved in ethanol (I) and deionized water (II) added to $\beta$ -lactoglobulin-sodium alginate soluble complexes (sodium alginate/ $\beta$ -lactoglobulin weight ratio of 0.75) (Hosseini et al., 2015). .....	26
Figure 2. 9. Schematic representation of the entrapment of nutraceuticals in the soluble nanocomplexes between $\beta$ -lactoglobulin and sodium alginate (Hosseini et al., 2015). .	27
Figure 2. 10. Schematic representation of the formation of SSPS-based films by esterification of OSA (Liu et al., 2018). ....	28
Figure 2. 11. Schematic representation of the encapsulation of $\beta$ -carotene by WPI-Gum Acacia coacervates (Jain et al., 2015). ....	29

Figure 2. 12. Schematic representation of the encapsulation of $\beta$ -carotene by casein-gum tragacanth coacervates (Jain et al., 2016). .....	30
Figure 2. 13. Freeze-dried microcapsules of gelatin-cashew gum complex coacervates with lipid extract rich in astaxanthin from shrimp waste (Gomez-Estaca et al., 2016)..	31
Figure 3. 1. Absorbance values of mixtures of 0.5% NWPI (A, C, E) or HWPI (B, D, F) and OSA-modified starch at protein to polysaccharide concentration ratios of 1:1, 1:10 and 1:20 as a function of pH. 0.5% NWPI or HWPI and corresponding concentration of OSA-modified starch solutions were measured as control. ....	42
Figure 3. 2. Mean particle diameter of 0.5% NWPI (A) and HWPI (B) as a function of pH.....	48
Figure 3. 3. Mean particle diameter of mixtures of 0.5% NWPI (A) or HWPI (B) and OSA-modified starch at protein to polysaccharide concentration ratios of 1:1, 1:10 and 1:20 as a function of pH.....	51
Figure 3. 4. Volume distribution of mixtures of 0.5% NWPI (A, C, E) or HWPI (B, D, F) and OSA-modified starch at protein to polysaccharide concentration ratios of 1:1, 1:10 and 1:20 over the pH range examined. ....	52
Figure 3. 5. $\zeta$ -potential of mixtures of 0.5% NWPI (A, C, E) or HWPI (B, D, F) and OSA-modified starch at protein to polysaccharide concentration ratios of 1:1, 1:10 and 1:20 as a function of pH. 0.5% NWPI or HWPI and corresponding concentration of OSA-modified starch solutions were measured as control. ....	56
Figure 3. 6. Absorbance values (A) and phase separation (B) of mixtures of 0.5% HWPI and 5% OSA-modified starch with different Mw at pH 4.5. 5% OSA-modified starch with different Mw were measured as control. Note: the phase separation of samples was observed after 7 days. Different capital and lowercase letters indicate significant	

differences ( $p < 0.05$ ) in the absorbance values of the mixtures and the starch solution, respectively. ....	60
Figure 3. 7. Absorbance values (A) and phase separation (B) of mixtures of 0.5% HWPI and 5% OSA-modified starch with different DS values at pH 4.5. 5% OSA-modified starch with different DS values were measured as control. Note: the phase separation of samples was observed after 7 days. Different capital and lowercase letters indicate significant differences ( $p < 0.05$ ) in the absorbance values of the mixtures and the starch solution, respectively.....	62
Figure 3. 8. Conformations of OSA-modified starch (A) and HWPI (B) in solutions with decreasing pH values from 7 to 4.5. (C) Schematic representation of mixtures of HWPI and OSA-modified starch at pH 7 and possible conformations of their complexes at pH 4.5. Note: sizes are not proportional to the physical size of the molecules. ....	64
Figure 4. 1. (A) Concentration of $\beta$ -carotene bound with different samples. (B) Visual observations of $\beta$ -carotene in water and different $\beta$ -carotene-loaded samples after filtration. Note: different lowercase letters indicate significant differences ( $p < 0.05$ ) in the concentration of $\beta$ -carotene bound with different samples after encapsulation.....	79
Figure 4. 2. TEM micrographs of different samples before and after encapsulation of $\beta$ -carotene. The scale bar represents 100 nm.....	85
Figure 4. 3. Visual observations of different freeze-dried samples before (A) and after (B) encapsulation of $\beta$ -carotene. ....	87
Figure 4. 4. SEM micrographs of $\beta$ -carotene, OSA-modified starch and WPI original powder (The scale bar represents 50 $\mu\text{m}$ ) and different freeze-dried samples before and after encapsulation of $\beta$ -carotene (The scale bar represents 500 $\mu\text{m}$ )......	89



Figure 4. 5. Visual observations of the redispersion behaviour of different freeze-dried $\beta$ -carotene-loaded powders.....	92
Figure 4. 6. FT-IR spectra of $\beta$ -carotene, OSA-modified starch and WPI original powder (A); and different freeze-dried samples before and after encapsulation of $\beta$ -carotene (B-F). .....	98
Figure 4. 7. XRD spectra of different freeze-dried samples before (A) and after (B) encapsulation of $\beta$ -carotene. ....	100
Figure 4. 8. DSC patterns of $\beta$ -carotene, OSA-modified starch and WPI original powder (A); and different freeze-dried samples before and after encapsulation of $\beta$ -carotene (B-F). .....	102
Figure 4. 9. Z-Ave of the samples before (A) and after (B) encapsulation of $\beta$ -carotene as a function of storage time. ....	106
Figure 4. 10. Schematic representation of all the samples before and after encapsulation of $\beta$ -carotene. Note: sizes are not proportional to the physical size of the molecules..	108

## List of Tables

Table 4. 1. Mean particle diameter of different samples before and after encapsulation of $\beta$ -carotene.....	82
Table 4. 2. Mean particle diameter of different $\beta$ -carotene-loaded samples before and after redispersion. ....	94
Table 4. 3. $\beta$ -Carotene retention rate in redispersions of different freeze-dried $\beta$ -carotene-loaded samples. Note: different lowercase letters indicate significant differences ( $p < 0.05$ ) in the $\beta$ -carotene retention rate of these samples after redispersion. ....	95
Table 4. 4. $\beta$ -carotene retention in $\beta$ -carotene-loaded samples during storage. Note: different lowercase letters indicate significant differences ( $p < 0.05$ ) in the $\beta$ -carotene retention rate of these samples during storage. ....	104



## List of Abbreviations

ASSP: acid soluble soy protein

CMC: carboxymethylcellulose

DE: degrees of esterification

DMSO: dimethyl sulfoxide

DS: degrees of substitution

DSC: differential scanning calorimetry

FT-IR: Fourier transform infrared spectroscopy

HWPI: heated WPI

Mw: molecular weight

NWPI: non-heated WPI

OSA: octenyl succinic anhydride

pI: Isoelectric point

SC: soluble complexes

SEM: scanning electron microscope

SSPS: soy soluble polysaccharide

TCNN: *trans*-cinnamaldehyde

TEM: transmission electron microscopy

WPC: whey protein concentrate

WPI: whey protein isolate

v/v: volume/volume

w/v: weight/volume

w/w: weight/weight

XRD: X-ray diffraction

## Chapter 1 Introduction

### 1.1. Background

Proteins and polysaccharides are frequently used in food industry, and the knowledge of the interactions between these two macromolecules in food systems are of great significance for food manufacturers, which can greatly affect the properties of food products such as the texture and stability (de Kruif & Tuinier, 2001; Ye, 2008).

The protein-polysaccharide interactions have been studied extensively over decades (de Kruif & Tuinier, 2001; de Kruif, Weinbreck, & de Vries, 2004; Dickinson, 1998, 2008; Doublier, Garnier, Renard, & Sanchez, 2000; Patino & Pilosof, 2011; Schmitt, Sanchez, Desobry-Banon, & Hardy, 1998; Schmitt & Turgeon, 2011; Tolstoguzov, 1991, 1997, 1998; Ye, 2008), which can be either attractive or repulsive. Strong attractive protein-polysaccharide interactions could lead to the formation of insoluble complexes (i.e., complex coacervates), which often occur at pH values below the isoelectric point (pI) of the protein (Schmitt et al., 1998). Below pI, there are strong electrostatic interactions between the proteins carrying positive charges and the anionic polysaccharides. At pH values above the pI of the protein, the anionic polysaccharides can have electrostatic interactions with the positively charged patches on the proteins, which could lead to the formation of soluble complexes (Dickinson, 1998; Schmitt et al., 1998). Except for the formation of soluble or insoluble complexes, it has been demonstrated that stable nanoparticles could be formed under specific conditions, which are stable over a quite range of pH (Anal, Tobiasen, Flanagan, & Singh, 2008; Ye, Flanagan, & Singh, 2006). The complex formation between proteins and polysaccharides is mainly dependent on the physical conditions of the biopolymer solutions, including pH, ionic strength, the

concentration and ratio of the biopolymers, and the characteristics of the biopolymers, including charge density, conformation and Mw. Meanwhile, the processing factors such as temperature, pressure and shear rate can also affect the complex formation (Schmitt et al., 1998; Schmitt & Turgeon, 2011; Ye, 2008).

Due to the low price and good emulsifying capacity of OSA-modified starch, it has been used as a substitute for some food ingredients including lipids, proteins and Gum Arabic (Sweedman, Tizzotti, Schäfer, & Gilbert, 2013). The presence of free carboxyl groups renders it anionic at certain pH values, which may lead to their interactions between positively charged proteins (Nilsson & Bergenståhl, 2007). Whey protein, which accounts for about 20% of bovine milk protein, is now recognized as an important nutritional ingredient in food industry all over the world (de Wit, 1990). Since they are both common ingredients in food products, their interactions need to be understood for the development of food production.

Currently, most studies are mainly focused on the interactions between milk proteins (casein, whey protein and  $\beta$ -lactoglobulin), plant proteins (soybean protein and pea protein) or gelatin and non-starch polysaccharides including Gum Arabic, pectin and carboxymethylcellulose (CMC) (Cuevas-Bernardino et al., 2018; Jones, Decker, & McClements, 2009; Jones & McClements, 2010; Liu et al., 2016; Salminen & Weiss, 2014; Santipanichwong, Supphantharika, Weiss, & McClements, 2008; Turgeon, Schmitt, & Sanchez, 2007; Ye et al., 2006; Zeeb, Mi-Yeon, Gibis, & Weiss, 2018). However, only a few studies reported on the interactions between protein and OSA-modified starch. Puerta-Gomez and Castell-Perez (2016, 2017) have investigated the self-assembly interactions between WPI and OSA-modified waxy rice starch with different DS values at pH 7 by rheology, and the entrapment efficiency of WPI at its pI in combination with

OSA-modified waxy rice starch for *trans*-cinnamaldehyde (TCNN). It has been demonstrated that the DS value of OSA-modified polysaccharides affects the amount of molecules interacting with the proteins. However, few studies have focused on the interactions between WPI and OSA-modified starch at different pH values. There are also some reports on the interactions between OSA-modified starch and other proteins such as gelatin (Wu & McClements, 2015; Zhao et al., 2018), casein (Sun, Liang, Yu, Tan, & Cui, 2016) and egg yolk protein (Magnusson & Nilsson, 2011), which have confirmed that OSA-modified starch can have strong electrostatic interactions with these proteins at pH under their pI values. Therefore, it is necessary to investigate the complex formation between WPI and OSA-modified starch as a function of pH, which can be useful for better knowledge of their interactions. In addition, the studies above did not focus on the interactions between the preheated protein and OSA-modified starch. It has been proved that the preheated whey protein could influence their interactions with polysaccharides, which could be attributed to the exposure of more hydrophobic groups and the increasing of their effective Mw by thermal denaturation (Bryant & McClements, 2000; Chun et al., 2014; Kim, Decker, & McClements, 2006). Hence, it is meaningful to investigate the interactions between heat-denatured WPI and OSA-modified starch, which may be very different from those between native WPI and OSA modified starch.

Many reports have focused on the application of the protein-polysaccharide complexes to encapsulate either hydrophilic or lipophilic bioactive compounds, and most of them used complex coacervates between proteins and polysaccharides rather than their soluble complexes (Eratte, Dowling, Barrow, & Adhikari, 2017; Eratte et al., 2015; Eratte, Wang, Dowling, Barrow, & Adhikari, 2014; Gomez-Estaca, Comunian, Montero, Ferro-Furtado, & Favaro-Trindade, 2016; Hernández-Rodríguez, Lobato-Calleros, Pimentel-González, & Vernon-Carter, 2014; Ilyasoglu & El, 2014; Jain, Thakur, Ghoshal, Katare, & Shivhare,



2015, 2016; Koupantsis, Pavlidou, & Paraskevopoulou, 2014; Zhao et al., 2018). Some researchers have used the binding capacity of  $\beta$ -lactoglobulin for lipophilic bioactive compounds after which inducing the ternary soluble complexes between polysaccharide and the primary complexes by the addition of polysaccharide solution before adjusting the pH of the mixture. However, there is no data about encapsulating lipophilic bioactive compounds directly into the already formed soluble complexes between proteins and polysaccharides, which warrants further investigation.

## 1.2. Aim and objectives

The aim of this study was to investigate the complexation process between WPI and OSA-modified starch and explore the application of their interactions in the encapsulation of lipophilic bioactive compounds.

The objectives of this study are: (i) to investigate the effects of the structural characteristics of WPI (native and denatured) and OSA-modified starch (Mw and DS) on the complex formation between WPI and OSA-modified starch; (ii) to characterize the complexes formed between WPI and OSA-modified starch; (iii) to encapsulate lipophilic bioactive compounds ( $\beta$ -carotene was used as a model) into the soluble complexes between HWPI and OSA-modified starch; (iv) to evaluate the storage stability of the  $\beta$ -carotene-loaded soluble complexes.

## Chapter 2 Literature review

This chapter covers the knowledge of milk protein, whey protein, modified starch and OSA-modified starch as the background for this Master's thesis. The interactions between proteins and polysaccharides and the applications of their interactions in the encapsulation of lipophilic bioactive compounds are discussed and reviewed, with emphasis on the nature of the complexation, the factors affecting the interactions and the applications of their interactions in the encapsulation of  $\beta$ -carotene.

### 2.1. Milk protein

Milk is a fluid secreted by all female mammals, which is primarily to satisfy the complete nutrients demands of neonates. Milk has become one of the main sources of dietary nutrition for most people around the world (Fox, 2003). The main components of milk are proteins, lactose, lipids and water (Fox, 2009). There are two major milk proteins that have been studied extensively by their physical properties and chemical composition, which are casein (~80% of bovine milk protein) and whey protein (~20% of bovine milk protein) (Fox, McSweeney, & Paul, 1998).

#### 2.1.1. Whey protein

Whey protein is prepared by any methods for casein preparation because it is soluble at pH 4.6, or in saturated NaCl, or after casein coagulation by rennet, and not precipitated after ultracentrifugation (Fox, 2009). Once it was considered as waste products in dairy industry; however, it is now recognized as an important nutritional ingredient by food industry all over the world (de Wit, 1990). Commercial whey protein products can be

divided into two categories based on the content of whey protein, which are whey protein concentrate (WPC, 30-85% whey protein) and whey protein isolate (WPI, ~95% whey protein) (Fox, 2003). The major proteins of whey protein include  $\beta$ -lactoglobulin (~50% of whey protein and ~12% of total protein in milk),  $\alpha$ -lactalbumin (~20% of whey protein and ~3.5% of total protein in milk), bovine serum albumin and immunoglobulins (Fox, 2003). It also contains several other protein or peptide such as lysozyme, lacto-peroxidase and lactoferrin (Qi & Onwulata, 2011).

The native structure of whey protein in solutions is compact, globular and organised, which is because of the disulphide bonds formed by the large amounts of sulphur-containing amino acids in whey protein (Fox et al., 1998). The major forces that maintain the structure include hydrophobic interactions, hydrogen bond and van der Waals' force. The native structure of whey protein can unfold into the random and disordered structure when it is denatured by changes in solution and temperature, which is shown in Figure 2.1. The thermal denaturation temperature range of whey protein is 62-89°C (Singh & Havea, 2003), and generally they can be completely denatured when heating at 90°C for 10 min (Fox, 2009). Since the pI of whey protein is near pH 5, they are negatively charged at neutral pH value.

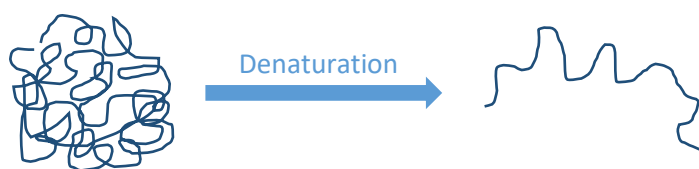


Figure 2. 1. Structure of native and denatured whey protein.

## 2.2. Modified starch

Starch is the major energy reserve in plants, which is one of the most abundant carbohydrates found in nature (Blennow, 2004). It is the most important food polysaccharide and a major energy source in daily life. Two common resources of starch are seeds and roots, including wheat, corn, rice, potato, etc. (Peris-Tortajada, 2004). Starch, regardless of the origin, consists of two major components, which refer to amylose and amylopectin. Amylose is a mainly linear polymer consisting of  $\alpha$  (1 $\rightarrow$ 4) glycosidic links and a few branches attached in  $\alpha$  (1 $\rightarrow$ 6) position. Amylopectin has the same structure as amylose except that the polymer is extensively branched, which makes it much larger (Bertoft, 2004).

Although starch has been commercially produced for food applications for more than a hundred years, the use of native starch in industrial applications has been limited by its physical and chemical properties (Luallen, 2004). Generally, the native starch granules have poor solubility in cold water and require heating to achieve the dispersion. In addition, the viscosity of the native starch dispersion is too high to use it in industrial applications (Wurzburg, 1986). Therefore, modified starch is designed to overcome the above limitations, and the introduction of modified starch enhanced the utilization of starch in food applications in the past decades (Luallen, 2004). There are three different starch modification methods, including enzymatic, physical and chemical modification (Chen, Kaur, & Singh, 2018). Modified starch has a number of applications in foods, which are often used as emulsifier, stabiliser, thickener, fat replacer and flavour carrier (Taggart, 2004).

### 2.2.1. OSA-modified starch

OSA-modified starch has been used as a food additive over half-century in food industry. The modification of native starch through esterification with dicarboxylic acids was derived from the patent of Caldwell and Wurzburg (1953), which was the most commonly cited genesis of modifying starch with OSA although it did not substitute the starch with OSA. Starch esterification with OSA involves the partial substitution of hydroxyl groups with OSA groups, which are hydrophobic substituents. Thereby the OSA-modified starch is then given an amphiphilic character and interfacial properties, as shown in Figure 2.2. It is an approved food additive in Europe and its E-number is 1450 (Tesch, Gerhards, & Schubert, 2002). Due to its low price, good emulsifying capacity and safety, OSA-modified starch is now widely used in a variety of food systems as an emulsifier, stabilizer, thickener, etc. Although OSA-modified starch in food industry has been used for some time, a great interest in this starch is growing in recent years as evidenced by its increasingly frequent appearance in publications (Sweedman et al., 2013).

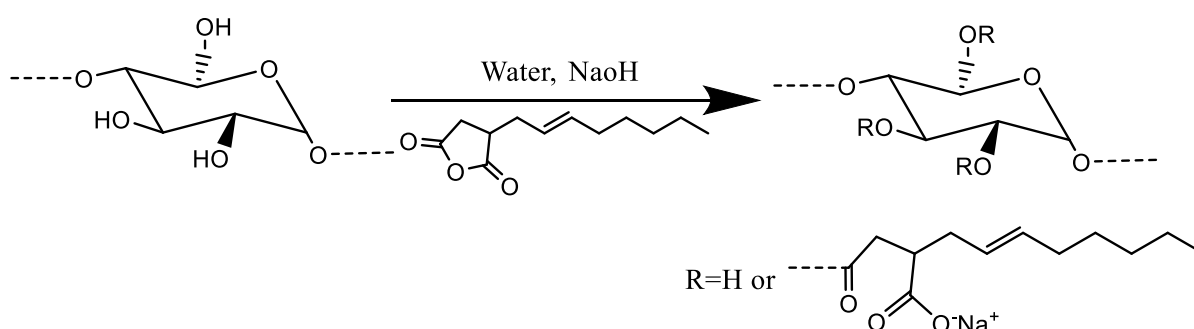


Figure 2. 2. Structure of OSA-modified starch.

### **2.3. Interactions between proteins and polysaccharides**

Mixed systems of proteins and polysaccharides are commonly used in food formulations, and the interactions between different components in food systems can greatly affect the properties of food products. Therefore, the knowledge of the interactions between proteins and polysaccharides is of great significance for food manufacturers. The protein-polysaccharide interactions in solutions or on interfaces have been studied extensively. Now there are growing interests in utilizing their complexes as carriers in food applications.

When proteins and polysaccharides are mixed in one solution, any of three main types of phenomenon can arise, including compatibility, incompatibility and complexation, among which complexation can be the formation of soluble or insoluble complexes between proteins and polysaccharides (de Kruif & Tuinier, 2001; de Kruif et al., 2004; Schmitt et al., 1998; Tolstoguzov, 1991). The possible behaviour of protein-polysaccharide mixed systems is shown in Figure 2.3.

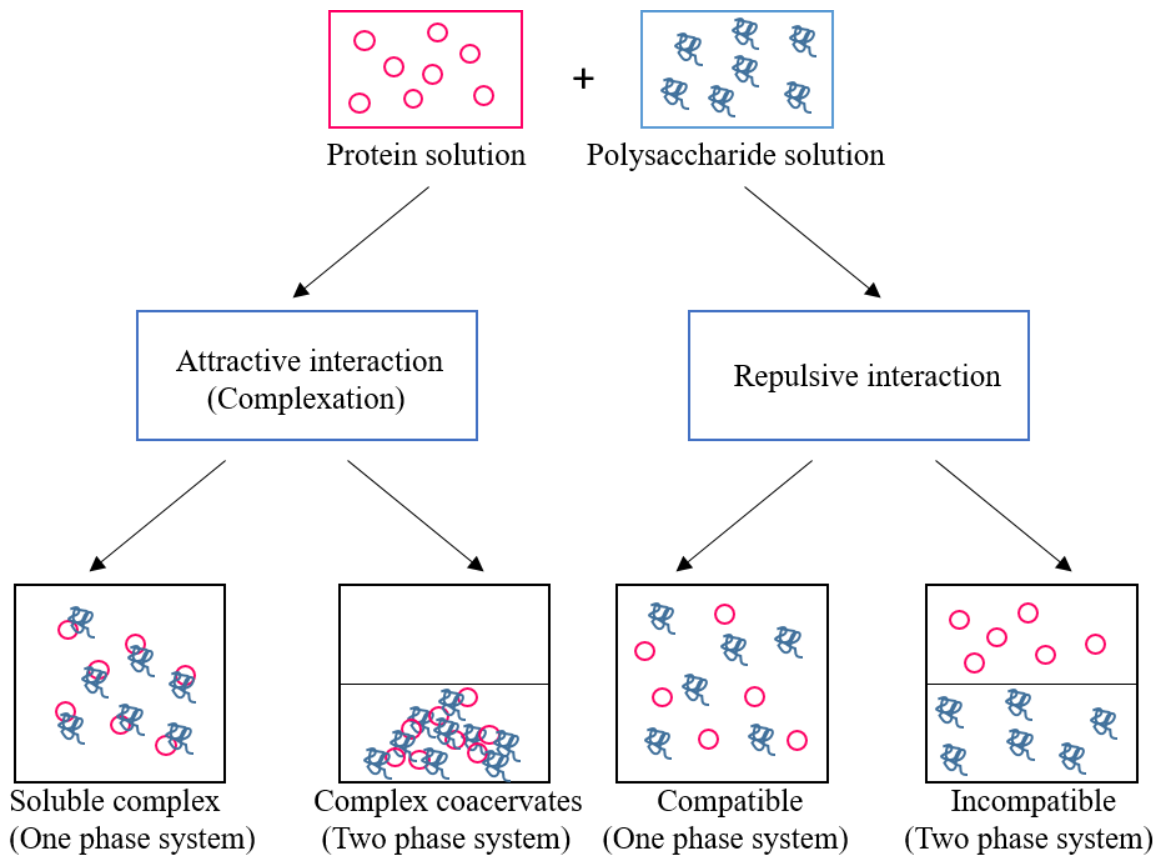


Figure 2. 3. Main trends in the behaviour of mixed systems of protein and polysaccharide.

In very dilute mixed systems of proteins and polysaccharides, these two biopolymers can be co-soluble in the solution because of the domination of mixing entropy, which leads to a homogeneous one-phase solution. However, the mixed system may become unstable with the increasing concentration of the biopolymers because of thermodynamic incompatibility (de Kruif & Tuinier, 2001; Grinberg & Tolstoguzov, 1997). Two non-interacting biopolymers can form a two-phase mixed system where each phase mainly enriched in either of the biopolymers (Tolstoguzov, 1991). Thermodynamic incompatibility may also happen when the solvent-polymer interactions (protein or polysaccharide) have a preference for the protein-polysaccharide interactions. The incompatible system of protein and polysaccharide is highly dependent on the ionic

strength and pH of the mixed solution, especially when the solution contains neutral polysaccharide and protein or the protein and polysaccharide carry the same charge at neutral pH (Goh, Sarkar, & Singh, 2014). When the mixed system of proteins and polysaccharides contains casein micelles, the phase separation phenomenon can also occur because of the depletion flocculation between casein micelles, which is due to their large particle size. In addition, there are greater attractive forces between the casein micelles with increasing polysaccharide concentration in the mixed system (de Kruif, 1999).

The attractive protein-polysaccharide interactions can lead to the formation of protein-polysaccharide complexes. Complex coacervation refers to the formation of insoluble complexes between proteins and polysaccharides driven by strong attractive electrostatic forces, which also eventually result in the phase separation of the mixed system (Goh et al., 2014). The upper phase mainly contains the solvent and little colloid and the lower phase enriched in the complex coacervates with a high viscosity between two biopolymers. A photograph of such complex coacervates was shown in Figure 2.4. This phenomenon was first investigated by Tiebackx in 1911 when he mixed gelatin and Gum Arabic in acetic acid solution. The term coacervation was introduced by Bungenberg de Jong and Kruyt in 1929. Instead of the formation of complex coacervates, protein and polysaccharide also can form soluble complexes by weak attractive electrostatic forces, which results in a stable one-phase system (Ye, 2008). The studies on these interactions between proteins and polysaccharides may bring about new applications in food industry.



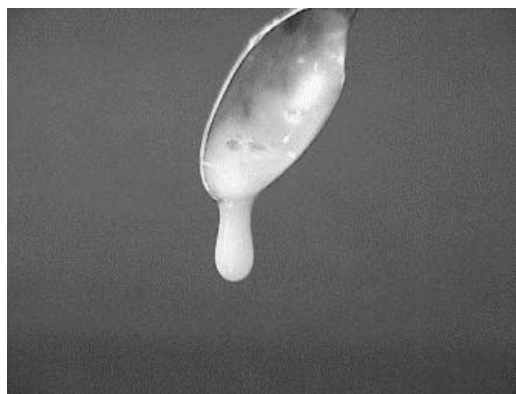


Figure 2. 4. Picture of the whey protein-Gum Arabic coacervates (de Kruif et al., 2004).

### 2.3.1. Nature of complexation between protein and polysaccharide

The main force, which contributes to the complex formation between proteins and polysaccharides, is the attractive electrostatic interaction. There are two types of protein-polysaccharide complexes produced by attractive electrostatic interactions, one is soluble complex and the other is insoluble complex. Strong attractive interactions lead to the formation of insoluble complexes, which refer to the complex coacervates (Dickinson, 1998; Schmitt et al., 1998). Complex coacervation often occurs between proteins and polysaccharides carrying opposite charges below the pIs of the proteins at very low ionic strength, where proteins are positively charged. The yield of coacervates can reach to the maximum value when the two biopolymers carry equal net opposite charges (Goh et al., 2014). Weak attractive interactions, which lead to the formation of soluble complexes, often occur at the pH above the pIs of the proteins, which is because of the electrostatic interactions between the negatively charged polysaccharides and the patches carrying positive charges on the negatively charged proteins (Schmitt et al., 1998; Ye, 2008). In addition, the soluble complexes can also be formed between the oppositely charged proteins and polysaccharides with different magnitude (Goh et al., 2014).

Compared to the attractive electrostatic interaction, other four types attractive forces, including van der Waals' force, hydrogen bonding, hydrophobic interaction and covalent bonding, play a less important role in the complex formation between proteins and polysaccharides. van der Waals' force is the very weak electrostatic force that comes from the temporary dipole interaction. Hydrogen bond is ionic and the hydrogen bonding is the interaction between hydrogen atoms attached to a negatively charged atom such as oxygen, sulphur and negatively charged atom, which is relatively weak at high temperature (Dickinson, 1998). Hydrophobic interaction is entropy-driven and long-range, which occurs between non-polar groups. It can be affected by the modifications of biopolymers in structure. Generally, this type of interaction can be promoted by unfolded polymers exposing hydrophobic groups. Contrary to hydrogen bonds, hydrophobic interactions are promoted with increasing temperature due to the increasing unfolded hydrophobic groups on polymers (Grinberg & Tolstoguzov, 1997). Covalent bonding refers to the chemical reactions between amino groups and carboxylic groups from proteins and polysaccharides respectively. Since the covalent bonding is stable to the changes in pH and ionic strength, it is used to make irreversible complexes in practice (Goh et al., 2014; Schmitt et al., 1998).

#### **2.4. Factors affecting the interactions between proteins and polysaccharides**

Among all the types of interactions discussed, attractive electrostatic interactions are the dominated driven forces in the complex formation between proteins and polysaccharides. Therefore, the factors influencing electrostatic interactions, such as pH, ionic strength, ratio and concentration of biopolymers, charge density, conformation, and Mw of biopolymers, have great influence on the protein-polysaccharide interactions. Except for the factors above, some processing factors such as temperature, shear rate and pressure

also can greatly affect the complex formation between proteins and polysaccharides (Schmitt et al., 1998). The factors are summarized in Figure 2.5.

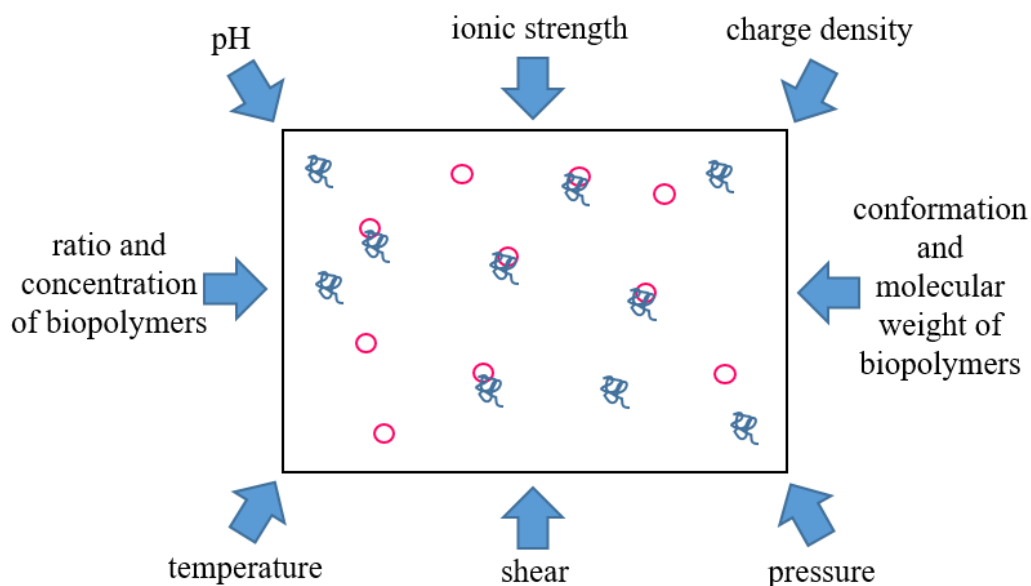


Figure 2. 5. Factors influencing the complex formation in protein-polysaccharide mixed systems.

### 2.4.1. pH

The pH value of the mixed systems of proteins and polysaccharides has great influence on the complex formation due to its effects on the ionized groups of proteins and polysaccharides, such as carboxylic and amino groups. Strong electrostatic interactions can occur between proteins and polysaccharides carrying opposite charges. Below the pI of the protein where proteins carry positive charges, strong electrostatic interactions can occur between proteins and anionic polysaccharides. Similarly, strong electrostatic interactions can also occur between proteins and cationic polysaccharides at pH above the pI of the protein (Dickinson, 2008; Schmitt et al., 1998; Xia & Dubin, 1994). The maximum yield of complex coacervates can be obtained at the electrical equivalence pH

where two biopolymers carry opposite charges with the same magnitude, leading to the maximum electrostatic interaction (Schmitt et al., 1998). Wu and McClements (2015) have investigated the effects of pH on the complex formation between gelatin and OSA-modified starch. The positive charges of gelatin solution decreased from 22.4 mV to 3 mV with the increasing pH from 3 to 7, where OSA-modified starch was negatively charged. In this study, pH 5 was selected to be the optimum pH for complex coacervation between gelatin and OSA-modified starch because of the similar magnitude of opposite charges (+8.7 mV and -13.5 mV) carried by these two biopolymers at this pH value, which indicated the maximum electrostatic interaction between them.

There are three critical pH values during the process of complexation between proteins and polysaccharides, including  $pH_c$ ,  $pH_{\Phi_1}$  and  $pH_{\Phi_2}$ .  $pH_c$  refers to the formation of initial soluble complexes where it is close to the pI of the protein, and  $pH_{\Phi_1}$  refers to the beginning of macroscopic phase separation (the formation of complex coacervates) of the mixed system (Schmitt et al., 1998). The third critical pH value,  $pH_{\Phi_2}$  refers to the dissociation of the complex coacervates between proteins and polysaccharides (Eghbal & Choudhary, 2017). In the study of Weinbreck et al (2003), the  $pH_c$  of the mixture of whey protein and Gum Arabic at a ratio of 2:1 was pH 5.3. The soluble complexes were formed by the weak electrostatic interactions between whey protein and Gum Arabic at pH close to the pI of protein because of the oppositely charged patches on whey protein. At the  $pH_{\Phi_1}$  of 4.8, the phase separation of the mixed system can be observed, and the final critical pH of the mixed system,  $pH_{\Phi_2}$  was found at pH 3. Another critical pH value,  $pH_{opt}$ , has been introduced in some studies that on the interactions between proteins and polysaccharides in recent years, which refers to the optimum pH for complex coacervation where the yield of coacervates is the highest (Azarikia & Abbasi, 2016;

Kaushik, Dowling, Barrow, & Adhikari, 2015; Khalesi, Emadzadeh, Kadkhodaei, & Fang, 2017; Mirpoor, Hosseini, & Yousefi, 2017).

#### **2.4.2. Ionic strength**

The ionic strength of the mixed systems, an important factor affecting the electrostatic interactions, is also critical for the protein-polysaccharide complexation. The mineral ions in the system may neutralize the charges carried by these two biopolymers, which can hinder the electrostatic interactions between proteins and polysaccharides (Schmitt et al., 1998; Xia & Dubin, 1994).

Low ionic strength has no significant effect on protein-polysaccharide interactions, however, with increasing ionic concentration in the mixed systems, the charges carried by proteins and polysaccharides decrease by interacting with the micro-ions, which leads to the reduction in electrostatic interactions between these biopolymers. In addition, the charges carried by the proteins and polysaccharides can be screened at high ionic strength, which thereby results in the suppression of electrostatic interactions and complex formation between proteins and polysaccharides (Weinbreck et al., 2003; Xia & Dubin, 1994; Ye, 2008). However, it was reported that salt addition at certain concentrations could improve the formation of protein-polysaccharide complexes, which was different from the salt screening effect (Wang, Lee, Wang, & Huang, 2007). The formation of complex coacervates between  $\beta$ -lactoglobulin and pectin at protein to polysaccharide ratio of 5:1 increased with increasing salt concentration under the critical salt concentration of 0.21M (0.01M-0.21M), which was suppressed by increasing salt concentration above the critical NaCl concentration (0.21M-0.41M).

### 2.4.3. Ratio and concentration of biopolymers

The concentration of the biopolymers in the mixed systems can affect the charge balance of the system, hence affecting the complexation between the macromolecules. The maximum complex coacervates between proteins and polysaccharides are obtained at a specific ratio under a specific condition, including pH and ionic strength. If one of the biopolymers is in excess in the mixture, soluble complexes could be formed due to the presence of non-neutralised charges, resulting in the decrease in turbidity (Weinbreck et al., 2003; Ye et al., 2006). Magnusson and Nilsson (2011) have investigated the interactions between egg yolk protein,  $\alpha$ - $\beta$ -livetins, and OSA-modified starch at different protein to polysaccharide ratios including 1:0, 5:1, 2:1, 1:1, 1:2 and 0:1. All the transmission values of the mixtures were obtained at pH 4, where the livetin is positively charged. The lowest transmission value was found at ratio of 2:1, which indicated the maximum formation of complex coacervates between livetin and OSA-modified starch. However, no phase separation was observed at the ratios of 5:1, 1:1 and 1:2, which could be attributed to the excess of one of the biopolymers in the mixture at these ratios, thereby leading to the formation of soluble complexes. Similar results were obtained in the study of Zhao et al. (2018), the turbidity of the gelatin-OSA-modified kudzu starch mixture at  $\text{pH}_{\text{opt}}$  (pH 6) varied from the different protein to polysaccharide ratios. The highest yield of complex coacervates was obtained at the ratio of 1:1. Further decrease (at ratio of 5:1, 3:1 or 2:1) or increase (at ratio of 1:2, 1:3 or 1:5) of the starch concentration in the mixture led to the decrease in its turbidity. Furthermore, at special protein to polysaccharide ratio of casein and Gum Arabic (Ye et al., 2006) or casein and chitosan (Anal et al., 2008) in the mixed systems, stable nanoparticles (Figure 2.6) could be formed over a quite range of pH where the two biopolymers carried opposite charges.

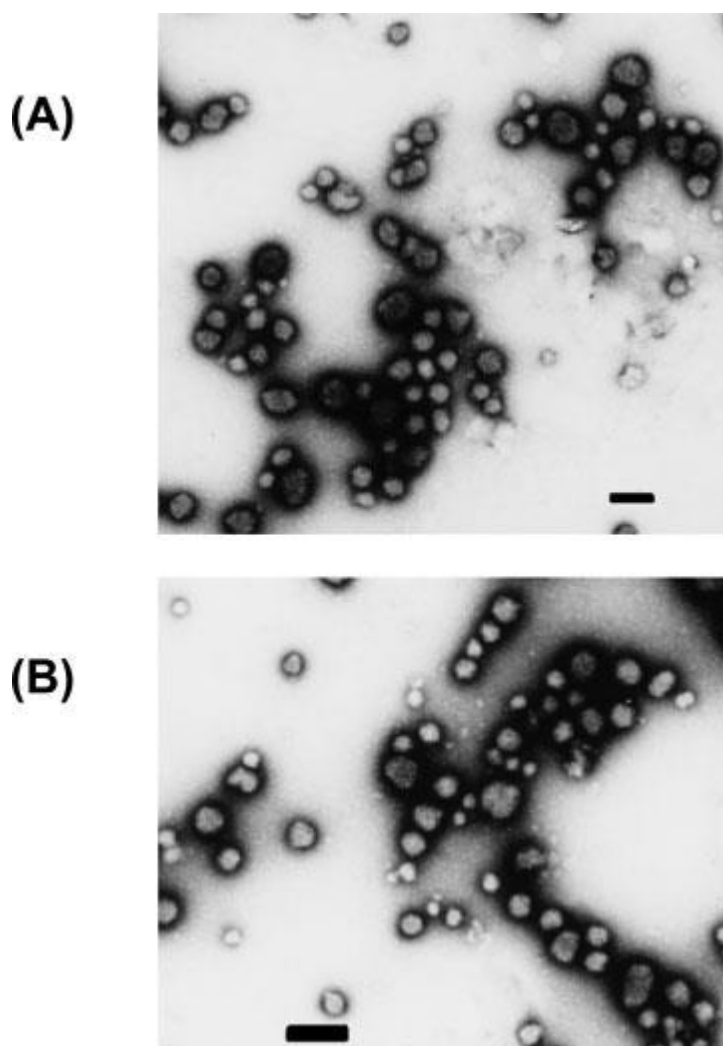


Figure 2. 6. TEM micrographs of complexes observed in the mixed system of 0.5% (w/w) sodium caseinate and 0.5% (w/w) Gum Arabic at pH 4.2. The scale bar represents 500 nm (Ye et al., 2006).

Another explanation is that greater release of counter ions in the mixture at high biopolymer concentration suppresses the complex coacervation between macromolecules (Weinbreck et al., 2003). Moreover, phase separation may happen at high biopolymer concentrations through thermodynamic incompatibility when the solvent-polymer interactions (protein or polysaccharide) overcome the protein-polysaccharide interactions (Goh et al., 2014; Tolstoguzov, 1997).

#### 2.4.4. Charge density

The charge density refers to the net charges presented on the biopolymers per unit length (Schmitt et al., 1998). It plays an important role in the complexation between proteins and polysaccharides, which can be improved when the net opposite charges carried by the biopolymers increase (Ye, 2008). The effects of charge density on the complexation between proteins and polysaccharides have been investigated in many mixed systems, which usually contains a protein and a synthetic polysaccharide because of easier modification of its charge density (Schmitt et al., 1998). The charge density of pectin could determine the strength of its adsorption to proteins. Maroziene and de Kruif (2000) reported that greater amount of low methoxyl pectin was required for the full coverage of casein in milk than high methoxyl pectin. The effect of pectins with different degrees of esterification (DE) on the complexes between WPI and pectin was investigated by Salminen and Weiss (2014). It was found WPI could form relatively small complexes with 50, 55, 62 and 70 % DE pectins, and the WPI-71% DE pectin complexes showed major aggregation in this study, which could be attributed to the different charge density of pectins with different DE. Similar results have been demonstrated by Zeeb et al. (2018) that low methoxyl (DE 10%) pectin led to smaller initial size and higher surface charge magnitude of its complexes with WPI than those of high methoxyl pectin (DE 71%). Similar to pectins, the DS value of OSA-modified starch can affect its charge density, however, there is limited data about the effects of DS value on the interactions between protein and OSA-modified starch, which needs further investigation. Perez, Carrara, Sánchez, Patino and Santiago (2009) reported that the mixture of WPC and k-carrageenan showed stronger attractive interactions at all the concentrations examined than that of WPC and sodium alginate. Similar results were also obtained by the study on the interactions between canola protein isolate and alginate or ι-carrageenan (Klassen, Elmer,



& Nickerson, 2011). These results suggested that the interactions between protein and sulphated polysaccharides (carrageenan) were stronger than those between protein and carboxylated polysaccharides (alginate), which could be attributed to greater charge density of the sulphated polysaccharides.

#### **2.4.5. Conformation and molecular weight of biopolymers**

It has been proved that there are stronger interactions between flexible proteins, (e.g., casein and gelatin) and polysaccharides than globular proteins (e.g., bovine serum albumin or  $\beta$ -lactoglobulin) (Doublier et al., 2000; Ye, 2008). The possible reason for this phenomenon is that flexible molecules have more contact with the molecules carrying opposite charges, which favours the increasing concentration of interacting groups locally. Therefore, thermal denaturation of globular proteins, which can lead to conformational changes of the proteins exposing more hydrophobic groups, may enhance their interactions with polysaccharides. This has been demonstrated by the studies on native or heat-denatured whey protein with xanthan (Bryant & McClements, 2000), pectin (Kim et al., 2006) or carrageenan (Chun et al., 2014) in solution. In these studies, the heat-denatured whey protein promoted the thermodynamic incompatibility between WPI and polysaccharides. Kim et al. (2006) observed that the phase separation phenomenon did not occur when native WPI was used to replace heat-denatured WPI over the phase separation range of heat-denatured WPI and pectin. The authors proposed an explanation that the globular structure of WPI tends to form filaments at neutral pH during heat treatment above their thermal denaturation temperature, which is because of the partially unfolded globular protein and the exposure of the non-polar groups inducing the cross-linking between the protein molecules by hydrophobic interactions. The entropy of the mixed system greatly decreased when the protein molecules were cross-linked to high

molecular weight structures, which contributed to the thermodynamic incompatibility of the mixed system. Therefore, phase separation is much more favourable for heat-denatured WPI than native WPI with polysaccharides. Conversely, polysaccharides with low charge density would rather interact with ordered (helix) conformational proteins with more charges than disordered (random coil) conformational proteins with less charges (Ye, 2008).

Different from other properties of biopolymers, the influence of the Mw of biopolymers on the protein-polysaccharide complex formation is rarely taken into account. In theory, the compatibility in mixed systems of proteins and polysaccharides decreases with increasing biopolymer molecular weight, hence the formation of coacervates should increase with the increasing biopolymer molecular weight (Schmitt et al., 1998). Some researchers have studied the effects of Mw of proteins on the protein-polysaccharide interactions. Since the cross-linking between the heat-denatured protein molecules by hydrophobic interactions can lead to higher effective molecular weight than native proteins, the thermodynamic incompatibility between proteins and polysaccharides was promoted when mixing with heat-denatured WPI (Bryant & McClements, 2000; Chun et al., 2014; Kim et al., 2006). However, the influence of Mw of polysaccharides on the interaction between proteins and polysaccharides is still unclear at present, which requires more investigations in the future.

#### **2.4.6. Processing factors**

Processing factors such as temperature, shear rate and pressure can also affect the complex formation between proteins and polysaccharides. Changes in temperature may affect the conformation of proteins or polysaccharides. When hydrophobic groups

attached to the backbone of the biopolymers, hydrophobic interactions may overcome electrostatic interactions (Schmitt et al., 1998; Ye, 2008). Conformational changes of proteins (thermal denaturation) and polysaccharides at high temperature lead to the exposure of more reactive groups and enhance the protein-polysaccharide interactions. The effect of temperature during the complex formation on the WPI or  $\beta$ -lactoglobulin-pectin system have been studied by Jones et al. (2009) and Jones and McClements (2010). In the study of Jones et al. (2009), the mixed system was under the thermal treatment of 83°C for 15 min. The thermal aggregation temperature of WPI increased in the presence of pectin, but aggregates of WPI was still observed when it was heated above 70°C. The obtained complexes were relatively small ( $d \approx 300$  nm) and stable over the range of pH values from 7 to 4.8. In addition, the particle size of  $\beta$ -lactoglobulin-pectin complexes decreased with increasing holding temperature (70 to 90°C) during thermal treatment of their mixture (Jones & McClements, 2010). The shear rate was also proved to have influence on the complexes between protein and polysaccharides. Protte et al. (2017) found that a higher shear rate led to a higher yield of WPI-pectin complexes with smaller particles on both the lab and pilot scale.

## **2.5. Applications in encapsulation of lipophilic bioactive compounds**

Lipophilic bioactive compounds such as polyunsaturated fatty acids, carotenoids, hydrophobic vitamins and nutraceuticals have an increasing attraction in food industry in recent years because of their health benefits to human. However, their instability to environmental conditions has limited their use in food industry (Wang, Akanbi, Agyei, Holland, & Barrow, 2018). Encapsulation refers to the entrapment of small particles, including solid, liquid or gas inside a shell (coating material) as small capsules. Biopolymers such as proteins and polysaccharides, are commonly used combined or

alone for encapsulation in food industry (Eghbal & Choudhary, 2017). Encapsulation of bioactive compounds can enhance the shelf life of food products and protect the sensitive flavours or bioactive compounds against changes in external conditions such as temperature, moisture, light, etc. Moreover, it can also help to control the release of bioactive compounds to specific gastrointestinal targets (Schmitt & Turgeon, 2011).

Now there are great interests in the encapsulation of bioactive compounds by the complex coacervates between proteins and polysaccharides (de Kruif et al., 2004; Devi, Sarmah, Khatun, & Maji, 2017; Evans, Ratcliffe, & Williams, 2013). It is generally used in emulsion-based delivery system rather than use them directly to encapsulate bioactives except for hydrophilic bioactive compounds such as thiamine (Bédié, Turgeon, & Makhoul, 2008) and probiotics (Bosnea, Moschakis, & Biliaderis, 2014; Eratte et al., 2015, 2017; Hernández-Rodríguez et al., 2014). It is considered as a potential technique for fabricating nanoparticles with a lipid core (Aloys et al., 2016), which is effective for encapsulation of lipophilic bioactive compounds. Once complex coacervation is induced, the coacervates are formed and can entrap the lipid core containing lipophilic bioactive compounds (McClements, Decker, & Weiss, 2007). Many reports on the encapsulation of lipophilic bioactive compounds by milk protein-polysaccharide complex coacervates have been published in recent years (Eratte et al., 2014; Jain et al., 2015, 2016; Koupantsis et al., 2014). As shown in Figure 2.7, two methods were developed for encapsulation of lipophilic bioactive compounds by protein-polysaccharide complex coacervates.

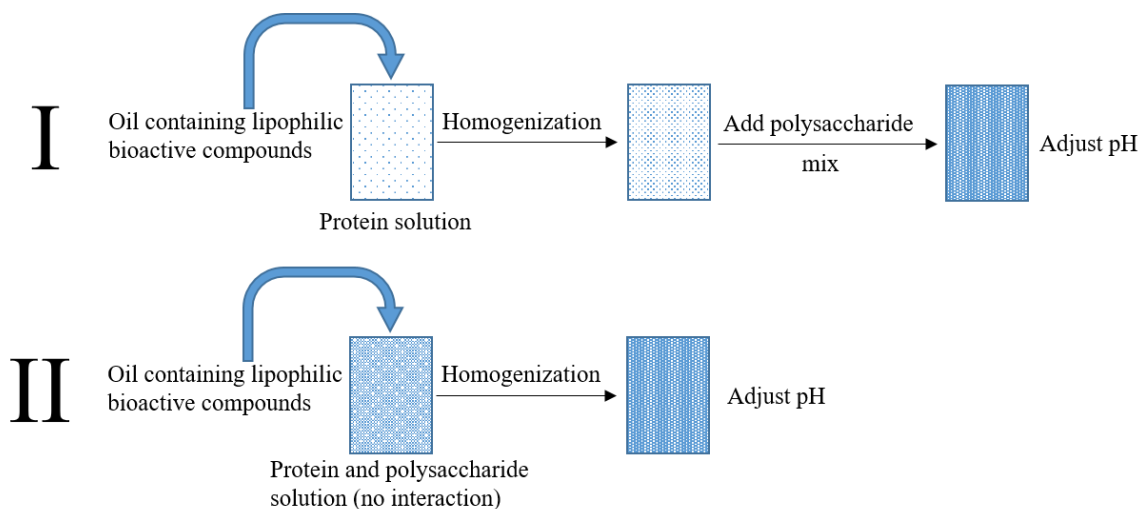


Figure 2. 7. Two preparation methods for encapsulation of lipophilic bioactive compounds by protein-polysaccharide complex coacervates.

In the first method, oil containing lipophilic bioactive compounds is added to a protein solution and homogenized to get a primary emulsion prior to the addition of a polysaccharide solution, followed by the adjustment of pH to the optimum pH value for complex coacervation. This method is applied by most of the studies (Eratte et al., 2014, 2015, 2017; Gomez-Estaca et al., 2016; Ilyasoglu & El, 2014; Jain et al., 2015, 2016; Junxia, Hai-yan, & Jian, 2011; Koupantsis et al., 2014; Zhao et al., 2018). For example, Eratte et al. (2014) used WPI and Tuna oil rich in omega-3 fatty acids to prepare the primary emulsion before the addition of Gum Arabic solution. After mixing with Gum Arabic solution, the mixture was adjusted to pH 3.75, which is the optimum pH for WPI-Gum arabic complex coacervation at protein to polysaccharide ratio of 3:1. The spray-dried microcapsules of tuna oil encapsulated by WPI-Gum Arabic coacervates showed high encapsulation efficiency and were quite stable against oxidation. In the second method, oil containing lipophilic bioactive compounds is added to a mixed solution of protein and polysaccharide and homogenized before adjusting to the optimum pH value for complex coacervation. Koupantsis et al. (2014) used WPI-CMC or casein-CMC coacervates to

encapsulate  $\beta$ -pinene (lipophilic flavour compound). The complex coacervation between WPI or casein and CMC was found to be favoured at pH 2.8. Therefore, the O/W emulsion with  $\beta$ -pinene made by either WPI-CMC or casein-CMC mixed solution was acidified to this pH value to induce complex coacervation, thereby leading to the formation of microcapsules coated by complex coacervates. In this study, the WPI-CMC coacervates showed higher encapsulation efficiency (36.90%) than the casein-CMC coacervates (29.02%).

This emulsion-based encapsulation method has also been used in WPI-OSA-modified polysaccharide mixed system to encapsulate lipophilic bioactive compounds. Puerta-Gomez & Castell-Perez (2017) encapsulated a lipophilic bioactive compound, TCNN, using the electrostatic precipitates of WPI in combination with OSA-modified waxy rice starch or phytoglycogen with different DS values. The primary O/W emulsion of TCNN was prepared by the mixture of WPI and OSA-modified polysaccharides before adjusting to pH 4.5, the pI of the protein solution. The maximum entrapment of TCNN was found at the WPI to OSA-modified polysaccharide ratio of 1:10 in both WPI-OSA-modified waxy rice starch mixed system and WPI-OSA-modified phytoglycogen mixed system. This could be attributed to the high concentration of OSA-modified polysaccharide, which may unfold the WPI in the mixture leading to more opportunities for the binding of exposed hydrophobic groups to OSA-modified polysaccharides, and hence to encapsulate more amounts of TCNN.

Except for the protein-polysaccharide complex coacervates, some researchers have explored the potential applications of soluble complexes between proteins and polysaccharides for encapsulation of either hydrophilic or lipophilic bioactive compounds in recent years (Hosseini, Emam-Djomeh, Sabatino, & Van der Meeren, 2015; Ilyasoglu

& El, 2014; Mirpoor et al., 2017; Ron, Zimet, Bargarum, & Livney, 2010; Zimet & Livney, 2009). Hosseini et al. (2015) found that the binding capacity of  $\beta$ -lactoglobulin for lipophilic bioactive compounds (curcumin) was higher than hydrophilic bioactive compounds (folic acid). The samples containing curcumin and folic acid are shown in Figure 2.8.

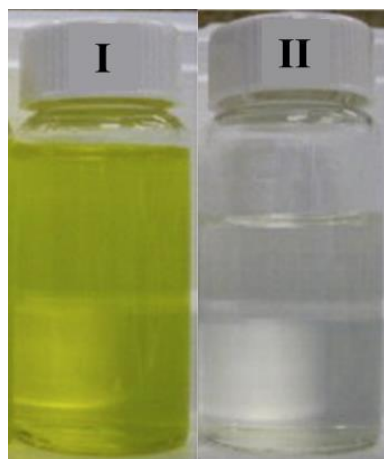


Figure 2. 8. Curcumin and folic acid nano-encapsulation at pH 4.25: curcumin dissolved in ethanol (I) and deionized water (II) added to  $\beta$ -lactoglobulin-sodium alginate soluble complexes (sodium alginate/ $\beta$ -lactoglobulin weight ratio of 0.75) (Hosseini et al., 2015).

Most of the research used  $\beta$ -lactoglobulin to bind lipophilic compounds since it is a lipocalin, which binds small hydrophobic ligands (Kontopidis, Holt, & Sawyer, 2004). Generally, the lipophilic bioactive compounds are dissolved in absolute ethanol at specific concentration, which has no appreciable effect on protein structure, before adding into the  $\beta$ -lactoglobulin solution. After the formation of the complexes between  $\beta$ -lactoglobulin and the lipophilic bioactive compounds under vortex for some time, the polysaccharide solution will be added and adjust pH to induce the formation of the ternary

complex between  $\beta$ -lactoglobulin-bioactive compounds complex and the polysaccharide by attractive electrostatic interactions (Figure 2.9).

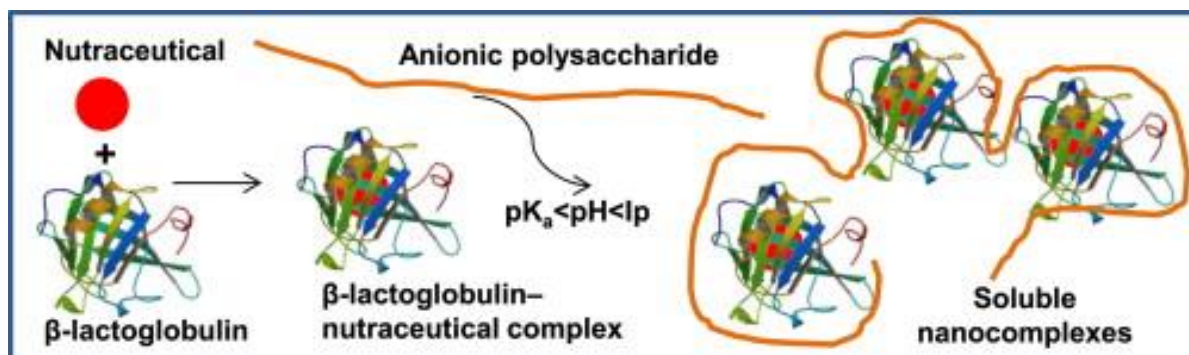


Figure 2. 9. Schematic representation of the entrapment of nutraceuticals in the soluble nanocomplexes between  $\beta$ -lactoglobulin and sodium alginate (Hosseini et al., 2015).

Liu et al. (2016) obtained soluble complexes (162.1 nm) between acid soluble soy protein (ASSP) and soy soluble polysaccharide (SSPS) at protein to polysaccharide weight ratio of 1:5 and pH 3.5, which was able to stabilize Pickering emulsions. Liu, Wang, Qi, Huang and Xiao (2018) then used this Pickering emulsion to encapsulate oregano essential oil before the formation of soybean polysaccharide films by esterification of OSA. It has been proved to be an effective method to improve the antimicrobial ability of polysaccharide films encapsulated with essential oil (Figure 2.10).



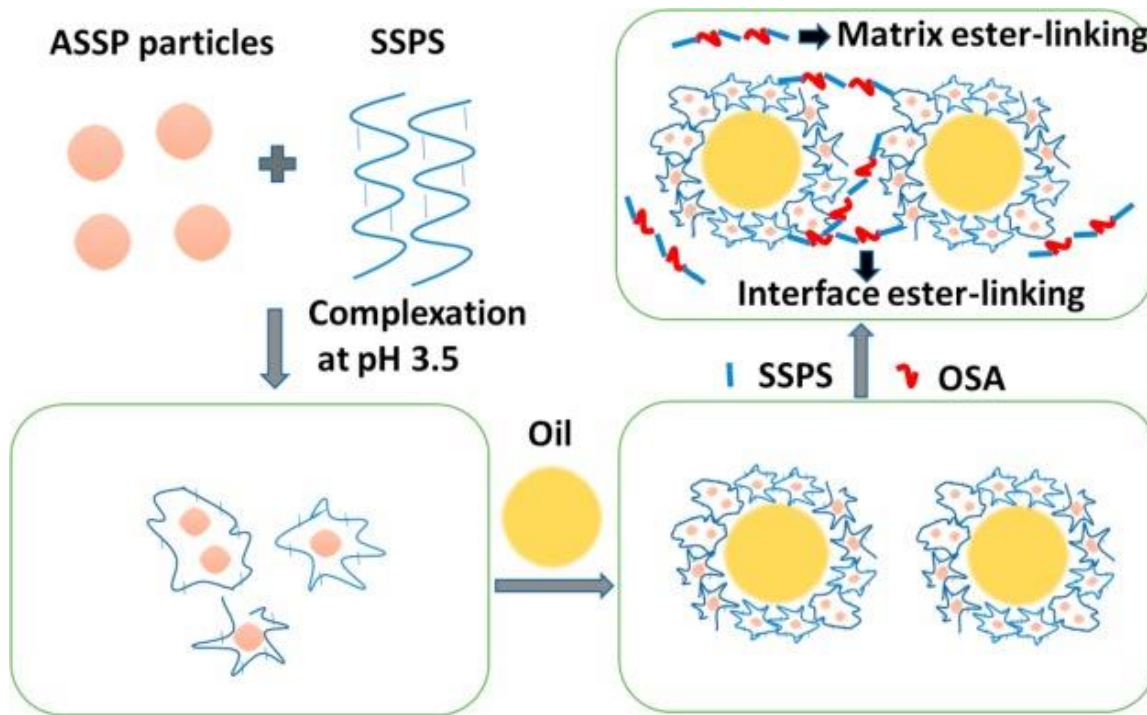


Figure 2. 10. Schematic representation of the formation of SSPS-based films by esterification of OSA (Liu et al., 2018).

### 2.5.1. Encapsulation of $\beta$ -carotene

$\beta$ -Carotene is the most significant carotenoid over more than 600 different carotenoids, which is highly conjugated and water-insoluble (Jain et al., 2016). It is one of the major carotenoids present in the diet and responsible for the colour in yellow, orange and red vegetables and fruits (Boon, McClements, Weiss, & Decker, 2010). As a good source of provitamin A, it has benefits for eye health, and its antioxidant properties help human body withstand free radical damage (Wang et al., 2018).  $\beta$ -Carotene is often used as subject matter in research works because of the above reasons (Jain et al., 2016). However, its poor water solubility and chemical instability have limited its utilization in food industry (Jain et al., 2015).

Jain et al. (2015, 2016) used protein-polysaccharide complex coacervates to encapsulate  $\beta$ -carotene (Figure 2.11 & 2.12). The encapsulation efficiency of  $\beta$ -carotene was almost 77.3 % when the ratio of WPI and Gum Acacia was 2:1 at pH 4.2 (Jain et al., 2015). Similarly, 79.36% of encapsulation efficiency was achieved by the casein-gum tragacanth coacervation at ratio of 2:1 and pH 4.35 (Jain et al., 2016). Results of both studies showed the encapsulation of  $\beta$ -carotene into the coacervates between proteins and polysaccharides improved the stability of  $\beta$ -carotene during storage. Another study also showed that  $\beta$ -carotene could be effectively encapsulated by the casein-Guar Gum coacervates (65.95%), which greatly enhanced the photo-stability of  $\beta$ -carotene (Thakur, Jain, Ghoshal, Shivhare, & Katare, 2017).

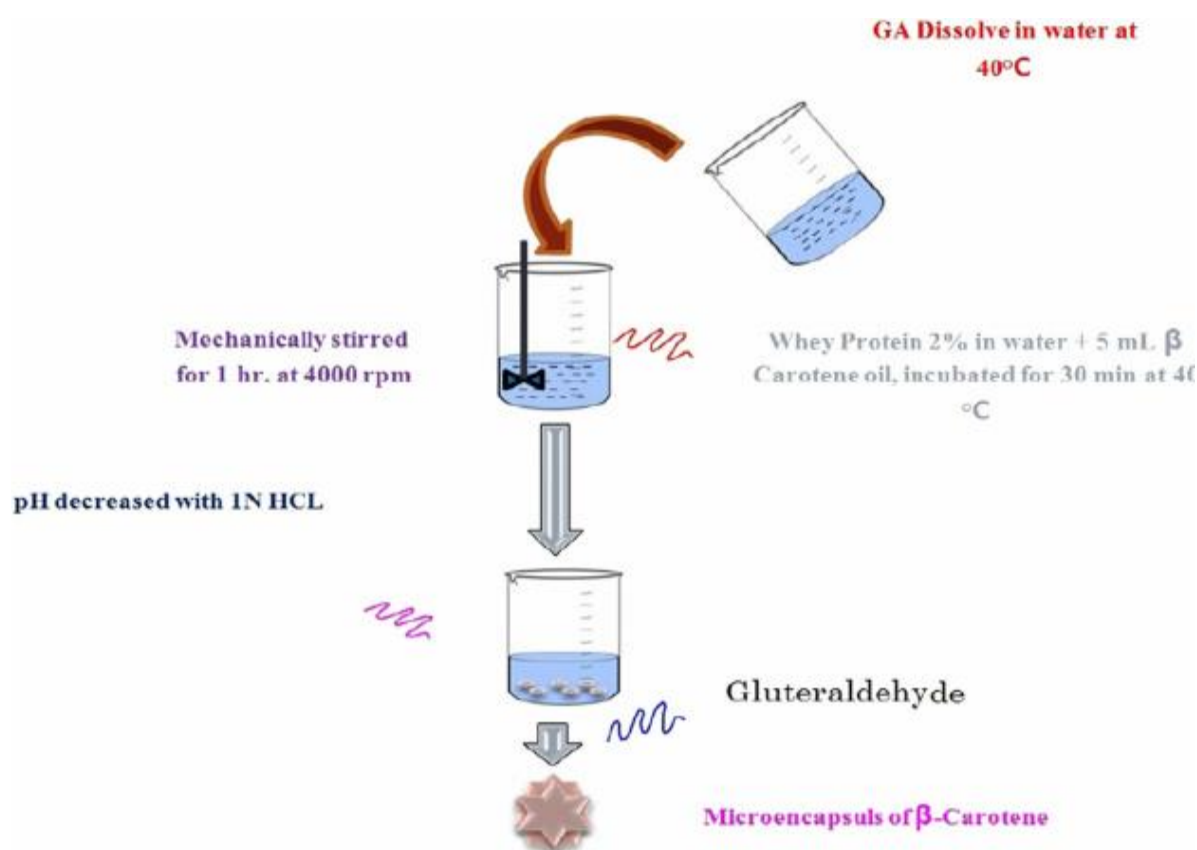


Figure 2. 11. Schematic representation of the encapsulation of  $\beta$ -carotene by WPI-Gum Acacia coacervates (Jain et al., 2015).

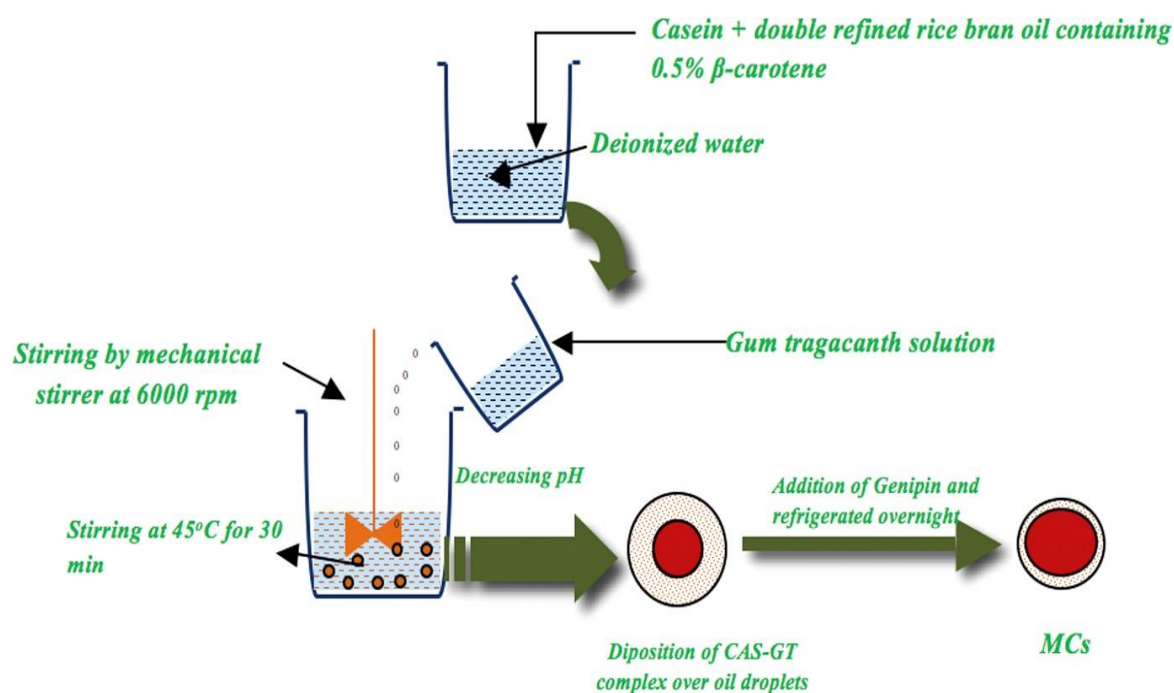


Figure 2. 12. Schematic representation of the encapsulation of  $\beta$ -carotene by casein-gum tragacanth coacervates (Jain et al., 2016).

There are also some reports on encapsulation of other carotenoids such as astaxanthin by complex coacervation, e.g. gelatin-cashew gum complex coacervates (Figure 2.13) (Gomez-Estaca et al., 2016) and gelatin-OSA-modified kudzu starch complex coacervates (Zhao et al., 2018). All of these studies were followed the first method mentioned above for encapsulation of lipophilic bioactive compounds using protein-polysaccharide complex coacervates.

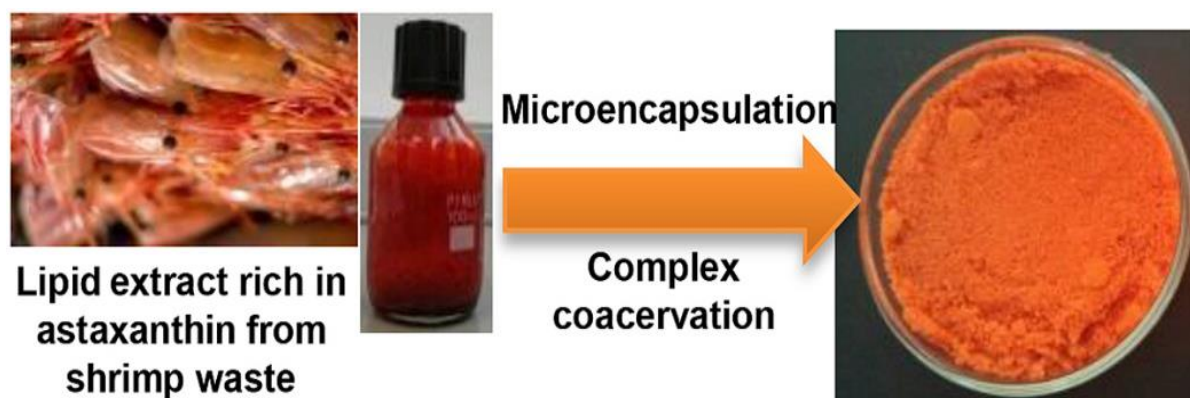


Figure 2. 13. Freeze-dried microcapsules of gelatin-cashew gum complex coacervates with lipid extract rich in astaxanthin from shrimp waste (Gomez-Estaca et al., 2016).

$\beta$ -Carotene can also be encapsulated into the protein-polysaccharide soluble complexes. Hosseini et al. (2015) encapsulated  $\beta$ -carotene by using the binding capacity of  $\beta$ -lactoglobulin for lipophilic bioactive compounds. The binding affinity of  $\beta$ -carotene to  $\beta$ -lactoglobulin has been evaluated under neutral pH (pH 7) and acidic pH (pH 4.25). The results showed that there was stronger binding affinity at pH 4.25, which could be attributed to the increasing hydrophobic interactions around the pI of  $\beta$ -lactoglobulin.

## 2.6. Conclusion

Currently, there are extensive studies on the interactions between whey protein and many different types of polysaccharide. However, only a few reports on the interaction between whey protein and OSA-modified starch have been published. Heat treatment of protein could induce changes in conformation and Mw of WPI, which has been proved to affect the interactions between proteins and polysaccharides. It can be inferred that the interactions between OSA-modified starch and heat-denatured WPI should be very different from those between native WPI. Except for the characteristics of WPI, the

characteristics of OSA-modified starch including Mw and DS may also affect their complexation, however, the influence was still unclear at present and requires further investigation. Therefore, it is necessary to investigate the complexation between native or heat-denatured WPI and OSA-modified starch with different DS or Mw for better knowledge of their interactions. It was demonstrated that the heat-denatured protein may form stable core-shell nanoparticles with polysaccharides over a specific pH range.  $\beta$ -Lactoglobulin aggregates can form stable core-shell nanoparticles with pectin, it can be hypothesised that heat-denatured WPI may form stable core-shell nanoparticles with OSA-modified starch under specific condition, which can be used as delivery systems in food applications. There is a growing interest in the application of the protein-polysaccharide complexes to encapsulate either hydrophilic or lipophilic bioactive compounds in recent years, but most of the researchers have focused on using complex coacervates between proteins and polysaccharides rather than their soluble complexes. Encapsulation of lipophilic bioactive compounds by protein-polysaccharide complex coacervates in the emulsion-based delivery systems has been proved to be a relatively effective way to protect the encapsulated bioactive compounds against the changes in the environment during the storage. However, there is no data about encapsulating lipophilic bioactive compounds directly into the already formed soluble complexes between proteins and polysaccharides. Therefore, it is interesting to seek the potential application of the soluble complexes between WPI and OSA-modified starch in this field, which can provide new ideas for food manufacturers in the production of functional foods.

## **Chapter 3 Formation of insoluble and soluble complexes between WPI and OSA-modified starch**

### **3.1. Abstract**

Mixed systems of protein and polysaccharide are frequently used in food industry, and the knowledge of their interactions is of great significance for food manufacturers. In this study, the formation of complexes between WPI and OSA-modified starch was investigated as a function of pH (7-3), the heat treatment of WPI, and the ratio of WPI and OSA-modified starch (1:1, 1:10, 1:20). The colloidal behaviour of the mixture under specific conditions was evaluated by absorbance measurement (at 515nm) and dynamic light scattering. The OSA-modified starch was more likely to interact with heated WPI rather than non-heated WPI, and the optimum condition for their complexation was at ratio of 1:10 and pH 4.5, which was driven by both electrostatic and hydrophobic interactions. The effects of OSA starch molecular characteristics including the Mw and DS on the complexation with HWPI under optimum condition were also investigated. OSA-modified starch with higher Mw was difficult to form a dense precipitation phase with HWPI due to its higher viscosity restricting the movement of any particles present. Stable soluble complexes could be formed between HWPI and OSA-modified starch with higher DS value under the same condition, which may be attributed to the stronger steric hindrance of OSA-modified starch with higher DS value. It is postulated that the complexes between HWPI and OSA-modified starch comprise a protein aggregate core and attached with OSA-modified starch. The complexation process was induced by electrostatic interactions, while the structural properties of the complexes were determined by hydrophobic interactions. The strong hydrophobic interactions between the protein aggregates and the OSA groups of the OSA-modified starch with higher DS

value lead to the presence of enough hydrophilic portion of OSA-modified starch outside the aggregate cores, which could sterically stabilize the protein aggregates and consequently prevent further aggregation. However, the OSA groups of OSA-modified starch with lower DS values may be insufficient for strong hydrophobic interactions with protein aggregate cores and consequently result in the further aggregation of the complexes. These stable soluble complexes between HWPI and OSA-modified starch may be used as delivery systems for lipophilic bioactive compounds.

### **3.2. Introduction**

The protein-polysaccharide interactions can have great influence on the properties of food products such as the texture and stability (de Kruif & Tuinier, 2001; Ye, 2008), which can be either attractive or repulsive. Strong attractive interactions between these two macromolecules often occur at pH values below the pI of the protein where the proteins carry positive charges, leading to the formation of complex coacervates (Schmitt et al., 1998). At pH value above the pI of the protein, anionic polysaccharides could have weak electrostatic interactions with the positively charged patches on the proteins, which can lead to the formation of soluble complexes (Dickinson, 1998; Schmitt et al., 1998). Except for the formation of insoluble or soluble complexes, it has been demonstrated that stable nanoparticles can be formed under specific condition, which are stable over a range of pH (Anal et al., 2008; Ye et al., 2006). The complex formation between proteins and polysaccharides is mainly dependent on the physical conditions of the biopolymer solutions, including pH, ionic strength, the ratio and concentration of the biopolymers, and the molecular characteristics of the biopolymers, including charge density, conformation and Mw. Meanwhile, the processing factors such as temperature, pressure



and shear rate can also affect the formation of complex (Schmitt et al., 1998; Schmitt & Turgeon, 2011; Ye, 2008).

Due to the low price and good emulsifying capacity of OSA-modified starch, it has been used as a good substitute for lipids, proteins and Gum Arabic (Sweedman et al., 2013). The presence of free carboxyl groups renders OSA-modified starch anionic at certain pH values, which may lead to interactions with positively charged proteins (Nilsson & Bergenståhl, 2007). Whey protein, which accounts for about 20% of bovine milk protein, is now recognized as an important nutritional ingredient in food industry all over the world (de Wit, 1990). Since they are both common ingredients in food products, their interactions need to be understood for the development of food production.

Currently, most studies are mainly focused on the interactions between milk proteins (casein, whey protein and  $\beta$ -lactoglobulin), plant proteins (soybean protein and pea protein) or gelatin and non-starch polysaccharides including Gum Arabic, pectin and CMC. (Cuevas-Bernardino et al., 2018; Jones et al., 2009; Jones & McClements, 2010; Kim et al., 2006; Liu et al., 2016; Salminen & Weiss, 2014; Santipanichwong et al., 2008; Turgeon et al., 2007; Ye et al., 2006; Zeeb et al., 2018). However, only a few studies have been reported on the interactions between protein and OSA-modified starch. It has been demonstrated that OSA-modified starch can have strong electrostatic interactions with the proteins including gelatin (Wu & McClements, 2015; Zhao et al., 2018), casein (Sun et al., 2016) and egg yolk protein (Magnusson & Nilsson, 2011) at pH under their pI values. Since few studies have focused on the interactions between WPI and OSA-modified starch at different pH values, it is necessary to investigate the complexation process between WPI and OSA-modified starch as a function of pH, which can be useful for better knowledge of their interactions. In addition, the previous studies did not focus



on the interactions between the preheated protein and OSA-modified starch. Since heat treatment could induce the changes in conformation and the effective Mw of whey protein, which has been proved to promote the thermodynamic incompatibility between proteins and polysaccharides at neutral pH (Bryant & McClements, 2000; Chun et al., 2014; Kim et al., 2006), it can be inferred that the interactions between OSA-modified starch and heat-denatured whey protein should be very different from those between OSA-modified starch and native whey protein. Except for the characteristics of whey protein, the characteristics of OSA-modified starch including Mw and DS value may also affect their complexation. The DS value of OSA-modified polysaccharides has been proven to have influence on the amount of molecules interacting with the proteins (Puerta-Gomez & Castell-Perez, 2016, 2017). However, the influence of Mw of OSA-modified starch on the interactions with whey proteins was still unclear at present and requires further investigation.

The aim of this study was to investigate the interactions between WPI and OSA-modified starch as a function of pH (7-3). The effects of the structural characteristics of WPI including native and denatured WPI and the concentration ratios of biopolymers on the complex formation between WPI and OSA-modified starch were evaluated. Furthermore, the influence of the Mw and DS value of OSA-modified starch on their interactions were also investigated.

### **3.3. Materials**

Whey protein isolate powder (WPI 895) was purchased from Fonterra Co-operative Group Ltd. (Palmerston North, New Zealand). Native waxy maize starch was a gift from Ingredion (Auckland, New Zealand). High purity OSA were purchased from Sigma–Aldrich (St. Louis, MO, USA) and were used without further purification. All the other

chemicals used were of analytical grade and obtained from either Merck Millipore Co. (Darmstadt, Germany) or Sigma Chemical Co. (St. Louis, MO) unless otherwise specified. Milli-Q water (Millipore Corp., Bedford, MA, USA) was used in all experiments.

### **3.4. Methods**

#### **3.4.1. Preparation of OSA-modified starch**

The preparation of OSA-modified starch including the acid hydrolysis of the native waxy maize starch and the esterification of hydrolysed starch was carried out following the method described by Lin, Liang, Zhong, Ye, & Singh (2018a) with slight modifications.

##### **(1) Hydrolysis of starch**

Native waxy maize starch (75 g, dry basis) was suspended in 0.68M HCl (375 mL) with agitation for 1 h, 6 h or 12 h in a water bath of 50 °C to perform the acid hydrolysis of starch. This reaction was stopped by adding 1.0 M NaHCO<sub>3</sub> to adjust the pH of the mixture to neutral (~pH 7). The slurry of the acid hydrolysed starch was centrifuged at 4500 rpm for 10 min (Multifuge 3SR Plus; Thermo Scientific Inc., USA) and then washed with deionized water for three times and 70% aqueous alcohol for twice. After drying in an oven at 40 °C for 24 h, the collected dried starch was ground and then sieved by a 100 mesh sieve.

##### **(2) Esterification of hydrolysed starch**

The hydrolysed waxy maize starch was suspended in Milli-Q water (35%, w/w) with magnetic stirring. The suspension was adjusted to pH 8.5 with 3% NaOH. The OSA (3.0, 5.0, 7.0, or 9.0% of the hydrolysed starch weight starch) solution (obtained by diluting the high purity OSA three times with absolute alcohol, v/v) was added slowly within 120

min to the hydrolysed starch slurry, which was maintained at pH 8.5 by the continuous addition of 3% NaOH. In order to react completely, the incubation was continued for another two hours. This reaction was stopped by adjusting the pH to 6.5 with the addition of 3% HCl. The slurry of the starch was centrifuged at 4500 rpm for 10 min (Multifuge 3SR Plus; Thermo Scientific Inc., USA) and then washed with deionized water for three times and 70% aqueous alcohol for twice. It was dried in an oven at 40 °C for 24 h, and then the dried starch was ground and sieved by a 100 mesh sieve.

### 3.4.2. Determination of DS of OSA-modified starch

The DS of the OSA-modified starch was measured by a titration method from Lin et al. (2018a). 5 g (dry basis) of OSA-modified starch sample was dispersed and stirred magnetically for 30 min in 2.5M HCl-isopropyl alcohol solution (25 mL) before the addition of 90% (v/v) aqueous isopropyl alcohol solution (100 mL), which was stirred for another 10 min. The suspension was centrifuged at 4500 rpm for 10 min (Multifuge 3SR Plus; Thermo Scientific Inc., USA) and then washed with 90% isopropyl alcohol solution until there were no chloride ions in the supernatant, which can be detected by adding 0.1M AgNO<sub>3</sub> solution. The washed starch was suspended in deionized water (300 mL) and heated in a water bath of 95 °C for 20 min. The gelatinized starch solution was added with phenolphthalein as an indicator and then titrated with 0.1M standard NaOH solution. Hydrolysed starch without esterification was titrated as control.

The DS value was calculated using the following equation:

$$DS = \frac{0.162 \times \frac{A \times M}{W}}{1 - [0.210 \times \frac{A \times M}{W}]}$$

where A is the titration volume (mL) of the NaOH solution, M is the molarity of the NaOH solution, and W is the dry weight (g) of the starch.

### 3.4.3. Determination of Mw of OSA-modified starch

10 mg of each OSA-modified starch samples were added to 10 mL of 50 mmol/L NaNO<sub>3</sub>/dimethyl sulfoxide (DMSO) solution with stirring for 30 min in a water bath at 90 °C, which were then agitated at 50 °C for 24 h to completely dissolve the samples. The dissolved samples were centrifuged at 10,000 rpm for 3 min and then filtered through 0.45 µm syringe filters. The filtrated samples were then injected into a high performance size exclusion column chromatography system with multi-angle laser light scattering detector (Dawn DSP-F, Wyatt Technology, Santa Barbara, CA) with a He–Ne laser source ( $\lambda = 632.8$  nm), a K-5 flow cell, and a refractive index (RI) detector, an HP 1050 series pump (model ERC-7512, ERMA Inc., Tokyo, Japan), and an injector valve (Hewlett-Packard, Valley Forge, PA) with a 100 µL injection loop. Two organic SEC columns (Styragel HMW 6E DMF and HMW 2 MF columns, Waters, Massachusetts State, USA) were connected in series to determine the Mw of the OSA-modified starch. The column temperature was set at 40 °C and the flow rate was at 0.6 mL/min with a mobile phase of 50 mmol/L NaNO<sub>3</sub>/DMSO solution. The collected data was analyzed by Astra software (version 5.3.4, Wyatt Technology), and the molecular weight distributions of starch in NaNO<sub>3</sub>/DMSO were calculated by the second-order Berry method with a refractive index of 1.479 and a dn/dc value of 0.07.

### 3.4.4. Preparation of mixtures of WPI and OSA-modified starch

The WPI stock solution (5%, w/v) was prepared by dispersing WPI powder in Milli-Q water and stirring gently for 5 h at room temperature to enable complete hydration. Sodium azide (0.02%, w/w) was added to the solution to inhibit the growth of

microorganisms. The WPI stock solution was then divided into two parts. A part was named as NWPI, and another part was heated at 90 °C in a water bath for 20 min to enable the complete denaturation of WPI and named as HWPI. These two solutions were then stored at 4 °C prior to further usage. The OSA-modified starch stock solution (20%, w/v) was prepared by dispersing OSA-modified starch powder in Milli-Q water and then gelatinized in a water bath of 95 °C for 20 min to obtain a homogeneous solution. Since the OSA-modified starch was prepared in the lab that may contain some impurities, the gelatinized OSA-modified starch solution was centrifuged (Multifuge 3SR Plus; Thermo Scientific Inc., USA) at 4000 rpm for 2 min to remove the impurities. Considering that starch is susceptible to retrogradation, fresh starch solution was prepared every time before experiment. Sodium azide (0.02%, w/w) was added to the starch solution after preparation.

Mixtures of NWPI or HWPI and OSA-modified starch at different protein to polysaccharide concentration ratios (1:1, 1:10 and 1: 20) were prepared by diluting the stock solutions in Milli-Q water. The pH (7.0-3.0) of the biopolymer mixtures were adjusted by the addition of 0.1-1 M HCl or NaOH. The samples were stored at room temperature after measurement.

### **3.4.5. Absorbance measurement**

The turbidity of the mixtures of NWPI or HWPI and OSA-modified starch at different ratios with a range of pH values (pH 7.0-3.0) were measured from the apparent absorbance according to a previous study (Ye et al., 2006), using a UV/Visible spectrophotometer (Genesys 10-S; Thermo Fisher Scientific Inc., USA) at a wavelength of 515 nm. Milli-Q water was used as a blank reference. Solutions of NWPI, HWPI and OSA-modified starch alone were measured as control.

### **3.4.6. Particle size and $\zeta$ -potential measurement**

The particle size and  $\zeta$ -potential of the mixtures were determined by zetasizer (Nano-ZS, Malvern Instruments Ltd, Malvern, Worcestershire, UK), which is a combined dynamic light scattering and electrophoresis motilities instrument. All the samples were measured without dilution.

### **3.4.7. Statistical analysis**

All experiments were performed three times, and the results were reported as the calculated means and standard deviations. Statistical analysis program, SPSS 19.0 (IBM Inc., Armonk, NY), was used to perform analysis of variance with Duncan test to compare the mean values with a defined significance level at  $p < 0.05$ .

## **3.5. Results and discussion**

### **3.5.1. Effect of the characteristics of WPI**

The characteristics of WPI such as native (non-heated) or denatured (heated) has been proved to affect the interactions between proteins and polysaccharides, since the thermal denaturation of globular proteins can lead to conformational changes of the proteins exposing more hydrophobic groups (Bryant & McClements, 2000; Chun et al., 2014; Kim et al., 2006). pH is an important factor affecting the protein-polysaccharide interactions due to its effects on the ionized groups of proteins and polysaccharides, such as carboxylic and amino groups (Dickinson, 2008; Schmitt et al., 1998). Figure 3.1 shows the absorbance profiles at a wavelength of 515 nm as a function of pH (7-3) of the mixtures of 0.5% NWPI or HWPI and OSA-modified starch at protein to polysaccharide concentration ratios of 1:1, 1:10 and 1:20. The OSA-modified starch (H12-OSA-5%, hereinafter to be referred as OSA in this Chapter) was acid hydrolysed for 12 h and then

esterified with OSA at 5% of the hydrolysed starch weight, which had a DS value of  $2.54 \pm 0.04$  % and Mw of  $19.24 \pm 0.07 \times 10^4$  g/mol. The pure 0.5% NWPI or HWPI solution and corresponding concentration of OSA-modified starch solutions were measured as control.

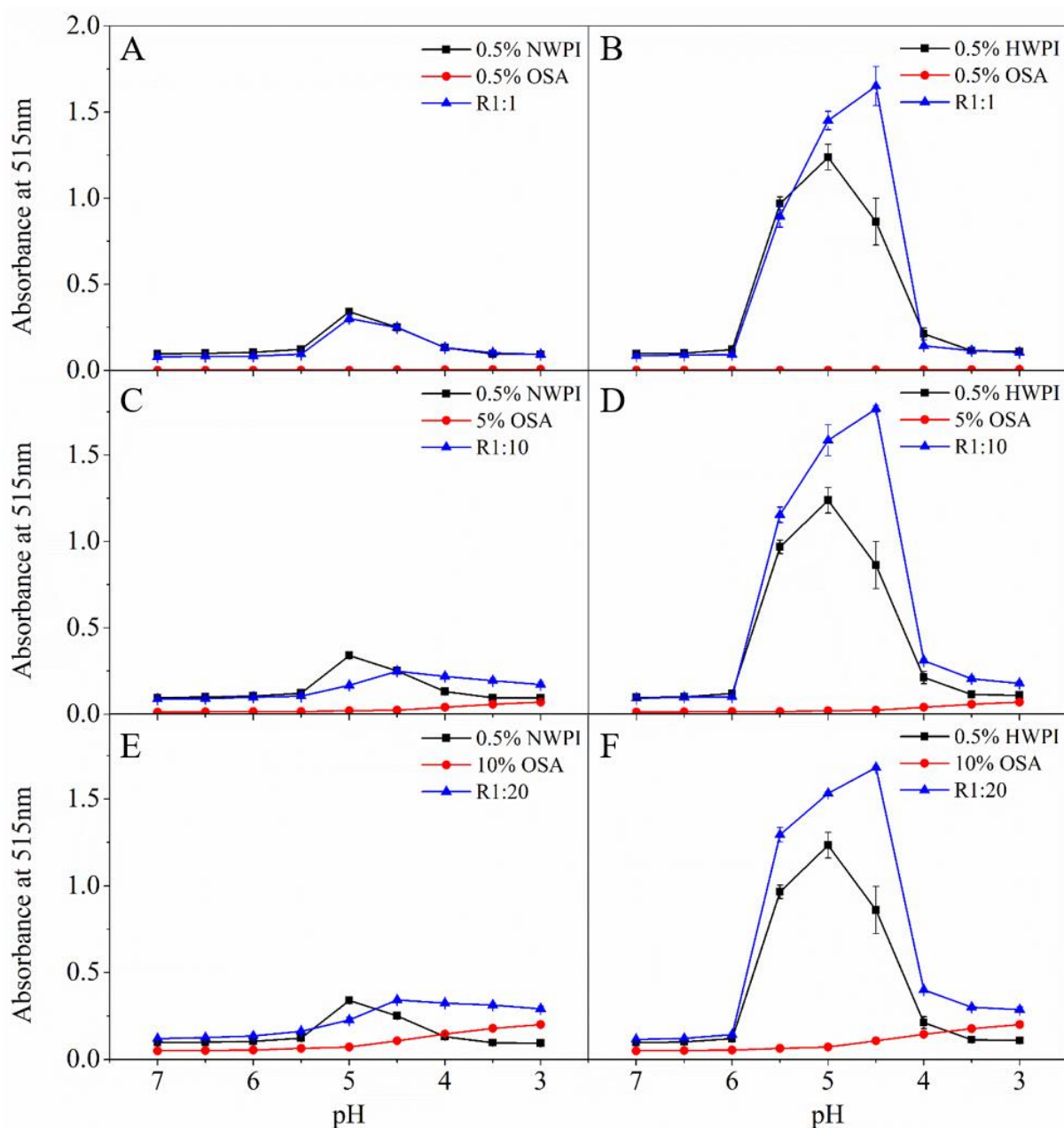


Figure 3. 1. Absorbance values of mixtures of 0.5% NWPI (A, C, E) or HWPI (B, D, F) and OSA-modified starch at protein to polysaccharide concentration ratios of 1:1, 1:10 and 1:20 as a function of pH. 0.5% NWPI or HWPI and corresponding concentration of OSA-modified starch solutions were measured as control.

The maximum absorbance value of either NWPI or HWPI was observed at pH 5. Since  $\beta$ -lactoglobulin is the major component of whey protein (~50% of whey protein), it dominates the self-assembly behaviour of whey protein (Puerta-Gomez & Castell-Perez, 2017). Similar pI value (~5) of  $\beta$ -lactoglobulin was reported in previous studies (Jones, Decker, & McClements, 2010; Jones et al., 2009; Santipanichwong et al., 2008), which indicated the extensive aggregation of protein due to the weakened electrostatic repulsion between the protein molecules at this pH value (Bryant & McClements, 2000; Jones et al., 2009). However, the absorbance value of HWPI at pH 5 was much larger than that of NWPI at this pH value, which could be attributed to the exposure of more hydrophobic groups of WPI molecules during heat treatment above their thermal denaturation temperature, thereby inducing stronger hydrophobic interactions at its pI (Zeeb et al., 2018). The increase in the absorbance of the NWPI solution at pH 5 may be because of the presence of a small amount of denatured whey protein in commercial WPI powder (Singh & Havea, 2003). The absorbance values of the pure OSA-modified starch solutions increased with increasing concentration over the whole pH range examined. The OSA-modified starch solutions at all concentration showed low absorbance values ( $< 0.2$ ) over the whole pH range examined. It can be seen that the absorbance values of OSA-modified starch solutions at concentration of 5% and 10% showed continuously increasing absorbance values when being acidified to pH values below 5, which may be due to the less negative charges carried by OSA-modified starch leading to the reduction of electrostatic repulsion. However, this trend was not observed in the 0.5% OSA-modified starch solution. The possible reason could be the concentration of the OSA-modified starch was too low so that it was difficult to observe the changes in absorbance values. The extent of initial increase in absorbance values of the OSA-modified starch solutions from pH 5 to 4.5 was proportional to the concentration of OSA-modified starch.



The mixtures of NWPI and OSA-modified starch at concentration ratios of 1:10 and 1:20 displayed similar absorbance values to the sum of the absorbance values of the NWPI solution and the corresponding concentration of OSA-modified starch solution over the pH range from 7 to 5.5. Nevertheless, the absorbance values of the mixture of NWPI and OSA-modified starch at these two concentration ratios at pH 5 were lower than that of NWPI solution. This phenomenon indicated the presence of OSA-modified starch reduced the aggregation of the NWPI near its isoelectric point, which could be attributed to the formation of complexes carrying more negative charges than NWPI alone (Jones et al., 2009; Weinbreck et al., 2003; Weinbreck, Tromp, & de Kruif, 2004). The slight increase in absorbance values at pH 5.5 ( $pH_c$ ) indicated the formation of primary soluble complexes between NWPI and OSA-modified starch. The absorbance values then increased abruptly from pH 5 ( $pH_{\Phi 1}$ ) because of the initial formation of insoluble complexes and reached to the maximum value at pH 4.5 ( $pH_{opt}$ ) by further titration (Figure 3.1C, E) (de Kruif & Tuinier, 2001; Schmitt et al., 1998; Weinbreck et al., 2003). However, the absorbance curve of NWPI and OSA-modified starch at ratio of 1:1 almost coincided with that of 0.5% NWPI alone (Figure 3.1A). It seems that the protein was in excess for complex formation in the mixture and the aggregation of proteins takes precedence over the protein-polysaccharide interactions when mixing NWPI and OSA-modified starch at this ratio over the whole pH range examined.

Different from the absorbance curves of the mixtures containing NWPI, all the mixtures of HWPI and OSA-modified starch at different concentration ratios displayed the same trend in absorbance curves over the pH range examined (Figure 3.1B, D, F). The absorbance values of the mixtures containing HWPI over the pH range from 5.5 to 4.5 were remarkably higher than those of the mixtures containing NWPI. An abrupt increase in absorbance values was observed from all the mixtures of HWPI and OSA-modified

starch at pH 5.5. The extent of increase was proportional to the concentration of OSA-modified starch in the mixture. The maximum absorbance values of all the mixtures containing HWPI were observed at pH 4.5, which was consistent with those of NWPI and OSA-modified starch mixtures at ratios of 1:10 and 1:20. Higher starch concentration in the mixtures of either NWPI or HWPI and OSA-modified starch led to higher absorbance values over the pH range from 4 to 3. Since the solubility of OSA-modified starch was relatively low at low pH values, the amount of insoluble particles increased with increasing starch concentration, thereby leading to higher absorbance values over this pH range.

Based on these results, it seems that the OSA-modified starch was more likely to interact with the unfolded whey protein molecules rather than the native whey protein molecules. The optimum condition for the complexation between HWPI and OSA-modified starch was at pH 4.5 and ratio of 1:10. Stronger hydrophobic interactions between these two macromolecules at the optimum condition were caused by the increased hydrophobicity of WPI molecules after heat treatment above their thermal denaturation temperature and the weakened electrostatic repulsion near its pI. The changes in the absorbance values of the mixtures of NWPI and OSA-modified starch at ratio of 1:10 and 1:20 could also be attributed to the small amount of denatured whey protein in commercial WPI powder (Singh & Havea, 2003), as discussed above for the pure NWPI solution. The absorbance value of the mixture at ratio of 1:20 was larger than that of 1:10 at pH 4.5, which was probably due to the increasing concentration of the OSA-modified starch inducing the exposure of more hydrophobic groups of  $\beta$ -lactoglobulin in WPI, which could continue unfold with the increasing OSA-modified starch concentration in the mixtures containing NWPI (Puerta-Gomez & Castell-Perez, 2017). In combination with the decrease in electrostatic repulsion forces between whey protein molecules near its pI ( $\sim 5$ ), these

conformational changes could lead to their stronger hydrophobic interactions with OSA-modified starch. Consequently, there was an increment of binding more OSA-modified starch and then an increase in absorbance values over the complexation pH range at ratio of 1:20. Another possibility could be the originally higher absorbance values of 10% OSA-modified starch solution than those of 5% OSA-modified starch solution over the whole pH range examined.

Less changes in absorbance values of the mixed systems of HWPI and OSA-modified starch with changes in the concentration ratios were observed suggested that the structural characteristic of WPI has great influence on protein-polysaccharide interactions in their mixture. Heat treatment of WPI above their thermal denaturation temperature could form soluble protein aggregates exposing more hydrophobic groups on their surface (Bryant & McClements, 2000; Fioramonti, Perez, Aríngoli, Rubiolo, & Santiago, 2014; Santipanichwong et al., 2008), which shaped in long filamentous structure and have higher Mw than individual whey protein molecules (Bryant & McClements, 2000; Chun et al., 2014; Kim et al., 2006). The increasing Mw of biopolymer could decrease the compatibility in protein-polysaccharide mixed systems (Schmitt et al., 1998), which may then promote the complex coacervation in the mixed systems. In addition, the unfolding and aggregation of heat-denatured whey protein molecules near its pI may affect the nature of protein-polysaccharide interactions and protein-protein interactions, which could also contribute to the remarkably different behaviours of mixtures containing NWPI and HWPI over the pH range from 5.5 to 4.5 (Bryant & McClements, 2000).

The results of the absorbance measurement of the 0.5% NWPI and HWPI solution were supported by the mean particle diameter measurements (Figure 3.2). The particle size of pure protein solution of 0.5% NWPI or HWPI remarkably increased when the pH value reduced below 5.5 or 6, which indicated that the NWPI molecules tend to form large aggregates from pH 5.5 and the HWPI molecules tend to form large aggregates from pH 6 during acid titration. This could be attributed to the weakened repulsive forces between whey protein molecules near their pI (~5) (Bryant & McClements, 2000; Jones et al., 2009). The maximum particle size of WPI was obtained at its pI, and the size of HWPI was remarkably larger than that of NWPI. Since the unfolded HWPI exposing more hydrophobic groups on the surface, the HWPI was more likely to aggregate than NWPI at pH near its pI and form larger aggregates with greater hydrophobic interactions between whey protein molecules (Salminen & Weiss, 2014).

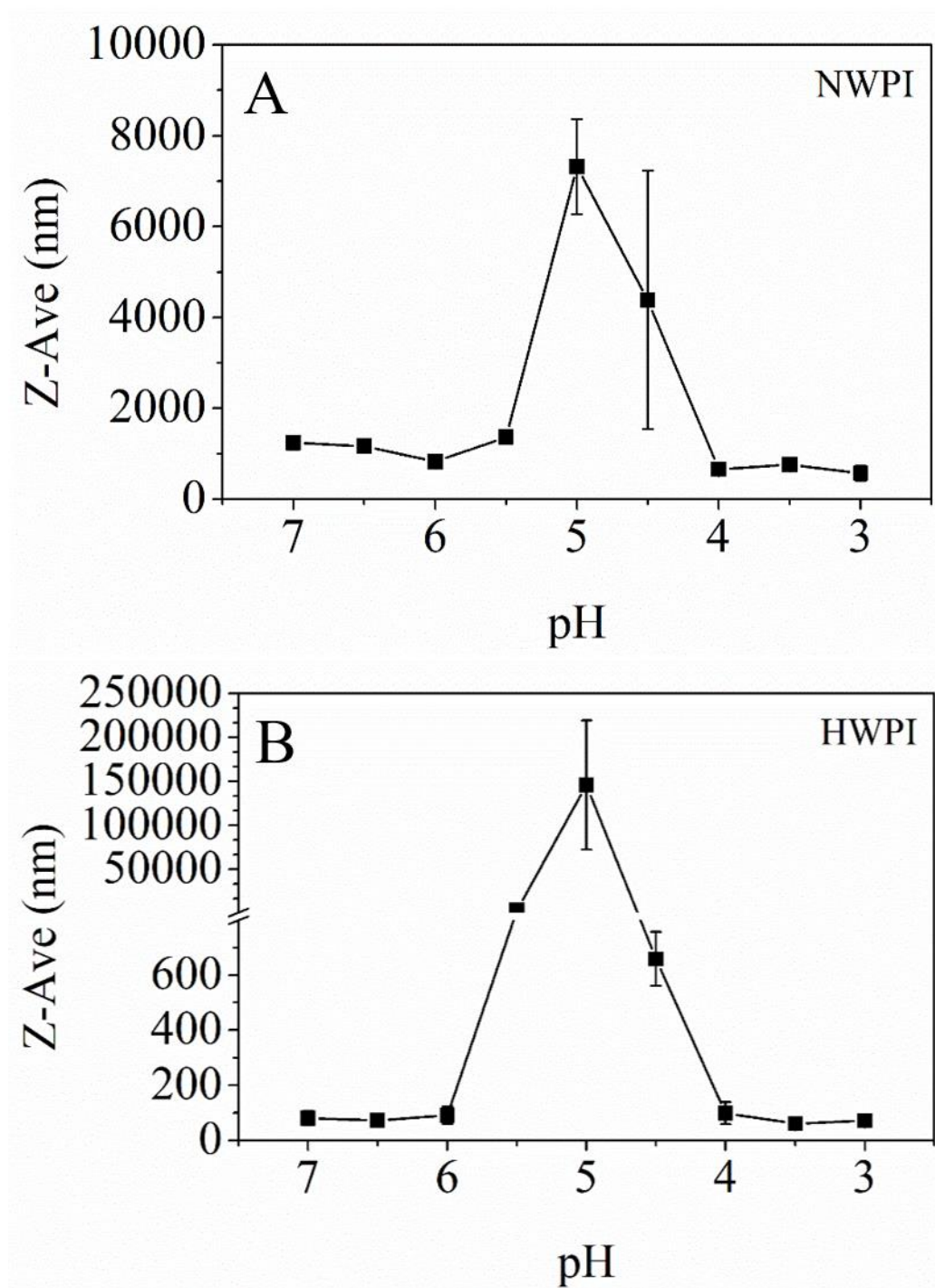


Figure 3. 2. Mean particle diameter of 0.5% NWPI (A) and HWPI (B) as a function of pH.

The mean particle size and volume distribution of mixtures of 0.5% NWPI or HWPI and OSA-modified starch at concentration ratio of 1:1, 1:10 and 1:20 over the pH range examined were shown in Figure 3.3 and 3.4. As can be seen in Figure 3.3, the trend in particle size of the mixtures containing NWPI at different concentration ratios was consistent with that in absorbance values over the whole pH range examined (Figure 3.1). The largest particle size of the mixture containing NWPI at ratio of 1:1 was observed at pH 5, whereas the size was much smaller than that of pure NWPI solution at this pH value. In combination with the result of its volume distribution, this phenomenon was probably due to the presence of OSA-modified starch in the mixture which could form nano-sized micelles in aqueous solution (Lin et al., 2018a). Another possibility could be the particle size of some large particles exceeded the instrument range. The pure NWPI solution formed large aggregates over the pH range from 5.5 to 4. However, the mixtures of NWPI and OSA-modified starch at ratio of 1:10 and 1:20 formed large aggregates over the pH range from 5 to 4, indicating the formation of complexes between NWPI and OSA-modified starch over this pH range. The volume distribution showed another peak except for the peak of starch micelles (~10 nm) from pH 5 at ratio of 1:10 also suggest the formation of complexes between NWPI and OSA-modified starch over this pH range. However, the volume distribution of the mixture at ratio of 1:20 only show peaks of starch micelles over this pH range, which could be attributed to a mass of starch in the mixture at this ratio. The largest particle size of the mixtures containing NWPI at these two ratios was observed at pH 4.5, which increased with the increasing OSA-modified starch concentration in the mixture. The possible reason could be the continuous unfolding of  $\beta$ -lactoglobulin in WPI when the OSA-modified polysaccharide to protein ratio was higher than 1:1 (Puerta-Gomez & Castell-Perez, 2017), which contributed to the formation of larger aggregates in the mixture containing NWPI at ratio of 1:20 than 1:10

because of binding more OSA-modified starch. Peaks around 10 nm presented the starch micelles could be detected at all pH values (Figure 3.4A, C, E), which indicated that the OSA-modified starch was in excess at all ratios, leading to the presence of free OSA-modified starch micelles. Although the results of absorbance and particle size measurements showed that the NWPI was in excess in the mixture at ratio of 1:1, the volume distribution showed the presence of free OSA-modified starch micelles at all pH values at this ratio. This confirmed the hypothesis above that the OSA-modified starch was more likely to interact with unfolded WPI rather than globular WPI molecules. There is a minority of denatured whey protein in commercial WPI powder (Singh & Havea, 2003), which may make the rest of native whey protein molecules be in excess in the mixture at this ratio.

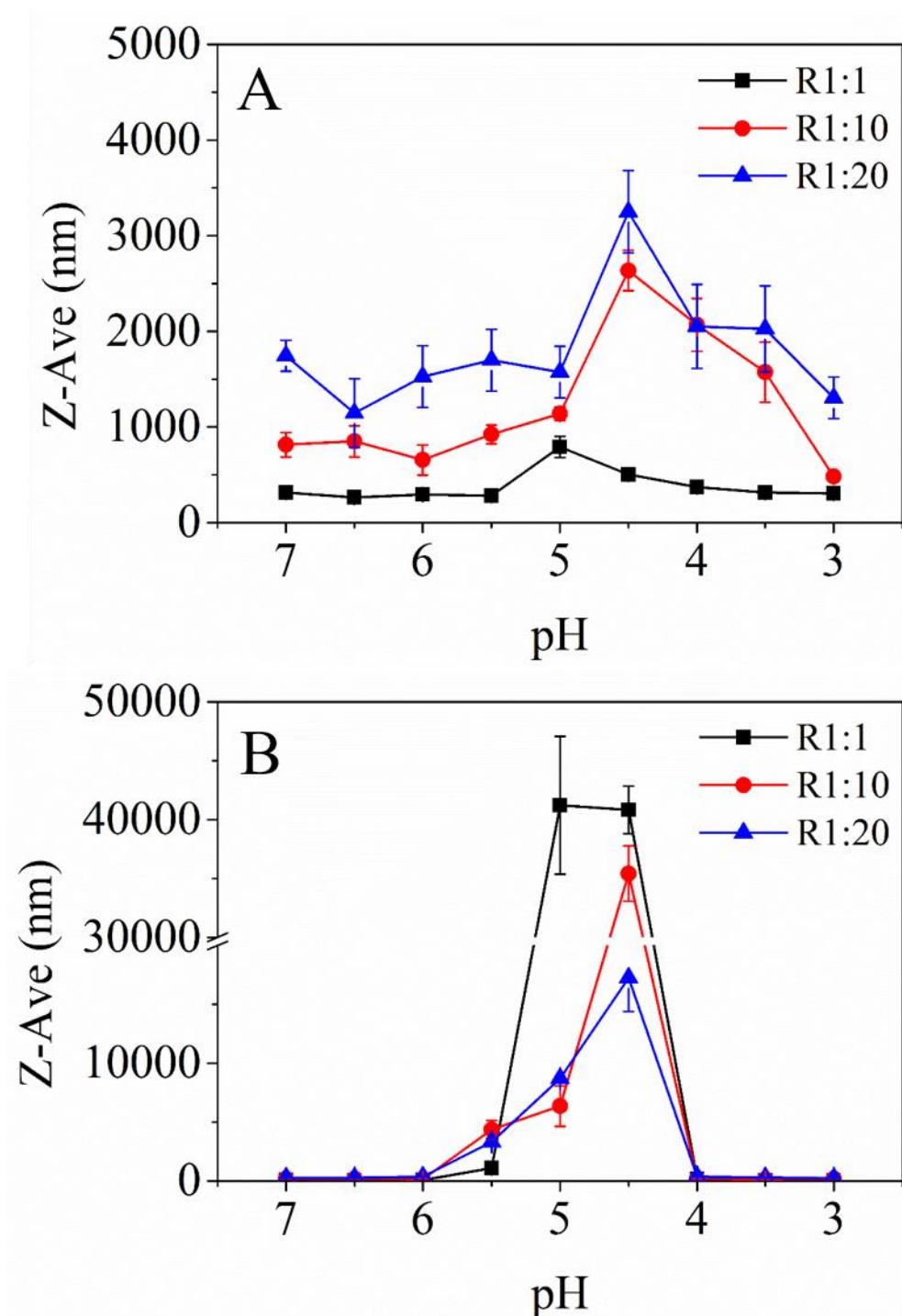


Figure 3. 3. Mean particle diameter of mixtures of 0.5% NWPI (A) or HWPI (B) and OSA-modified starch at protein to polysaccharide concentration ratios of 1:1, 1:10 and 1:20 as a function of pH.



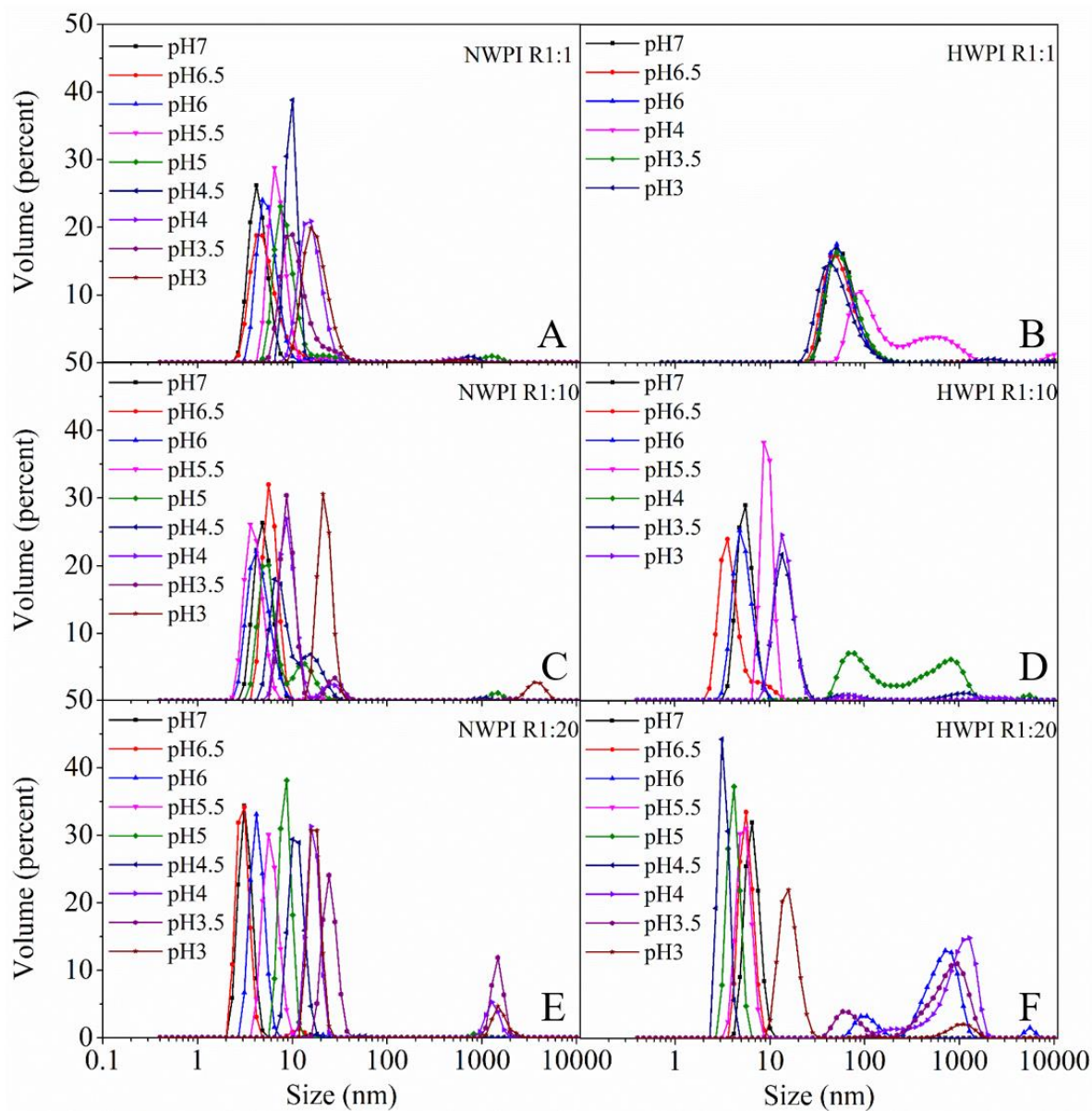


Figure 3. 4. Volume distribution of mixtures of 0.5% NWPI (A, C, E) or HWPI (B, D, F) and OSA-modified starch at protein to polysaccharide concentration ratios of 1:1, 1:10 and 1:20 over the pH range examined.

The formation of large aggregates in the mixture containing HWPI at ratio of 1:1 was observed at both pH 5 and 4.5, which was only observed at pH 4.5 at the other two ratios (Figure 3.3). This could be attributed to the formation of large protein aggregates at the pI (pH 5) of WPI. Therefore, it could be inferred that the HWPI in the mixture at ratio of 1:1 may be in excess during the complexation process. In addition, the volume distribution of the mixture displayed peaks around 100 nm instead of the peaks of starch micelles at the pH values where no phase separation had been observed (Figure 3.4B). These peaks may refer to the protein aggregates formed after heating, which should have a submicron-size of 100 to 300 nm (Santipanichwong et al., 2008). This proved the inference that the HWPI may be in excess in the mixture at this ratio. No volume distribution was obtained at pH 5.5, 5 and 4.5 (Figure 3.4B) because of the formation of large particles which exceeded the instrument range. However, the particle size of the mixture at pH 5.5 and 5 was markedly smaller than that of pure HWPI solution, probably due to the formation of complexes between HWPI and OSA-modified starch, which should be smaller than the protein aggregates. Based on the results of particle size measurement of pure HWPI solution, it could be inferred that the large particles obtained at pH 5.5 and 5 may be a mixture of whey protein aggregates and complexes between HWPI and OSA-modified starch, which needs further investigation. The proportion of the complexes in the mixture may increase by decreasing pH value. Further acidification to pH 4.5 led to the increase in the electrostatic repulsion between the whey protein molecules and then the increasing formation of insoluble complexes. At the ratios of 1:10 and 1:20, the largest particle size referred to the insoluble complexes between HWPI and OSA-modified starch was observed at pH 4.5, which was the optimum pH value for their complexation. The changes in the particle size of the mixtures at these two ratios were consistent with the results of absorbance measurements. Large particles that exceeded the

instrument range for volume distribution of the mixture at ratio of 1:10 (Figure 3.4D) were observed at pH 5 and 4.5, which was in line with the results of mean particle diameter at this ratio. The relatively smaller particle size of the mixture at ratio of 1:20 at pH 4.5 could be attributed to the existence of excess unreacted OSA-modified starch that presented as nano-sized micelles in the mixture, which could be supported by the volume distribution of the mixture at this ratio (Figure 3.4F).

The pH-dependent  $\zeta$ -potential values of the mixtures of 0.5% NWPI or HWPI and OSA-modified starch at different concentration ratios, and corresponding pure WPI or OSA-modified starch solutions were displayed in Figure 3.5. The  $\zeta$ -potential values of pure NWPI solution changed from negative ( $-31.05$  mV) to positive ( $+22.53$  mV) when the pH value decreased from 7 to 3 (Figure 3.5A, C, E), and those of HWPI showed the same trend from  $-39.13$  mV to  $+27.08$  mV over this pH range (Figure 3.5B, D, F). However, the HWPI carried more charges than NWPI at each pH values (Salminen & Weiss, 2014). Both NWPI and HWPI had no charges near pH 5, which referred to the pI of WPI. The measured pI of WPI was in line with the absorbance and particle size measurement results above and also in agreement with the previous studies ( $pI \approx 5$ ) (Jones & McClements, 2011; Salminen & Weiss, 2014). Similar results of  $\zeta$ -potential changes were obtained between non-heated and heated ( $85^\circ\text{C}$  for 15 min)  $\beta$ -lactoglobulin in a previous study (Schmitt et al., 2009), which could be attributed to the redistribution of the counterions on the surface of protein during heat treatment and the conformational changes in the structure of protein. The OSA-modified starch was negatively charged over the whole pH range examined, which could be attributed to the carboxylic group ( $-\text{COO}^-$ ) from OSA (Nilsson & Bergenst hl, 2007; Wu & McClements, 2015; Zhao et al., 2018). In theory, the charges carried by OSA-modified starch should increase by increasing concentration, whereas it decreased with increasing concentration from 0.5% to 10%. The possible

reason for this phenomenon could be the residual NaCl that generated during the preparation of OSA-modified starch, which had not been washed out completely. The starch solutions had relatively neutral charges from pH 4 to 3 at higher starch concentration (5% and 10%) because the dissociation of the carboxylic group was suppressed at low pH values (Wu & McClements, 2015). These relatively neutral charges could lead to the loss of electrostatic repulsion between OSA-modified starch micelles and consequently induce the formation of starch micelle aggregates, which may contribute to the relatively higher absorbance values of OSA-modified starch solution over this pH range.

For the mixed systems containing either NWPI or HWPI, the increasing of OSA-modified starch concentration in the mixture led to a decrease in the pH values of charge neutralization at which charge neutralisation occurred (Figure 3.5). In the mixtures of NWPI and OSA-modified starch, the pH value of charge neutralization changed from 4.5 to 3.5 as the OSA-modified starch concentration increased from 0.5% to 10% (Figure 3.5A, C, E). Similarly, it changed from pH 4.5 to 4 as the starch concentration increased from 0.5% to 10% in the mixtures containing HWPI (Figure 3.5B, D, F). The  $\zeta$ -potential values of the mixture of NWPI and OSA-modified starch at ratio of 1:1 seemed to be dominated by the NWPI molecules, which was similar to the results of absorbance and particle size measurements. These results confirmed that the NWPI should be in excess and present as free molecules, because it was assumed that OSA-modified starch tends to interact with unfolded WPI, of which is a minority in the commercial WPI powder. After the concentration of OSA-modified starch increased to 5% in the mixture, the  $\zeta$ -potential value of the mixture from pH 5.5 to 3 almost coincided with those of OSA-modified starch at corresponding concentration. This could be attributed to the excess OSA-modified starch presented in the mixture. Further increase in the concentration of OSA-

modified starch made it far excess in the mixture (1:20), which led to almost the same  $\zeta$ -potential values of the mixture as those of 10% OSA-modified starch at all pH values.

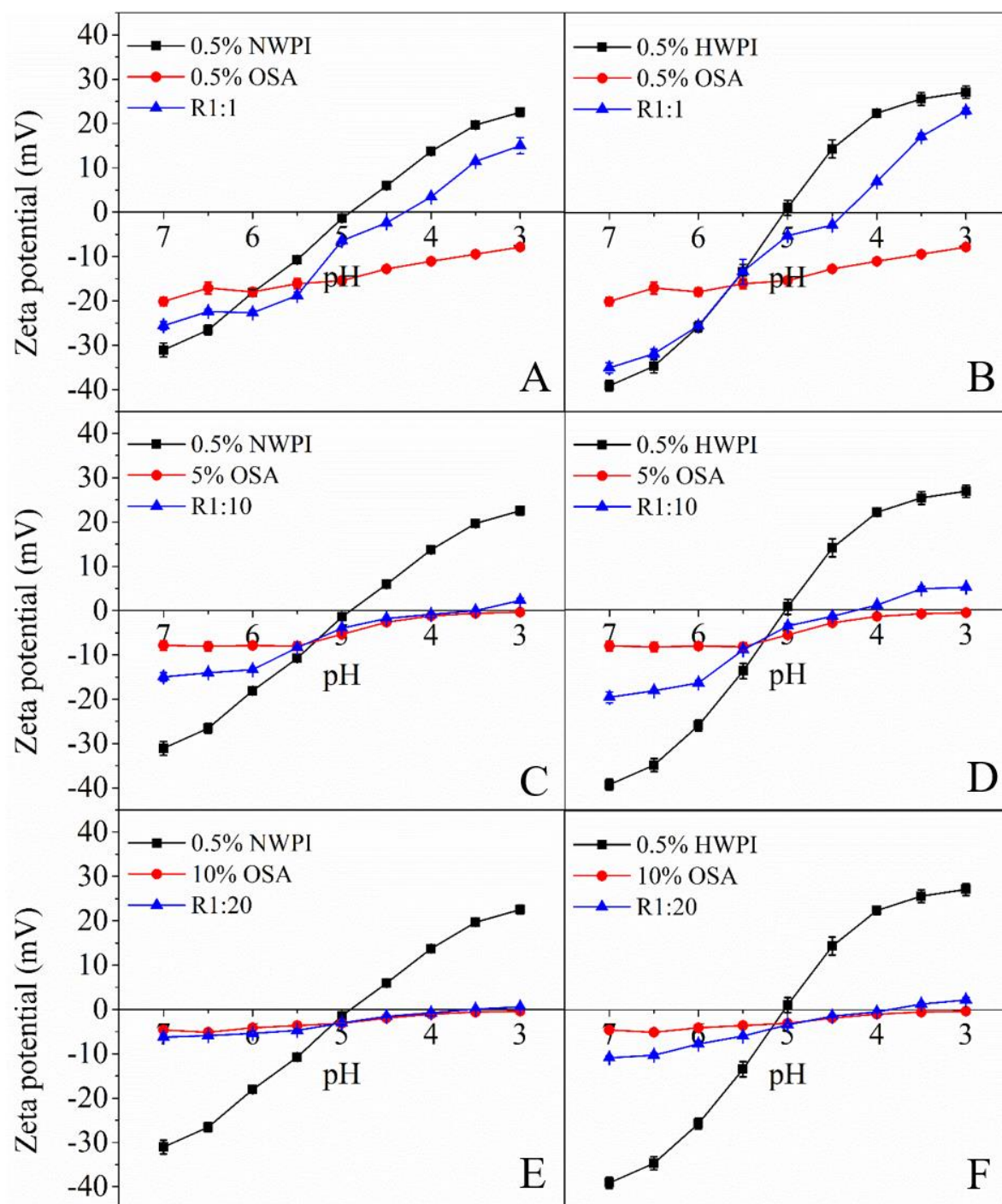


Figure 3. 5.  $\zeta$ -potential of mixtures of 0.5% NWPI (A, C, E) or HWPI (B, D, F) and OSA-modified starch at protein to polysaccharide concentration ratios of 1:1, 1:10 and 1:20 as a function of pH. 0.5% NWPI or HWPI and corresponding concentration of OSA-modified starch solutions were measured as control.

In the mixture of HWPI and OSA-modified starch at ratio of 1:1, the HWPI seemed to be excess for complexation with OSA-modified starch. The  $\zeta$ -potential values of the mixture at this ratio from pH 7 to 5.5 almost coincided with those of HWPI solution. Further acidification of the mixture led to the formation of extensive protein aggregates and complexes between HWPI and OSA-modified starch at the same time. The negative charges at pH 5 and 4.5 could be attributed to the OSA-modified starch that may be located on the surface of the complexes (Zeeb et al., 2018). At pH values those were lower than 4.5, the electrical characteristics seemed to be dominated by the excess HWPI in the mixture at this ratio again. These results confirmed the inference proposed above from absorbance and particle size measurements at this ratio. When the concentration of OSA-modified starch increased to 5%, the  $\zeta$ -potential value of the mixture at pH 4.5, where the largest absorbance value was obtained at this ratio, was close to zero but still negative ( $-1.12$  mV). The possible reason could be the OSA-modified starch may be located on the surface of the complexes (Zeeb et al., 2018). Similar to the mixture of NWPI and OSA-modified starch at ratio of 1:20, the electrical characteristics of the mixture of HWPI and OSA-modified starch at this ratio were also dominated by the OSA-modified starch, which may be far in excess in the mixture. However, since the HWPI carried more charges than NWPI over the whole pH range examined (Figure 3.5A, B), the  $\zeta$ -potential curve of HWPI and OSA-modified starch at ratio of 1:20 slightly deviated from that of OSA-modified starch at corresponding concentration compared to the mixture of NWPI and OSA-modified starch at this ratio.

Although the HWPI and OSA-modified starch carried opposite charges at the optimum condition for their complexation (Figure 3.5D), the negative charges carried by OSA-modified starch were much less than the positive charges carried by HWPI at the same pH. Theoretically, the soluble complexes could be generated in this case where



biopolymers carry opposite charges with different magnitude (Goh et al., 2014). However, the insoluble complexes were formed instead of the soluble complexes at this condition. Therefore, the complexation between HWPI and OSA-modified starch seemed to be induced by electrostatic interactions, but the structural properties of the complexes were dominated most likely by hydrophobic interactions rather than electrostatic interactions.

### 3.5.2. Effect of the characteristics of OSA-modified starch

Except for the characteristics of WPI, the characteristics of OSA-modified starch such as  $M_w$  may also affect the interactions between WPI and OSA-modified starch. The absorbance values of the mixtures of 0.5% HWPI and 5% OSA-modified starch with different  $M_w$  at pH 4.5 were shown in Figure 3.6A. These three OSA-modified starch had similar DS values (data not shown) with decreasing  $M_w$  of  $1243.0 \pm 10.0 \times 10^4$  g/mol,  $60.27 \pm 0.06 \times 10^4$  g/mol and  $19.24 \pm 0.07 \times 10^4$  g/mol, respectively. According to their acid hydrolysis time and the addition amount of OSA during esterification, they were named as H1-OSA-5%, H6-OSA-5% and H12-OSA-5%, respectively.

It was observed that OSA-modified starch with higher  $M_w$  led to higher absorbance values of the pure starch solution at pH 4.5. Significant differences ( $p < 0.05$ ) were observed in the absorbance values among these three starch solutions with decreasing  $M_w$ . This contributed to the significantly ( $p < 0.05$ ) higher absorbance value of the mixture containing OSA-modified starch with the highest  $M_w$  (H1-OSA-5%) than the mixtures containing OSA-modified starch with lower  $M_w$  (H6-OSA-5% and H12-OSA-5%). However, no significant difference ( $p > 0.05$ ) were observed in the absorbance values between the mixtures containing H6-OSA-5% and H12-OSA-5%, though significant difference was observed ( $p < 0.05$ ) in the absorbance values of H6-OSA-5% and H12-OSA-5%. Interestingly, the phase separation behaviours of these three mixtures

after 7 days were quite different (Figure 3.6B). There was no obvious phase separation observed for the mixture containing H1-OSA-5%. The yield of precipitation, which was determined by its proportion of phase, seemed to decrease with the decreasing Mw of OSA-modified starch. This phenomenon could be attributed to the fact that the higher viscosity of OSA-modified starch with higher Mw, which led to the higher viscosity of the mixture, thereby restricting the movement of any particles present (Jones et al., 2009). It suggested that HWPI could form denser (higher precipitation proportion of phase) insoluble complexes with OSA-modified starch with lower Mw. Another possibility should be the long chain starch molecules become smaller after the acid hydrolysis process, which makes the OSA groups on the OSA-modified starch with lower Mw more dispersed in its mixture with HWPI (Hong, Li, Gu, Wang, & Pang, 2017). Thereby the opportunities of interacting with HWPI greatly increased, and then resulting in the denser coacervates. Sun et al. (2016) found the OSA-modified starch could adsorb with casein and have effects on the steric stabilization, which could increase the tightness of the complex structure.



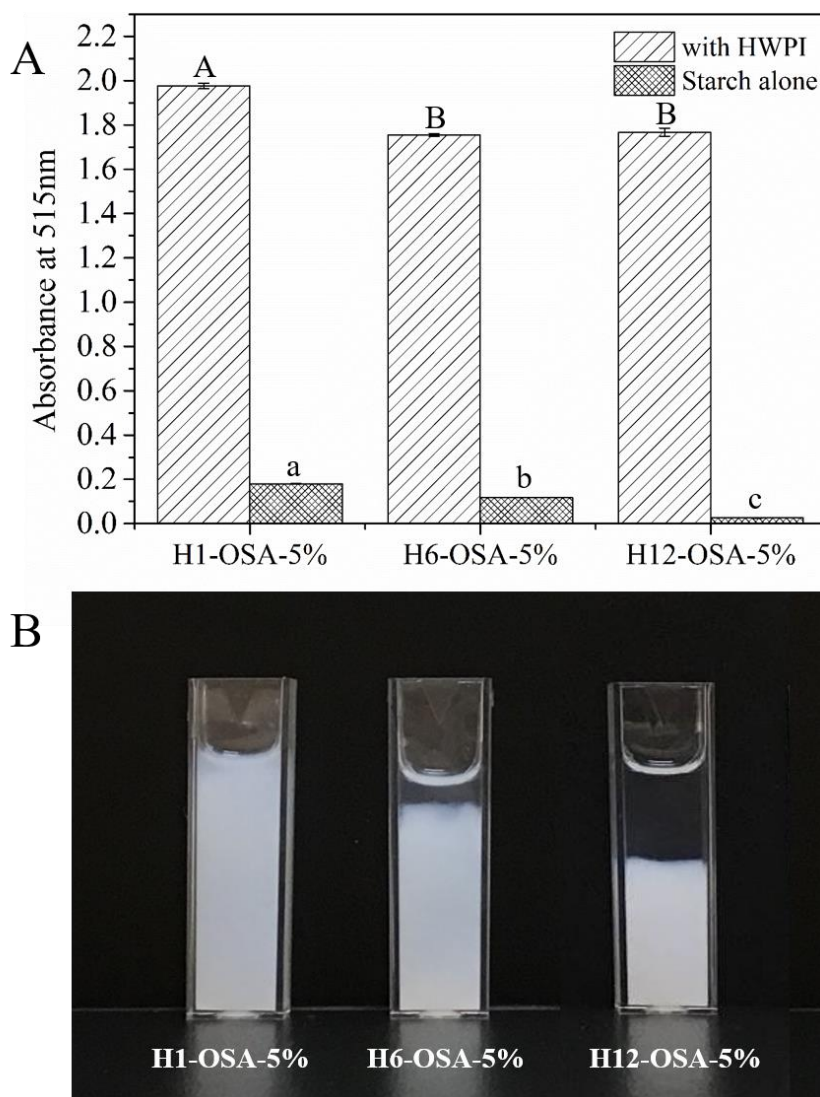


Figure 3. 6. Absorbance values (A) and phase separation (B) of mixtures of 0.5% HWPI and 5% OSA-modified starch with different Mw at pH 4.5. 5% OSA-modified starch with different Mw were measured as control. Note: the phase separation of samples was observed after 7 days. Different capital and lowercase letters indicate significant differences ( $p < 0.05$ ) in the absorbance values of the mixtures and the starch solution, respectively.

Another important characteristic of OSA-modified starch is the DS value, which has been proved to have influence on the amount of molecules interacting with the proteins

(Gomez-Estaca et al., 2016; Puerta-Gomez & Castell-Perez, 2017). The absorbance values of the mixtures of 0.5% HWPI and 5% OSA-modified starch with different DS values at pH 4.5 were shown in Figure 3.7A. These three OSA-modified starch had similar Mw (data not shown) with increasing DS values of  $1.12 \pm 0.09\%$ ,  $2.54 \pm 0.04\%$ ,  $3.66 \pm 0.01\%$  and  $4.29 \pm 0.11\%$ , respectively. According to their acid hydrolysis time and the addition amount of OSA during esterification, the other three were named as H12-OSA-3%, H12-OSA-5%, H12-OSA-7% and H12-OSA-9%, respectively.

It could be observed that the OSA-modified starch with higher DS value led to lower absorbance values of the pure starch solution at pH 4.5. Significant differences ( $p < 0.05$ ) were observed in the absorbance values among these four starch solutions with increasing DS values. Similarly, the absorbance values of the mixtures containing H12-OSA-3%, H12-OSA-5%, H12-OSA-7% or H12-OSA-9% decreased significantly ( $p < 0.05$ ) with increasing DS values of the OSA-modified starch. The phase separation behaviour of these four mixtures after 7 days was quite different. The precipitation yield of the mixture containing H12-OSA-3% was more than that of the mixture containing H12-OSA-5%, probably due to the insufficient OSA groups on H12-OSA-3% molecules, which cannot prevent the hydrophobic interactions of small protein aggregates and lead to a loose complex structure. The phase separation was observed in the mixture containing H12-OSA-3%, H12-OSA-5%, whereas no phase separation was observed in the mixtures containing H12-OSA-7% or H12-OSA-9%. This phenomenon could be attributed to the increasing OSA group on OSA-modified starch with increasing DS value, which may lead to stronger hydrophobic interactions with HWPI and stronger steric stabilization effects of OSA-modified starch molecules after adsorption to the HWPI. Therefore, the OSA-modified starch with higher DS values, such as H12-OSA-7% or H12-OSA-9% in

this study, could effectively prevent the aggregation of HWPI molecules at pH 4.5, which showed its great potential for applications in food development.

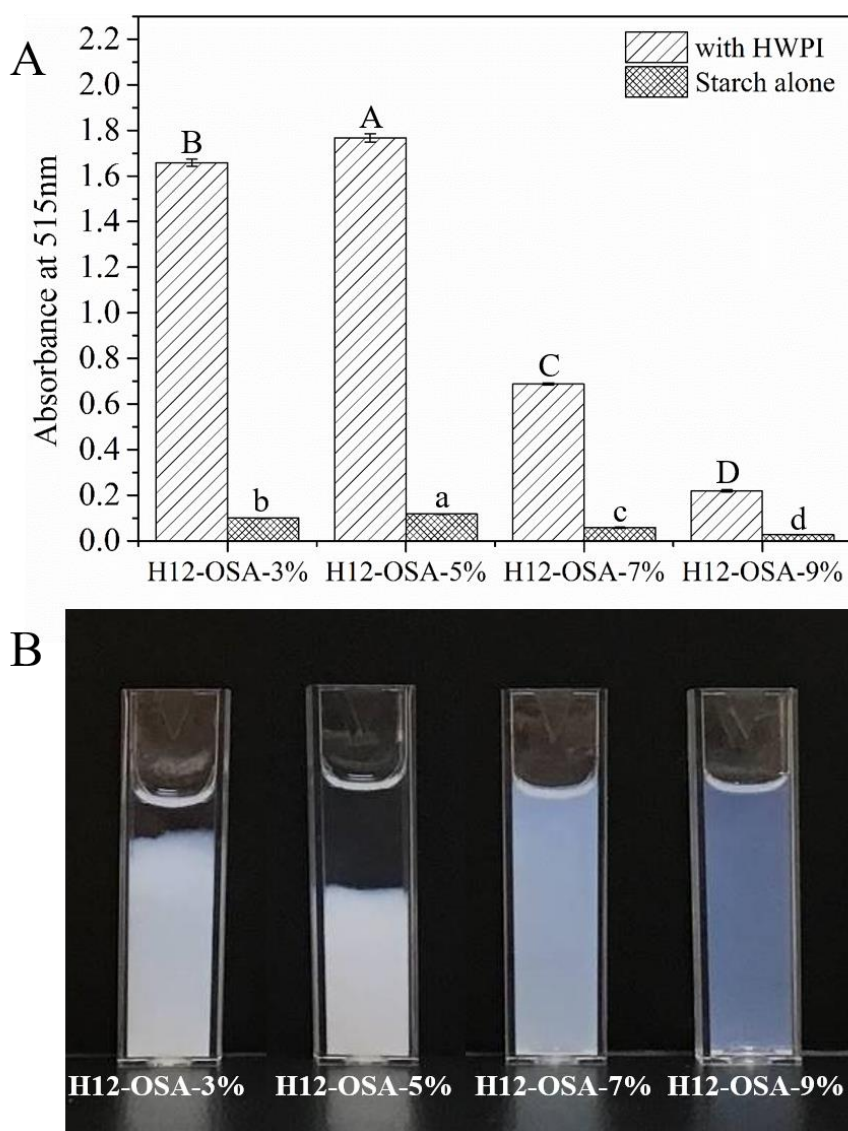


Figure 3. 7. Absorbance values (A) and phase separation (B) of mixtures of 0.5% HWPI and 5% OSA-modified starch with different DS values at pH 4.5. 5% OSA-modified starch with different DS values were measured as control. Note: the phase separation of samples was observed after 7 days. Different capital and lowercase letters indicate significant differences ( $p < 0.05$ ) in the absorbance values of the mixtures and the starch solution, respectively.

### **3.5.3. Proposed mechanism of the interactions between HWPI and OSA-modified starch**

The conformations of the OSA-modified starch and HWPI in solutions with decreasing from pH 7 to 4.5 were displayed in Figure 3.8A and 3.8B. The OSA-modified starch presented as nano-sized micelles in aqueous solution because of the hydrophobic bonding of OSA groups (Zhu, Li, Chen, & Li, 2013), and the HWPI molecules presented as filaments after heat treatment because of the partially unfolded globular protein and the exposure of the non-polar groups inducing the cross-linking between the protein molecules by hydrophobic interactions (Bryant & McClements, 2000). Based on the results of particle size and  $\zeta$ -potential measurements, the OSA-modified starch micelles seemed to form small aggregates due to the weakened electrostatic repulsion during acidification. For pure HWPI solution, it can be seen that small aggregates may be formed prior to the extensive aggregation of HWPI molecules near pH 5.

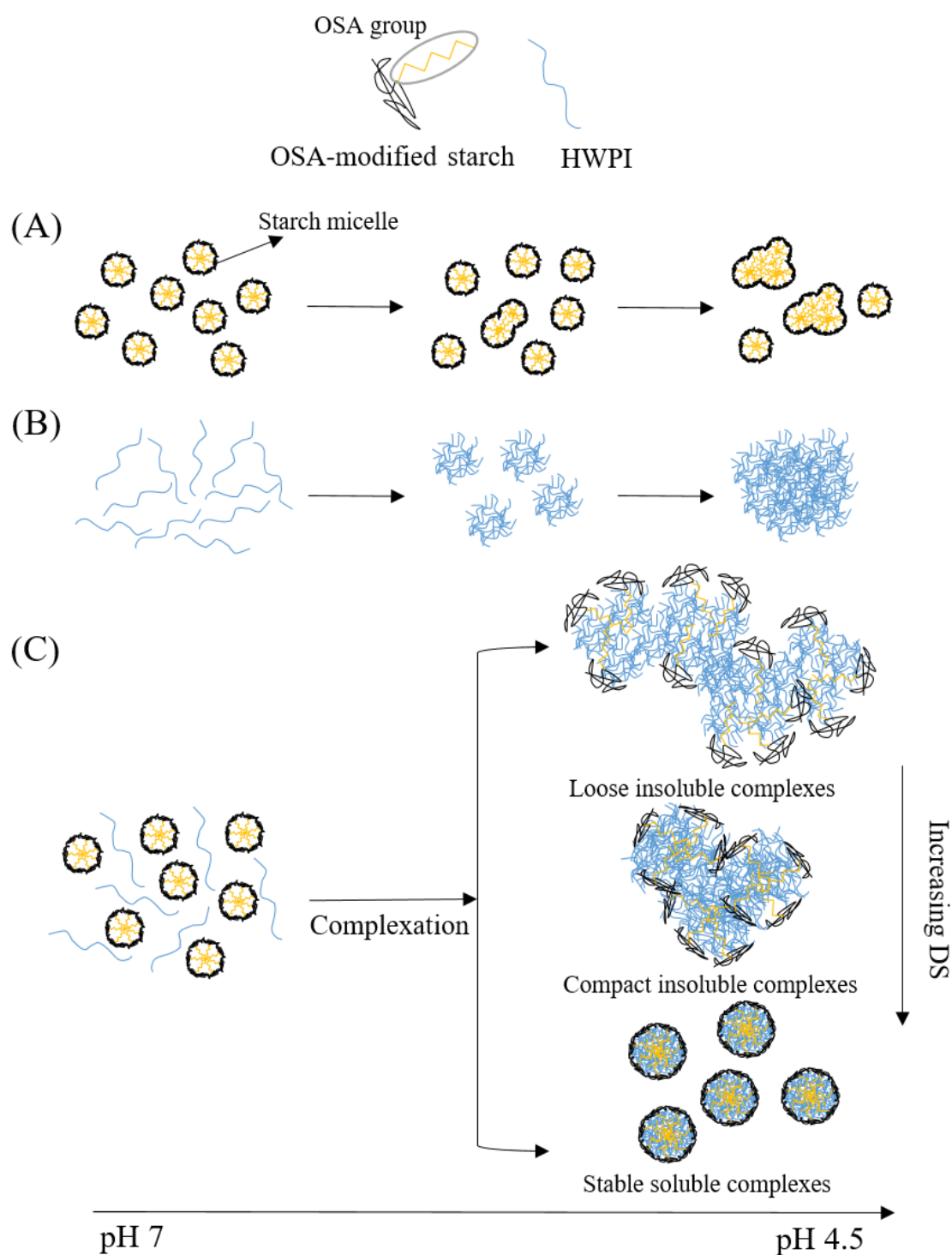


Figure 3. 8. Conformations of OSA-modified starch (A) and HWPI (B) in solutions with decreasing pH values from 7 to 4.5. (C) Schematic representation of mixtures of HWPI and OSA-modified starch at pH 7 and possible conformations of their complexes at pH 4.5. Note: sizes are not proportional to the physical size of the molecules.

We proposed that the possible conformation of the complexes between HWPI and OSA-modified starch may be based on the small self-aggregation of heat-denatured whey protein molecules that act as nuclei (Ye et al., 2006). The schematic representation of the mixtures of HWPI and OSA-modified starch at pH 7 and the conformations of the complexes composed of HWPI and OSA-modified starch with different DS values were shown in Figure 3.8C. Based on the results of  $\zeta$ -potential measurement, the HWPI molecules and OSA-modified starch micelles carrying enough negative charges were compatible due to the electrostatic repulsion at high pH values (7-6). When the pH values decreased below pH 6, the HWPI molecules tend to form small aggregates before the extensive aggregation at pH values close to their pI (pH 5). The OSA-modified starch micelles may attach to the small aggregates because of the electrostatic interactions between the negatively charged OSA-modified starch micelles and the positively charged patches on the surface of these small aggregates. Since the increased hydrophobic properties of the whey protein molecules after heat treatment (Zeeb et al., 2018), the exposed hydrophobic groups on the surface of the whey protein aggregates may promote the unfolding of attached OSA-modified starch micelles to expose the OSA groups from the core of the micelle. In this case, the hydrophobic interactions between the protein aggregates and the OSA groups of OSA-modified starch become stronger. As the  $\zeta$ -potential values of the soluble complexes between HWPI and OSA-modified starch with higher DS value are quite low, for example,  $-2.61$  mV and  $-2.87$  mV for the HWPI-H12-OSA-7% and HWPI-H12-OSA-9% soluble complexes at pH 4.5 (data not shown), respectively, which was not enough to make the complexes stable through electrostatic repulsion. Therefore, the steric hindrance should be the main stabilizing mechanism in this scenario. It could be inferred that the stronger hydrophobic interactions due to the increasing OSA groups of OSA-modified starch with increasing DS value lead to the

presence of enough hydrophilic portion of OSA-modified starch outside the small protein aggregates, which could sterically stabilize the protein aggregate cores and consequently prevent further aggregation. According to the particle size measurement results, the mean particle diameter of HWPI-H12-OSA-7% and HWPI-H12-OSA-9% soluble complexes was  $308.7 \pm 4.21$  nm and  $161.4 \pm 0.6$  nm, respectively (data not shown). It seemed that OSA-modified starch with higher DS value attaches to the HWPI aggregates in an earlier stage of the small-scale aggregation of HWPI molecules than those with lower DS value. This could determine the initial size of the protein aggregate core of the complexes, hence higher DS value of OSA-modified starch in the mixture with HWPI led to smaller soluble complexes at pH 4.5.

### **3.6. Conclusion**

This study investigated the complexation process between NWPI or HWPI and OSA-modified starch under different conditions. It was found that the OSA-modified starch was more likely to interact with the unfolded WPI rather than the native WPI, which could be attributed to the increased hydrophobic properties of WPI after heat treatment above its thermal denaturation temperature. The interactions between HWPI and OSA-modified starch seem to be highly dependent on pH, as no interaction could be observed at high pH (7-6). Besides, the protein to polysaccharide ratio seems to have great influence on the formation of insoluble complexes. The optimum condition for complexation between HWPI and OSA-modified starch was at protein to polysaccharide ratio of 1:10 (w/v) and pH 4.5. The structure of the complexes formed under the optimum condition could be affected by different molecular characteristics of OSA-modified starch including Mw and DS value. The short chain of OSA-modified starch with lower Mw made the OSA groups more dispersed in the mixture, which could lead to a denser coacervates phase because of



the increased opportunities for interacting with HWPI. It is worth mentioning that the OSA-modified starch with high DS values could form stable soluble complexes with HWPI under the optimum condition. In addition, the particle size of the soluble complexes could be tailored by the changes in the DS value of OSA-modified starch. Higher DS value of OSA-modified starch could lead to smaller particle size of the soluble complexes.

The complexation between HWPI and OSA-modified starch seemed to be firstly induced by electrostatic interactions. However, the structural properties of the complexes were most likely dominated by hydrophobic interactions rather than electrostatic interactions at pH 4.5. We proposed a possible mechanism of the complexation process that the OSA-modified starch attached to the surface of the HWPI aggregates via electrostatic attraction with the positively charged patches exposed on the surface, and then strong hydrophobic interactions occurred between the OSA groups of OSA-modified starch and hydrophobic groups on the surface of protein aggregates during further acidification. The presence of an increased amount of OSA groups of OSA-modified starch with higher DS value may provide increased steric stabilization for the complexes, which may explain the formation of stable soluble complexes at this pH value. The soluble complexes between HWPI and OSA-modified starch generated in this study may be beneficial for use as delivery systems for lipophilic bioactive components.





## Chapter 4 Encapsulation of $\beta$ -carotene in soluble complexes between HWPI and OSA-modified starch

### 4.1. Abstract

There are growing interests in the encapsulation of lipophilic bioactive compounds by soluble complexes between proteins and polysaccharides.  $\beta$ -Carotene is the most significant carotenoid with a variety of health benefits. However, its poor water solubility and chemical instability have limited its utilization in food industry. In this study, the soluble complexes formed between 0.5% (w/v) HWPI and 5% (w/v) OSA-modified starch (HWPI-OSA SC) at pH 4.5 were applied to encapsulate  $\beta$ -carotene. The apparent aqueous solubility of  $\beta$ -carotene was enormously improved ( $264.05 \pm 72.53 \mu\text{g/g}$ ) after encapsulation in the soluble complexes. Transmission electron microscopy (TEM) and scanning electron microscope (SEM) were used to evaluate the structure of the soluble complexes before and after encapsulation of  $\beta$ -carotene. There were no significant differences observed between the soluble complexes before and after encapsulation of  $\beta$ -carotene whether in a liquid or a powdered form. The results of Fourier transform infrared spectroscopy (FT-IR) suggested that the  $\beta$ -carotene was encapsulated into the soluble complexes via hydrophobic interactions. Therefore, we postulated that the  $\beta$ -carotene could bind to the protein aggregate cores and the OSA groups attached to the cores of the soluble complexes by hydrophobic forces. The results of X-ray diffraction (XRD) and differential scanning calorimetry (DSC) indicated that the  $\beta$ -carotene was in an amorphous form loaded inside the soluble complexes. In addition, the  $\beta$ -carotene-loaded freeze-dried soluble complexes showed good redispersion behaviour and a relatively high retention rate of  $\beta$ -carotene (89.75%), which indicated that the  $\beta$ -carotene-loaded soluble

complexes could be successfully converted into a powdered form. The accelerated stability study showed that the soluble complexes between HWPI and OSA-modified starch could effectively improve the chemical stability of  $\beta$ -carotene for long-term storage under low pH conditions. This study may be beneficial for the potential use of delivering lipophilic bioactive compounds by the soluble complexes between HWPI and OSA-modified starch in commercial applications.

## **4.2. Introduction**

Lipophilic bioactive compounds such as polyunsaturated fatty acids, carotenoids, hydrophobic vitamins and nutraceuticals have an increasing attraction in food industry in recent years due to their health benefits to human. However, the instability to environmental conditions of them has limited their use in food industry (Wang et al., 2018). Encapsulation of bioactive compounds can enhance the shelf life of food products and protect them against changes in external conditions such as temperature, moisture, light, etc. Moreover, it can also help to control the release of bioactive compounds to specific gastrointestinal targets (Schmitt & Turgeon, 2011).

There are growing interests in the encapsulation of bioactive compounds by the complexes between proteins and polysaccharides including complex coacervates and soluble complexes (de Kruif et al., 2004; Devi et al., 2017; Evans et al., 2013; Hosseini et al., 2015; Ilyasoglu & El, 2014; Mirpoor et al., 2017). Encapsulation of bioactive compounds by complex coacervation is generally used in emulsion-based delivery system rather than use them directly to encapsulate bioactives except for hydrophilic bioactive compounds such as thiamine (Bédié et al., 2008) and probiotics (Bosnea et al., 2014; Eratte et al., 2017; Eratte et al., 2015; Hernández-Rodríguez et al., 2014). Puerta-Gomez

& Castell-Perez (2017) used the electrostatic precipitates of WPI in combination with OSA-modified polysaccharides to encapsulate a lipophilic bioactive compound, TCNN. The primary O/W emulsion of TCNN was prepared by the mixture of WPI and OSA-modified polysaccharides before inducing the electrostatic precipitation of the mixed system. The maximum entrapment of TCNN was found at the WPI to OSA-modified polysaccharide ratio of 1:10. Some researchers have used the binding capacity of  $\beta$ -lactoglobulin for lipophilic bioactive compounds to encapsulate them in protein-polysaccharide soluble complexes (Hosseini et al., 2015; Mirpoor et al., 2017; Ron et al., 2010). After the formation of the complexes between  $\beta$ -lactoglobulin and the lipophilic bioactive compounds, the polysaccharide solution will be added and adjust pH to induce the formation of the ternary complex between  $\beta$ -lactoglobulin-bioactive compounds complex and the polysaccharide by attractive electrostatic interactions. However, there is no data about encapsulating lipophilic bioactive compounds directly into the already formed soluble complexes between proteins and polysaccharides, which needs further investigation.

$\beta$ -Carotene is the most significant carotenoid over more than 600 different carotenoids, which is one of the major carotenoids present in the diet and responsible for the colour in yellow, orange and red vegetables and fruits (Boon et al., 2010; Jain et al., 2016). As a good source of provitamin A, it has benefits for eye health, and its antioxidant properties help human body withstand free radical damage (Wang et al., 2018). However, its poor water solubility and chemical instability have limited its utilization in food industry (Jain et al., 2015). Jain et al. (2015, 2016) used WPI-Gum Acacia and casein-gum tragacanth complex coacervates to encapsulate  $\beta$ -carotene. Relatively high encapsulation efficiency of  $\beta$ -carotene (77.3% and 77.36, respectively) was obtained in these studies, and the encapsulation of  $\beta$ -carotene into the complex coacervates improved the stability of  $\beta$ -

carotene during storage. Results of another study also showed that  $\beta$ -carotene could be effectively encapsulated by the casein-Guar Gum coacervates (65.95%), which greatly enhanced the photo-stability of  $\beta$ -carotene during storage (Thakur et al., 2017). There are also some reports on encapsulation of other carotenoids such as astaxanthin by complex coacervation, e.g. gelatin-cashew gum complex coacervates (Gomez-Estaca et al., 2016) and gelatin-OSA-modified kudzu starch complex coacervates (Zhao et al., 2018). However, limited reports have been published on the encapsulation of  $\beta$ -carotene into the protein-polysaccharide soluble complexes, especially using the already formed soluble complexes to encapsulate  $\beta$ -carotene directly.

The aim of this study was to explore the feasibility of directly encapsulating lipophilic bioactive compounds into the already formed soluble complexes between HWPI and OSA-modified starch. As a common subject matter in research works due to its a variety of health benefits,  $\beta$ -carotene was chosen as a model of lipophilic bioactive compounds in this study. The concentration of the  $\beta$ -carotene bound with the soluble complexes was determined. The chemical stability of the  $\beta$ -carotene-loaded soluble complexes during storage was also investigated. The results may be beneficial for the potential application of soluble complexes between HWPI and OSA-modified starch in food industry.

### **4.3. Materials**

Whey protein isolate powder (WPI 895) was purchased from Fonterra Co-operative Group Ltd. (Palmerston North, New Zealand). OSA-modified starch, H12-OSA-9%, was made in own lab. All the other chemicals used were of analytical grade and obtained from either Merck Millipore Co. (Darmstadt, Germany) or Sigma Chemical Co. (St. Louis,

MO) unless otherwise specified. Milli-Q water (Millipore Corp., Bedford, MA, USA) was used in all experiments.

#### **4.4. Methods**

##### **4.4.1. Preparation of soluble complexes between HWPI and OSA-modified starch (HWPI-OSA SC)**

The WPI stock solution (5%, w/v) was prepared by dispersing WPI powder in Milli-Q water and stirring gently for 5 h at room temperature to enable complete hydration. Sodium azide (0.02%, w/w) was added to the solution to inhibit the growth of microorganisms. The HWPI stock solution was obtained by heating the WPI stock solution in a water bath of 90 °C for 20 min to enable the complete denaturation of WPI. It was then stored at 4 °C prior to further usage. The OSA-modified starch stock solution (20%, w/v) was prepared by dispersing OSA-modified starch powder in Milli-Q water and then gelatinized in a water bath of 95 °C for 20 min to obtain a homogeneous solution. Since the OSA-modified starch was prepared in the lab that may contain some impurities, the gelatinized OSA-modified starch solution was centrifuged (Multifuge 3SR Plus; Thermo Scientific Inc., USA) at 4000 rpm for 2 min to remove the impurities. Considering that starch is susceptible to retrogradation, fresh starch solution was prepared every time before experiment. Sodium azide (0.02%, w/w) was added to the starch solution after preparation.

Mixtures of HWPI and OSA-modified starch at protein to polysaccharide concentration ratio of 1:10 were prepared by diluting the stock solutions in Milli-Q water. The pH of

the biopolymer mixtures was adjusted to 4.5 by the addition of 0.1-1 M HCl. The samples were stored at room temperature after measurement.

#### **4.4.2. Encapsulation of $\beta$ -carotene**

The soluble complexes between HWPI and OSA-modified starch at ratio of 1:10 and pH 4.5 were used to encapsulate  $\beta$ -carotene. The mixture of HWPI and OSA-modified starch at pH 7, HWPI solution at pH 7, the OSA-modified starch solution at pH 7 and 4.5 were also used to encapsulate  $\beta$ -carotene as control. Briefly, 5 mg  $\beta$ -carotene powder was firstly suspended in 5 mL of each sample using a high-speed homogenizer (D-130, LabServ, New Zealand) for 1 min. It was then stirred at 1500 rpm for 24 h by a magnetic stirrer (C-MAG MS 4, IKA, Germany). Afterwards, the suspension was filtrated using 1.2  $\mu$ m syringe filters to remove the excess  $\beta$ -carotene crystals. Finally, a portion of each sample was taken out for TEM and another portion of each sample was freeze-dried for SEM, FT-IR, XRD and DSC measurements. The rest of each sample was stored under light with high intensity at room temperature for 10 days to evaluate the stability of the  $\beta$ -carotene-loaded samples.

#### **4.4.3. Determination of $\beta$ -carotene**

The  $\beta$ -carotene in each sample was extracted following the method of Lin, Liang, Zhong, Ye, & Singh (2018c) with some modifications. 50  $\mu$ L of the each filtrated sample after encapsulation was added with 5 mL dimethyl sulfoxide and vortexed for 30 s. Afterwards, 4 mL of solvent (n-hexane/dichloromethane, 4:1, v/v) was added immediately and then vortexed for 30 s before centrifugation (Multifuge 3SR Plus; Thermo Scientific Inc., USA) at 4000 rpm for 5 min. The upper yellow-coloured layer was measured for the absorbance

by spectrophotometer at a wavelength of 450 nm (Genesys 10-S; Thermo Fisher Scientific Inc., USA). The concentration of  $\beta$ -carotene extracted from each sample was determined from a calibration curve of absorbance versus  $\beta$ -carotene concentration in n-hexane/dichloromethane (4:1, v/v).

#### **4.4.4. Particle size measurement**

The particle size of the mixtures was determined by zetasizer (Nano-ZS, Malvern Instruments Ltd, Malvern, Worcestershire, UK), which is a combined dynamic light scattering and electrophoresis motilities instrument. All the samples were measured without dilution.

#### **4.4.5. Transmission electron microscopy**

Negative staining transmission electron microscopy was used to observe the microstructure of the samples. One drop of the sample ( $\sim 80 \mu\text{L}$ ) was placed on the Parafilm in a glass petri dish and then a formvar/carbon coated 200 mesh copper grid (Agar Scientific, coated in the lab) was placed on the sample droplet for 4 min. The excess sample on the copper grid was drained off by a Whatman No1 filter paper. Subsequently, it was then placed on a drop of 2% Phosphotungstic Acid in MilliQ water for another 4 min before being drained off again by a Whatman No1 filter paper. The grid was then imaged in a TEM (FEI Tecnai G2 Spirit BioTWIN, Czech Republic) at 100kV.

#### **4.4.6. Scanning electron microscope**

Scanning Electron Microscope was used to observe the morphology of the freeze-dried samples. A small amount of the freeze-dried samples was stuck onto aluminum stubs



using double-sided adhesive tapes. The excess was puffed away before sputter coating with gold (~100 nm, Baltec SCD 050 sputter coater). The coated samples were then imaged in an SEM (FEI Quanta 200, The Netherlands) at an accelerating voltage of 20 kV.

#### **4.4.7. Fourier-transform infrared spectroscopy**

The changes in the chemical structure of the samples encapsulated with  $\beta$ -carotene was qualitatively analysed using an FT-IR spectrometer (Nicolet 5700; Thermo Electron Co., Waltham, MA, USA). The samples were freeze-dried before measurement. All the spectrum was obtained at a resolution of 4  $\text{cm}^{-1}$  over the wavenumber range between 700 and 4000  $\text{cm}^{-1}$ .

#### **4.4.8. X-ray diffraction**

X-ray diffractometer (Spider; Rigaku Co., Japan) equipped with a copper anode was used to determine the molecular arrangements of the freeze-dried samples that encapsulated with  $\beta$ -carotene. The data was collected at an accelerating voltage of 40 kV and a tube current of 30 mA over an angular range from 5° to 55°.

#### **4.4.9. Differential scanning calorimetry**

The thermal behaviour of the freeze-dried samples that loaded with  $\beta$ -carotene was analysed by a differential scanning calorimetry (Q2000-2906; TA Instruments, Inc., USA). 5 mg sample was sealed in a standard aluminium pan. Another empty sealed pan was applied as a reference. The sealed samples were heated at a rate of 50-200°C with a 50 mL/min nitrogen flow.

#### 4.4.10. Accelerated stability study

1.5 mL of each filtrated samples obtained in section 4.4.2. were stored in a 2 mL glass container under four 58 W fluorescent tubes (Alto; Philips, Netherlands) with a distance of 20 cm for a period of 10 days at room temperature. An appropriate amount of samples was taken out on 0, 1, 3, 7 and 10 day. The concentration of the loaded  $\beta$ -carotene in samples and the particle size of the samples after encapsulation were measured following the method described in section 4.4.3 and 4.4.4. The retention of  $\beta$ -carotene ( $R_{BC}$ ) was calculated using the following equation:

$$R_{BC}(\%) = \frac{C}{C_0} \times 100$$

where  $C$  is the concentration of the retentive  $\beta$ -carotene in the samples on a specific day, and  $C_0$  is the concentration of the loaded  $\beta$ -carotene in the samples after filtration on 0 day.

#### 4.4.11. Statistical analysis

All experiments were performed three times, and the results were reported as the calculated means and standard deviations. Statistical analysis program, SPSS 19.0 (IBM Inc., Armonk, NY), was used to perform analysis of variance with Duncan test to compare the mean values with a defined significance level at  $p < 0.05$ .

## 4.5. Results and discussion

### 4.5.1. Concentration of $\beta$ -carotene bound with soluble complexes

Based on the results in Chapter 3, stable soluble complexes could be formed between HWPI and OSA-modified starch with a DS value of  $4.29 \pm 0.11\%$  (H12-OSA-9%, hereinafter to be referred as OSA in this Chapter) at ratio of 1:10 and pH 4.5. In this Chapter, the soluble complexes (SC) between HWPI and OSA-modified starch formed at pH 4.5 (HWPI-OSA SC) were applied to encapsulate  $\beta$ -carotene using the magnetic stirring method. The mixture of HWPI and OSA-modified starch at pH 7 (HWPI-OSA pH 7), OSA-modified starch solution at pH 7 (OSA pH 7) and 4.5 (OSA pH 4.5) and HWPI solution at pH 7 (HWPI pH 7) were followed the same procedures to help illustrate the encapsulation mechanism of the soluble complexes for lipophilic bioactive compounds. The HWPI solution at pH 4.5 was not prepared to encapsulate  $\beta$ -carotene because of the extensive protein aggregation.

The concentration of the  $\beta$ -carotene bound with these samples was displayed in Figure 4.1A. As can be seen, the concentration of the  $\beta$ -carotene bound with HWPI-OSA SC ( $264.05 \pm 72.53 \mu\text{g/g}$ ) and OSA pH 4.5 ( $283.78 \pm 67.54 \mu\text{g/g}$ ) was significantly ( $p < 0.05$ ) higher than those in other samples at pH 7. HWPI-OSA pH 7 ( $133.32 \pm 34.56 \mu\text{g/g}$ ) and OSA pH 7 ( $155.83 \pm 30.42 \mu\text{g/g}$ ) showed significantly ( $p < 0.05$ ) higher encapsulation capacity than HWPI pH 7 ( $111.34 \pm 34.41 \mu\text{g/g}$ ). All the samples presented deep orange colour after encapsulation of  $\beta$ -carotene (Figure 4.1B). However, there were no obvious macroscopic differences of the colours among these samples, which may be attributed to the high concentration of the  $\beta$ -carotene bound with these samples.

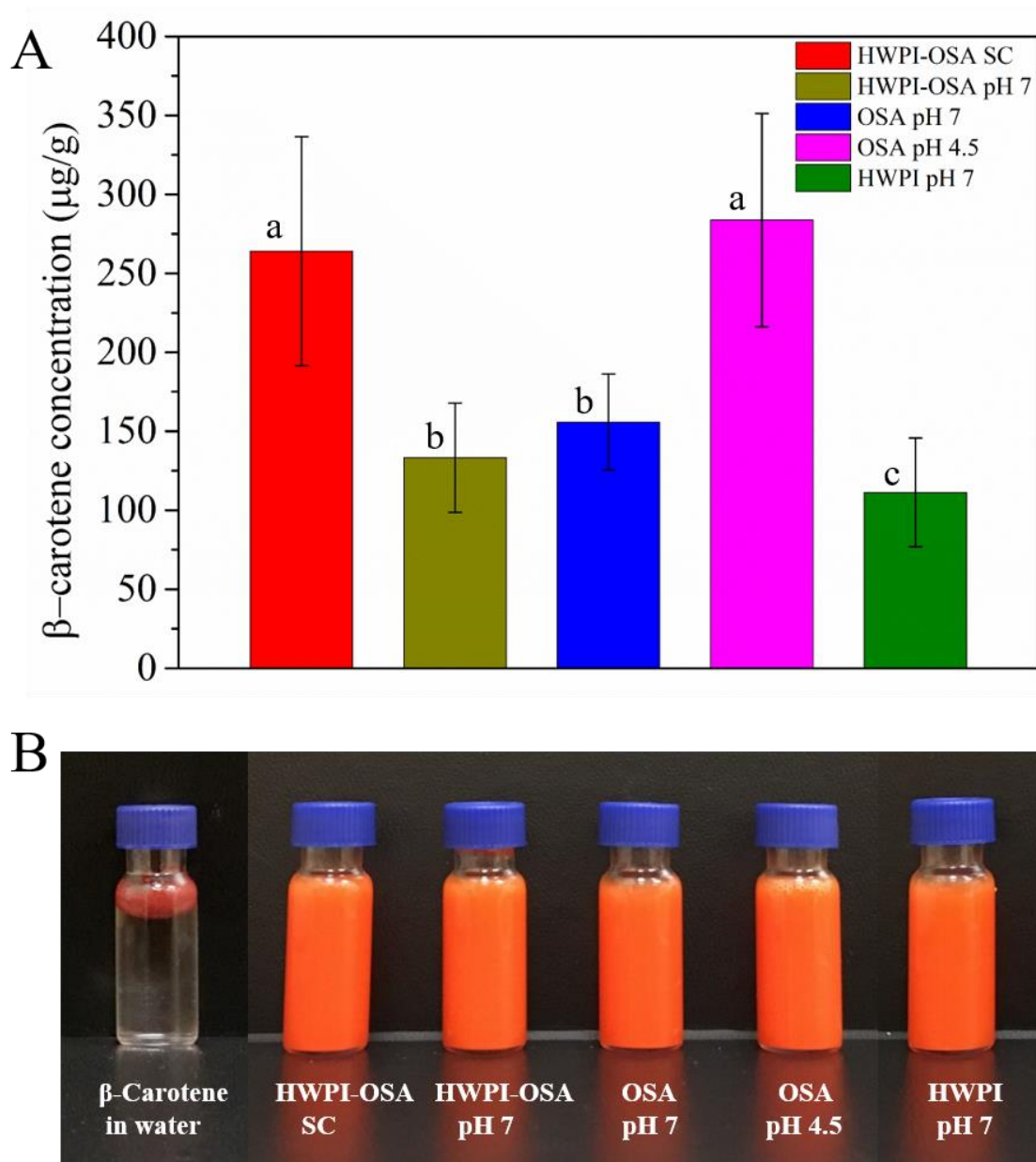


Figure 4. 1. (A) Concentration of  $\beta$ -carotene bound with different samples. (B) Visual observations of  $\beta$ -carotene in water and different  $\beta$ -carotene-loaded samples after filtration. Note: different lowercase letters indicate significant differences ( $p < 0.05$ ) in the concentration of  $\beta$ -carotene bound with different samples after encapsulation.

Compared with the estimated water solubility of  $\beta$ -carotene ( $1.5 \times 10^{-9}$  g/L) (McClements, 2012), the apparent aqueous solubility of  $\beta$ -carotene has been enormously improved after encapsulation in the soluble complexes. The  $\beta$ -carotene showed significantly greater binding affinity to either the soluble complexes or the OSA-modified starch at pH 4.5 than that to other samples at pH 7. This was in agreement with the previous study of Hosseini et al. (2015), which showed that there was stronger binding affinity of  $\beta$ -carotene to  $\beta$ -lactoglobulin at pH 4.25 than that at neutral pH. The authors inferred that it could be attributed to the increasing hydrophobic interactions around the pI of  $\beta$ -lactoglobulin. Therefore, the significantly higher concentration of the  $\beta$ -carotene bound with the soluble complexes may be attributed to the strong hydrophobic interactions between HWPI and OSA-modified starch at pH 4.5, which was the most likely dominated forces for the properties of the soluble complexes. Different from the soluble complexes, the OSA-modified starch micelles formed aggregates at pH 4.5 because of the weakened electrostatic repulsion, which could lead to the increasing interactions between the hydrophobic groups of the OSA-modified starch micelles and then result in the exposure of more hydrophobic groups. Therefore, the hydrophobic interactions between the hydrophobic groups of OSA-modified starch micelles and  $\beta$ -carotene may increase, leading to a significantly higher concentration of  $\beta$ -carotene bound with OSA-modified starch at pH 4.5 than that at pH 7. Since there should be no complexation between HWPI and OSA-modified starch at pH 7, it could be inferred that the loaded  $\beta$ -carotene in HWPI-OSA pH 7 was encapsulated by HWPI and OSA-modified starch independently. The binding affinity of  $\beta$ -carotene to HWPI pH 7 could be attributed to the small hydrophobic ligands bound on  $\beta$ -lactoglobulin (Kontopidis et al., 2004). In addition, the surface hydrophobicity of  $\beta$ -lactoglobulin increased after denaturation, thereby improving its encapsulation capacity for  $\beta$ -carotene (Mensi et al., 2013). It was different

that the binding affinity of  $\beta$ -carotene to OSA pH 7 could be attributed to the hydrophobic cores of OSA-modified starch micelles (Peng et al., 2018). The significantly lower concentration of  $\beta$ -carotene in these samples than that of the soluble complexes suggested that the formation of the soluble complexes may lead to the changes in the original structure of the HWPI molecules and OSA-modified starch micelles, and the new structure could greatly improve the encapsulation capacity for lipophilic bioactive compounds.

#### 4.5.2. Changes in particle size of soluble complexes after encapsulation of $\beta$ -carotene

Table 4.1 displays the particle size changes in different samples before and after encapsulation of  $\beta$ -carotene. As shown in the table, the mean particle diameter of HWPI-OSA SC, HWPI-OSA pH 7, OSA pH 7, OSA pH 4.5 and HWPI pH 7 increased by 1.83, 4.25, 15.95, 6.54 and 2.98 times after encapsulation of  $\beta$ -carotene, respectively. The extent of increase in the particle size of HWPI-OSA SC after encapsulation was greatly lower than that of other samples though it had significantly higher encapsulation capacity for  $\beta$ -carotene. For the samples of pure OSA-modified starch, the original Z-Ave of OSA pH 4.5 was larger than that of OSA pH 7. This may be attributed to the formation of OSA-modified starch micelle aggregates at pH 4.5. However, the particle size of OSA pH 7 after encapsulation of  $\beta$ -carotene was larger than that of OSA pH 4.5, which could be attributed the different structures of the starch micelles at pH 7 and pH 4.5. The particle size of HWPI pH 7 changed from  $80.85 \pm 25.88$  nm to  $321.46 \pm 9.36$  nm after encapsulating  $\beta$ -carotene, which was in line with the results in the previous study (Sneharani, Karakkat, Singh, & Rao, 2010). The authors found that the nanoparticles of  $\beta$ -lactoglobulin encapsulated with curcumin were polydispersed with the average size of  $142 \pm 5$  nm, which was larger than the original particle size of  $\beta$ -lactoglobulin before

encapsulation ( $\sim 60$  nm). The results of the particle size determination indicated that the introduction of  $\beta$ -carotene could lead to an increase in the particle size of all the samples examined in the present study, among which minimal changes were observed in the soluble complexes between HWPI and OSA-modified starch.

Table 4. 1. Mean particle diameter of different samples before and after encapsulation of  $\beta$ -carotene.

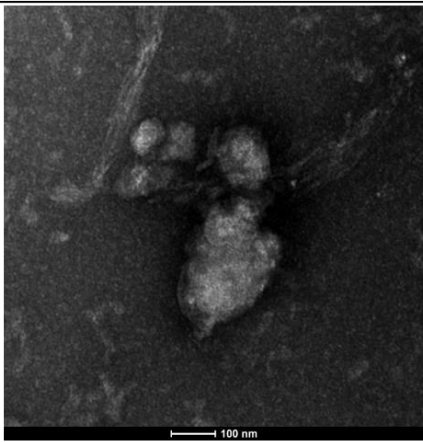
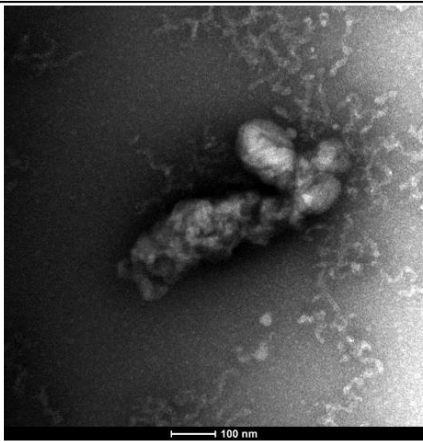
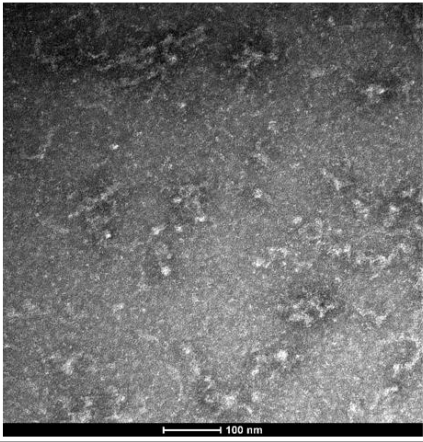
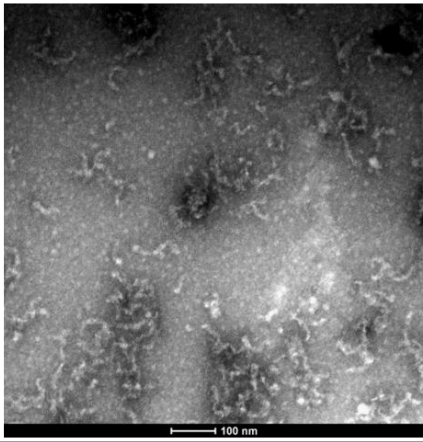
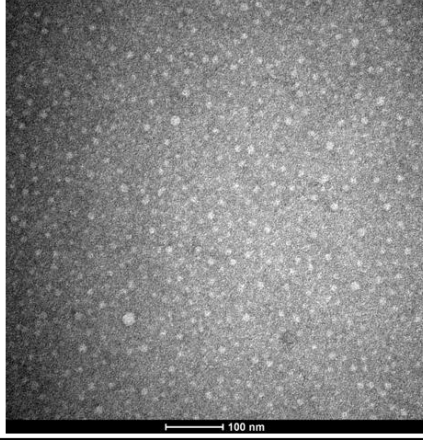
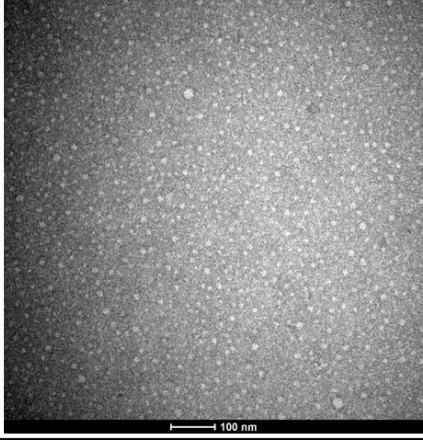
Sample	Z-Ave (nm)	
	Original	After encapsulation
HWPI-OSA SC	161.4 $\pm$ 0.6	456.43 $\pm$ 11.01
HWPI-OSA pH 7	112 $\pm$ 5.34	588.77 $\pm$ 28.38
OSA pH 7	38.49 $\pm$ 3.18	652.55 $\pm$ 53.43
OSA pH 4.5	63.21 $\pm$ 3.9	476.75 $\pm$ 15.96
HWPI pH 7	80.85 $\pm$ 25.88	321.46 $\pm$ 9.36

#### 4.5.3. TEM observation

The morphology of microstructure of different samples before and after encapsulation of  $\beta$ -carotene was investigated by TEM (Figure 4.2). It seemed that there were no significant differences between the microstructure of these samples before and after encapsulation of  $\beta$ -carotene. This result was inconsistent with the observation in the particle size determination where the remarkable increase in the particle size after encapsulation of  $\beta$ -carotene was observed. The particles observed in HWPI-OSA SC might be the soluble complexes between HWPI and OSA-modified starch, and the size was in agreement with the results of the particle size determination. In HWPI-OSA pH 7, it can be seen that the HWPI soluble aggregates and OSA-modified starch micelles were individually represented. The structure of HWPI in the mixture was curved and stranded. Similar structure of WPI soluble aggregates was also observed in the previous studies (Ryan et al., 2012; Schmitt, Bovay, Rouvet, Shojaei-Rami, & Kolodziejczyk, 2007). This result

could support the speculation that the  $\beta$ -carotene was encapsulated by HWPI and OSA-modified in the mixture at pH 7 independently. The OSA-starch micelles were spherical at pH 7 whereas they seemed to form aggregates at pH 4.5, which may be caused by the weakened repulsive electrostatic forces between the starch micelles. These observations were in agreement with the results of the particle size determination for these two samples. The loose structure of the starch aggregates could also be taken into consideration for the relatively higher encapsulation capacity for  $\beta$ -carotene. The HWPI at pH 7 alone showed a transparent and 'gluey' structure, which was composed of loosely packed aggregates, which was in agreement with the results in the study of Langton and Hermansson (1992). However, this morphology of HWPI was different from that observed in the mixture of HWPI and OSA-modified starch at pH 7, which could be attributed to the blocking effect in the presence of OSA-modified starch in the mixture.



Sample	Before encapsulation	After encapsulation
HWPI-OSA SC	 100 nm	 100 nm
HWPI-OSA pH 7	 100 nm	 100 nm
OSA pH 7	 100 nm	 100 nm

(Continued)

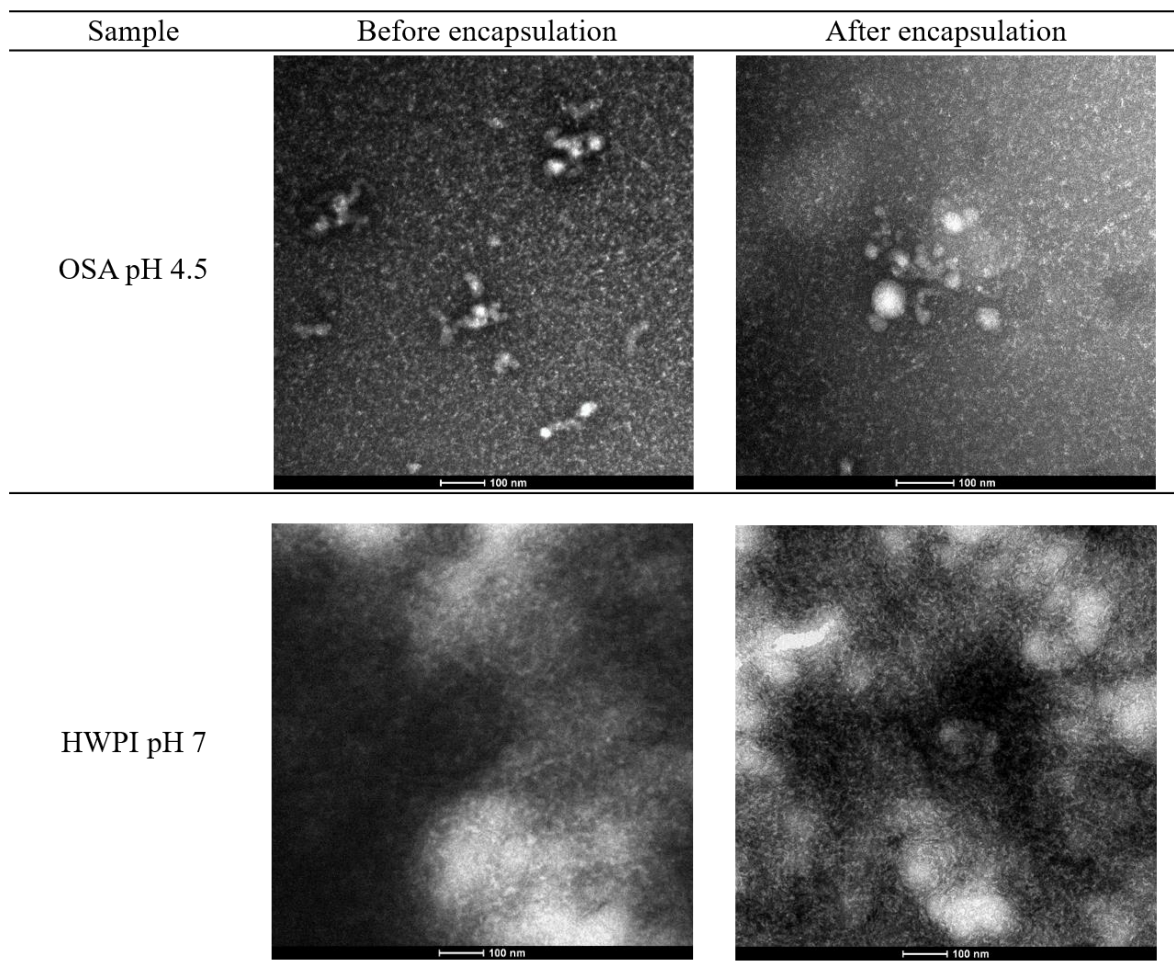


Figure 4. 2. TEM micrographs of different samples before and after encapsulation of  $\beta$ -carotene. The scale bar represents 100 nm.

#### 4.5.4. Properties of $\beta$ -carotene bound with soluble complexes in a powdered form

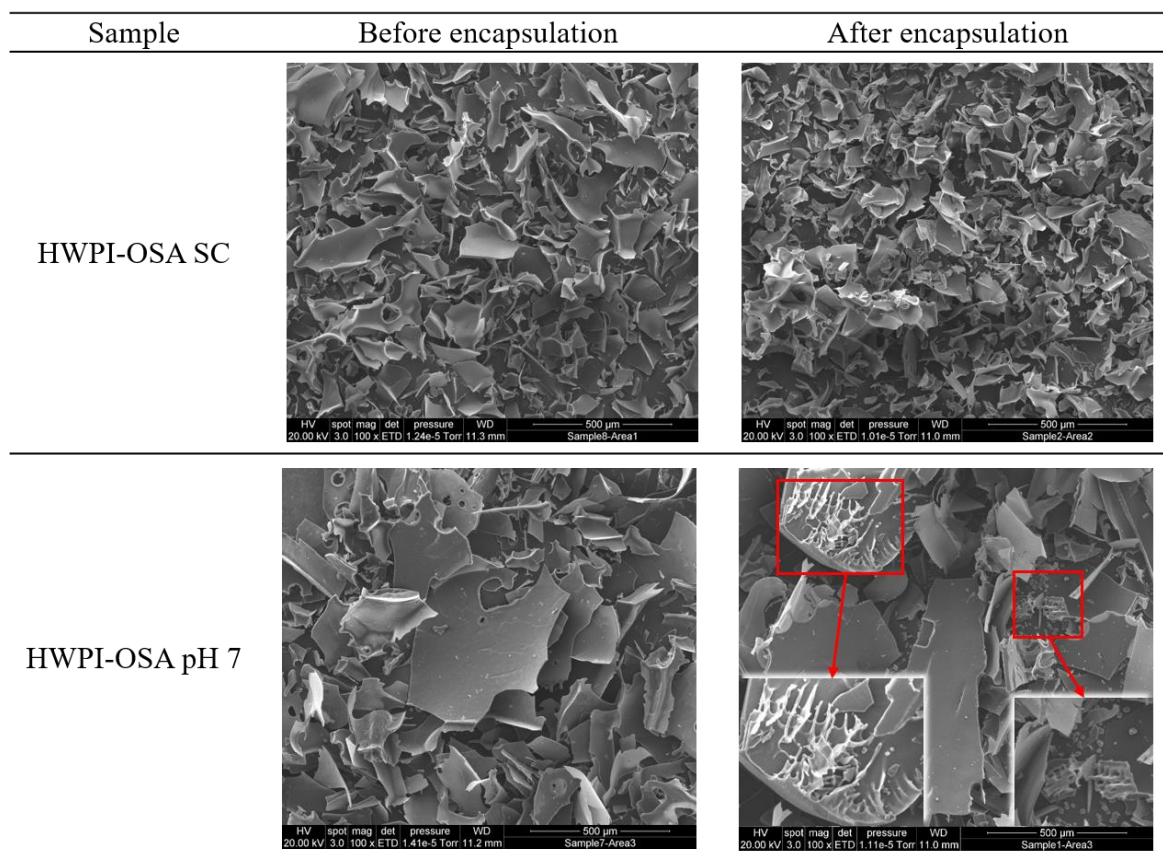
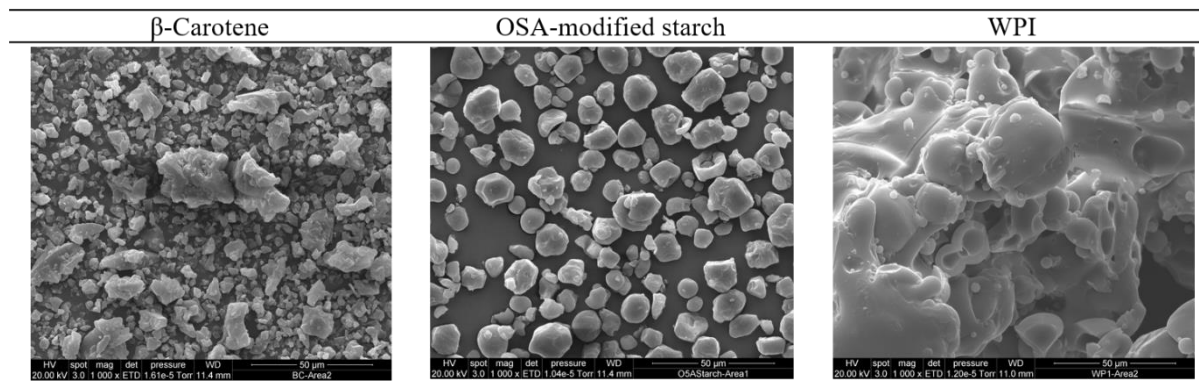
In commercial applications, it is better to deliver  $\beta$ -carotene in a powdered form rather than a liquid form. Freeze-drying is a considerable method to convert the  $\beta$ -carotene-loaded dispersions into powder form because it can effectively protect carotenoids from oxidation and isomerization during the process, which may occur in other drying methods such as spray drying and air drying (Soukoulis & Bohn, 2018). Therefore, all the  $\beta$ -carotene-loaded samples were freeze-dried, and the properties of the  $\beta$ -carotene bound with the soluble complexes were investigated. Figure 4.3B displays the different  $\beta$ -carotene-loaded freeze-dried samples, and the original samples without encapsulation of  $\beta$ -carotene were also freeze-dried as control (Figure 4.3A). The pictures of  $\beta$ -carotene-loaded freeze-dried samples before crush into powder were displayed beside the corresponding powder. As shown in Figure 4.3, compared to the white colour of the freeze-dried powder of the original samples, all the freeze-dried powders of  $\beta$ -carotene-loaded samples had a deep orange colour, which was similar to the colour of the solutions before freeze-drying (Figure 4.1B). Similar deep orange colour was observed in the freeze-dried gelatin-cashew gum coacervates encapsulating astaxanthin-containing lipid extract from shrimp waste (Gomez-Estaca et al., 2016). Since the dark red colour of the pure  $\beta$ -carotene crystals was not observed in these freeze-dried powders, it seemed that the loaded  $\beta$ -carotene was not separated out as crystal during freeze-drying. In addition, there were no distinct differences in visual observation of the colours of all the  $\beta$ -carotene-loaded freeze-dried samples. However, it is interesting that the structure of  $\beta$ -carotene-loaded freeze-dried HWPI pH 7 was quite different from other samples, which was soft and elastic so that was hard to be crushed into powder.



Figure 4. 3. Visual observations of different freeze-dried samples before (A) and after (B) encapsulation of  $\beta$ -carotene.

The morphology of  $\beta$ -carotene, OSA-modified starch and WPI powder and the samples loaded with or without  $\beta$ -carotene were observed using SEM (Figure 4.4). The pure  $\beta$ -carotene was crystals with size from several micrometres to tens of micrometres, which was similar to the morphology of  $\beta$ -carotene observed in the previous study (Tan & Nakajima, 2005). The OSA-modified starch used in the present study still maintained the granular morphology as native starch, whereas there were some pits or pores on the surface caused by esterification of OSA (Li et al., 2012). The morphology of the WPI powder was also in line with the previous study (Liu, Chen, Cheng, & Selomulya, 2016).





(Continued)

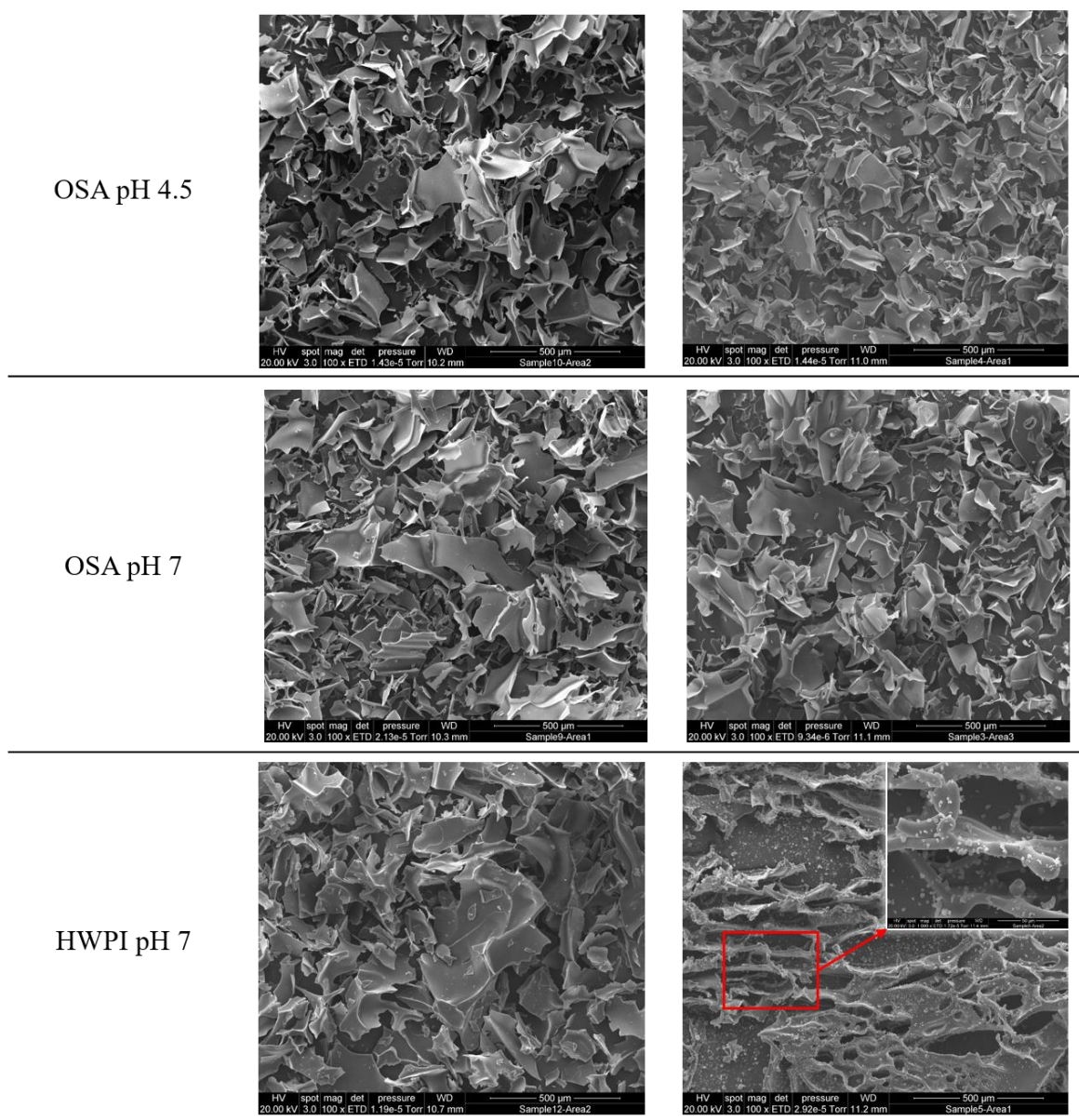


Figure 4. 4. SEM micrographs of  $\beta$ -carotene, OSA-modified starch and WPI original powder (The scale bar represents 50  $\mu$ m) and different freeze-dried samples before and after encapsulation of  $\beta$ -carotene (The scale bar represents 500  $\mu$ m).

All the freeze-dried samples without encapsulation of  $\beta$ -carotene showed quite similar morphology, which had a sheet-like structure with a smooth surface. The only difference between them could be the size of sheets in freeze-dried HWPI-OSA pH 7 and HWPI pH 7 was slightly bigger than other samples. These results showed that the OSA-modified starch granules were completely disrupted after gelatinization, which was consistent with the results of the study of Zhao et al. (2018). For the freeze-dried  $\beta$ -carotene-loaded HWPI-OSA SC, no structural changes were observed under SEM, which showed the same structure with the corresponding sample without encapsulating  $\beta$ -carotene. It suggested that the structure of the  $\beta$ -carotene-loaded soluble complexes between HWPI and OSA-modified starch were quite stable. The freeze-dried  $\beta$ -carotene-loaded samples of pure OSA-modified starch including OSA pH 7 and OSA pH 4.5 also showed no significant differences in the morphology compared with those samples without encapsulation. However, the freeze-dried HWPI pH 7 loaded with  $\beta$ -carotene displayed a sponge-like structure, which changed remarkably from its original sheet-like structure. In addition, it can be seen that there were amounts of particles interspersed through the 'sponge'. The possible reason for this type of structure could be that there were some interactions occurred between WPI and  $\beta$ -carotene during the freeze-drying process, thereby leading to the cross-linking of the molecules to form the 'sponge'. The particles could be the new complexes formed from WPI and  $\beta$ -carotene during the freeze-drying process or the separated-out  $\beta$ -carotene crystals, which needs further investigation. A portion of similar sponge-like structure and small particles were also observed in the freeze-dried HWPI-OSA pH 7 loaded with  $\beta$ -carotene, which was marked in the Figure of this sample. This confirmed that the  $\beta$ -carotene was encapsulated by HWPI and OSA-modified starch in the mixture at pH 7 independently. Furthermore, it seemed that the cross-linking of the molecules during the freeze-drying process was suppressed by the

presence of the OSA-modified starch. The majority of  $\beta$ -carotene-loaded OSA-modified starch micelles in the mixture may isolate the  $\beta$ -carotene-loaded HWPI molecules, consequently reduced the contact of these molecules and then prevent their interactions during freeze-drying. These structural changes were not observed in the freeze-dried  $\beta$ -carotene-loaded HWPI-OSA SC, which indicated that the formation of the soluble complexes leads to the changes in the original structure of the HWPI molecules. Therefore, no similar structural changes to the other two freeze-dried samples containing HWPI were observed in the  $\beta$ -carotene-loaded soluble complexes.

The redispersion behaviour of the  $\beta$ -carotene-loaded soluble complexes in a powdered form was also evaluated in our study. There were no distinct changes in visual observation of the colour between the original  $\beta$ -carotene-loaded HWPI-OSA SC (Figure 4.1B) and its redispersion (Figure 4.5). The freeze-dried  $\beta$ -carotene-loaded HWPI-OSA SC showed good redispersion behaviour. Other freeze-dried  $\beta$ -carotene-loaded samples also had good redispersion behaviour with no distinct changes in visual observation of the colour, except for the freeze-dried  $\beta$ -carotene-loaded HWPI pH 7, which could not be redispersed in aqueous. This may be attributed to its quite different sponge-like structure from other samples observed under SEM. However, the redispersion behaviour of freeze-dried  $\beta$ -carotene-loaded HWPI-OSA pH 7 was not affected, although a fraction of sponge-like structure was also observed under SEM for this sample. This confirmed the inference that the presence of the OSA-modified starch suppresses the cross-linking of the  $\beta$ -carotene-loaded HWPI molecules during the freeze-drying process, thereby leading to its better redispersion behaviour than that of the freeze-dried  $\beta$ -carotene-loaded HWPI pH 7.



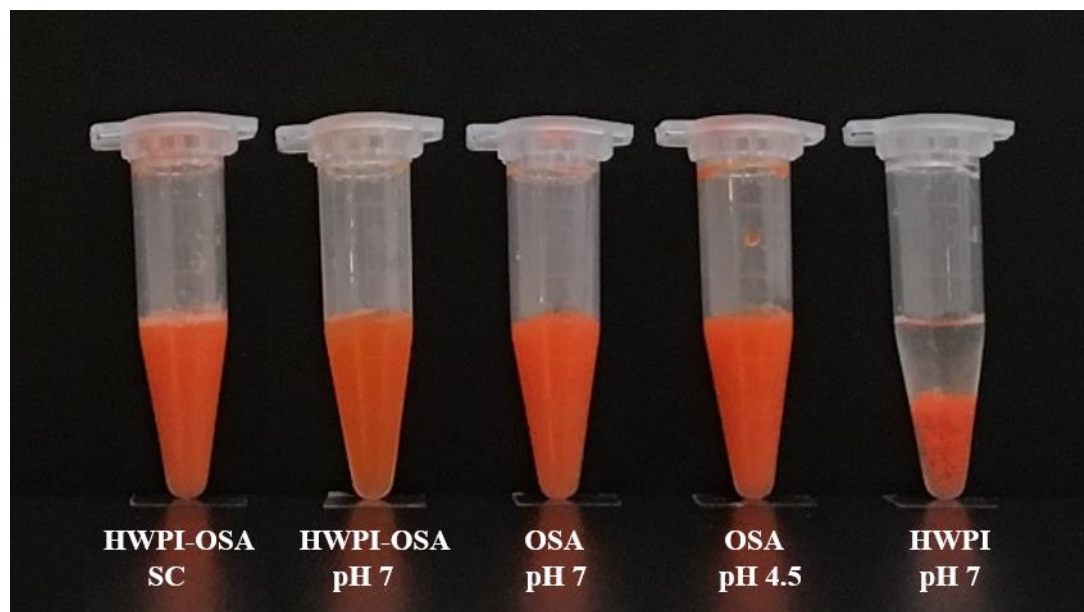


Figure 4. 5. Visual observations of the redispersion behaviour of different freeze-dried  $\beta$ -carotene-loaded powders.

The particle size measurement was carried out on the redispersions for further evaluation of the redispersion behaviour of the  $\beta$ -carotene-loaded HWPI-OSA SC (Table 4.2). There were almost no changes in the particle size of the  $\beta$ -carotene-loaded HWPI-OSA SC after redispersion. Combined with no morphology changes observed in the freeze-dried HWPI-OSA SC with or without encapsulating  $\beta$ -carotene, it could be postulated that the  $\beta$ -carotene was effectively encapsulated into the hydrophobic interior of the soluble complexes between HWPI and OSA-modified starch. Otherwise, the unloaded  $\beta$ -carotene crystals should be more susceptible to form large aggregates during freeze-drying (Peng et al., 2018), which could lead to an increase in the particle size of redispersions. No significant changes in the particle size were also observed in OSA pH 7 and OSA pH 4.5, which prove the  $\beta$ -carotene was effectively encapsulated into the hydrophobic cores of the OSA-modified starch micelles or their aggregates. However, the particle size of  $\beta$ -carotene-loaded HWPI-OSA pH 7 increased significantly. The remarkable increase in

particle size could be attributed to the structural changes of the  $\beta$ -carotene-loaded HWPI pH 7 molecules during the freeze-drying process. This provided further evidence to support our inference above that the HWPI and OSA-modified starch in HWPI-OSA pH 7 encapsulate the  $\beta$ -carotene independently during the encapsulation process. In addition, the presence of OSA-modified starch could effectively improve the redispersion behaviour of the  $\beta$ -carotene-loaded HWPI, which could not be redispersed in aqueous.

Based on these results, we can found that although the presence of OSA-modified starch in the mixture at pH 7 could greatly improve the redispersion behaviour of its freeze-dried sample, it could not prevent the structural changes of the  $\beta$ -carotene-loaded HWPI molecules during freeze-drying. This could be attributed to the fact that the HWPI molecules and OSA-modified starch micelles encapsulate the  $\beta$ -carotene independently in their mixture at pH 7. However, the  $\beta$ -carotene-loaded in HWPI-OSA SC could effectively avoid this problem, which had good redispersion behaviour with no changes in the structure or particle size. This result suggested the structure of soluble complexes provided a different binding approach with  $\beta$ -carotene to form a ternary complex among HWPI, OSA-modified starch and  $\beta$ -carotene, which had a better redispersion property in water than that of  $\beta$ -carotene bound with HWPI alone. The structure and possible binding approach of this ternary complex will be further investigated in future work.

Table 4. 2. Mean particle diameter of different  $\beta$ -carotene-loaded samples before and after redispersion.

Sample	Z-Ave (nm)	
	Before redispersion	After redispersion
HWPI-OSA SC	489.13 $\pm$ 5.75	494.33 $\pm$ 8.37
HWPI-OSA pH 7	534.83 $\pm$ 0.74	1160.33 $\pm$ 27.59
OSA pH 7	637.3 $\pm$ 4.68	656.5 $\pm$ 5.75
OSA pH 4.5	470.33 $\pm$ 7.89	492.36 $\pm$ 5.4
HWPI pH 7	321.83 $\pm$ 2.14	/

The concentration of the retentive  $\beta$ -carotene in the redispersed samples are shown in Table 4.3. It can be seen that the  $\beta$ -carotene retention rate in HWPI-OSA SC was significantly ( $p < 0.05$ ) higher than those in HWPI-OSA pH 7 and OSA pH 4.5. No significant ( $p > 0.05$ ) difference was observed in the  $\beta$ -carotene retention rate between HWPI-OSA pH 7 and OSA pH 4.5. The OSA pH 7 showed the highest  $\beta$ -carotene retention rate in all the samples, which was nearly no loss of  $\beta$ -carotene after redispersion. Theoretically, the  $\beta$ -carotene retention rate in samples at pH 7 should be significantly higher than those at pH 4.5, where the stability of  $\beta$ -carotene decreased significantly (Xu et al., 2013). Therefore, the  $\beta$ -carotene retention rate OSA pH 4.5 was significantly ( $p < 0.05$ ) lower than that in OSA pH 7. However, HWPI-OSA SC showed significantly ( $p < 0.05$ ) higher  $\beta$ -carotene retention rate than HWPI-OSA pH 7, which indicated that the structure of the soluble complexes between HWPI and OSA-modified starch provided effective protection for the loaded  $\beta$ -carotene against the effects of low pH values. The lowest  $\beta$ -carotene retention rate in HWPI-OSA pH 7 may be attributed to the presence of the  $\beta$ -carotene-loaded HWPI pH 7, which was greatly affected by the freeze-drying process. According to the study of Deng, Zhang and Tang (2017), there was only about 31.9% retention rate of  $\beta$ -carotene in free  $\beta$ -carotene crystals after freeze-drying. It could be inferred that a portion of the loaded  $\beta$ -carotene in HWPI at pH 7 may be separated out

as crystals during freeze-drying, which may thereby lead to the relatively high degradation rate. However, all the  $\beta$ -carotene-loaded redispersions showed over 80% retention rate of  $\beta$ -carotene after freeze-drying in the present study, which indicated the effective improvement of the stability of  $\beta$ -carotene after encapsulation in these samples.

Table 4. 3.  $\beta$ -Carotene retention rate in redispersions of different freeze-dried  $\beta$ -carotene-loaded samples. Note: different lowercase letters indicate significant differences ( $p < 0.05$ ) in the  $\beta$ -carotene retention rate of these samples after redispersion.

Redispersed sample	$\beta$ -Carotene retention (%)
HWPI-OSA SC	89.75 <sup>b</sup>
HWPI-OSA pH 7	83.2 <sup>c</sup>
OSA pH 7	98.57 <sup>a</sup>
OSA pH 4.5	85.58 <sup>c</sup>

The structure of HWPI-OSA SC showed effective protection to the bound  $\beta$ -carotene, which led to the good redispersion behaviour and a high retention rate of  $\beta$ -carotene in the  $\beta$ -carotene-loaded HWPI-OSA SC in a powdered form. These results indicated that the soluble complexes between HWPI and OSA-modified starch loaded with lipophilic compounds could be successfully converted into a powdered form, which showed its potential in commercial applications in food industry.

#### 4.5.5. FT-IR spectroscopy

The FT-IR spectroscopy was used to investigate the intermolecular interactions among HWPI, OSA-modified starch and  $\beta$ -carotene (Figure 4.6). As shown in Figure 4.6A, the peak of OSA-modified starch at  $3350\text{ cm}^{-1}$  corresponded to the O-H groups, and the peak at  $2929\text{ cm}^{-1}$  was attributed to the C-H stretching vibration of the glucose unit (Lin, Liang, Zhong, Ye, & Singh, 2018b). The residual bound water contributed to the absorption band at  $1648\text{ cm}^{-1}$  (Zhang et al., 2011). The characteristic peaks of OSA-modified starch were at  $1716$  and  $1566\text{ cm}^{-1}$ , which were assigned to the C=O stretching vibration of ester groups and the asymmetric stretching vibration of OSA groups, respectively (Zhao et al., 2018). The typical transmittance peaks of WPI occurred at  $1635$  and  $1535\text{ cm}^{-1}$ , which referred to amide I and amide II band, respectively (Yi, Lam, Yokoyama, Cheng, & Zhong, 2015). The FT-IR spectrum of  $\beta$ -carotene showed peaks at  $965$ ,  $1368$ ,  $1620$  and  $2915\text{ cm}^{-1}$ . The peaks at  $1368$  and  $2915\text{ cm}^{-1}$  were due to the C-H bending, and the peak at  $1620\text{ cm}^{-1}$  was attributed to the C=C stretching of the conjugated double bond (Saha, Samanta, Chaudhuri, & Dutta, 2015). In addition, the sharp peak at  $965\text{ cm}^{-1}$  was because of the presence of the alkene C-H with out of plane deformation (Yi et al., 2015).

All the samples showed the same characteristic peaks before and after encapsulation of  $\beta$ -carotene (Figure 4.6B-E), except for the HWPI pH 7 (Figure 4.6F). The characteristic peaks of  $\beta$ -carotene including  $965$ ,  $1368$ ,  $1620$  and  $2915\text{ cm}^{-1}$  were disappeared in all the spectra of these samples loaded with  $\beta$ -carotene. This result suggested that the  $\beta$ -carotene may be encapsulated into these samples via hydrophobic interactions, which was in agreement with the results in the previous study (Dai et al., 2017; Hu et al., 2015). It is interesting that the amide I peak increased by  $2\text{ cm}^{-1}$  and the amide II peak increased by  $10\text{ cm}^{-1}$  after encapsulation of  $\beta$ -carotene (Figure 4.6F). This confirms that the

encapsulation of  $\beta$ -carotene could affect the structure or conformation of the WPI (Yi et al., 2015). In addition, several new peaks occurred over the wavenumber range from 700 to 1200  $\text{cm}^{-1}$ , which was marked in Figure 4.6F. These changes indicated the significant variation in the structure of  $\beta$ -carotene-loaded HWPI pH 7 during freeze-drying, which led to the quite different sponge-like structure. Since there were no significant differences observed under TEM between the HWPI pH 7 before and after encapsulation of  $\beta$ -carotene, the impact of freeze-drying should be taken into consideration for these significant structural changes.

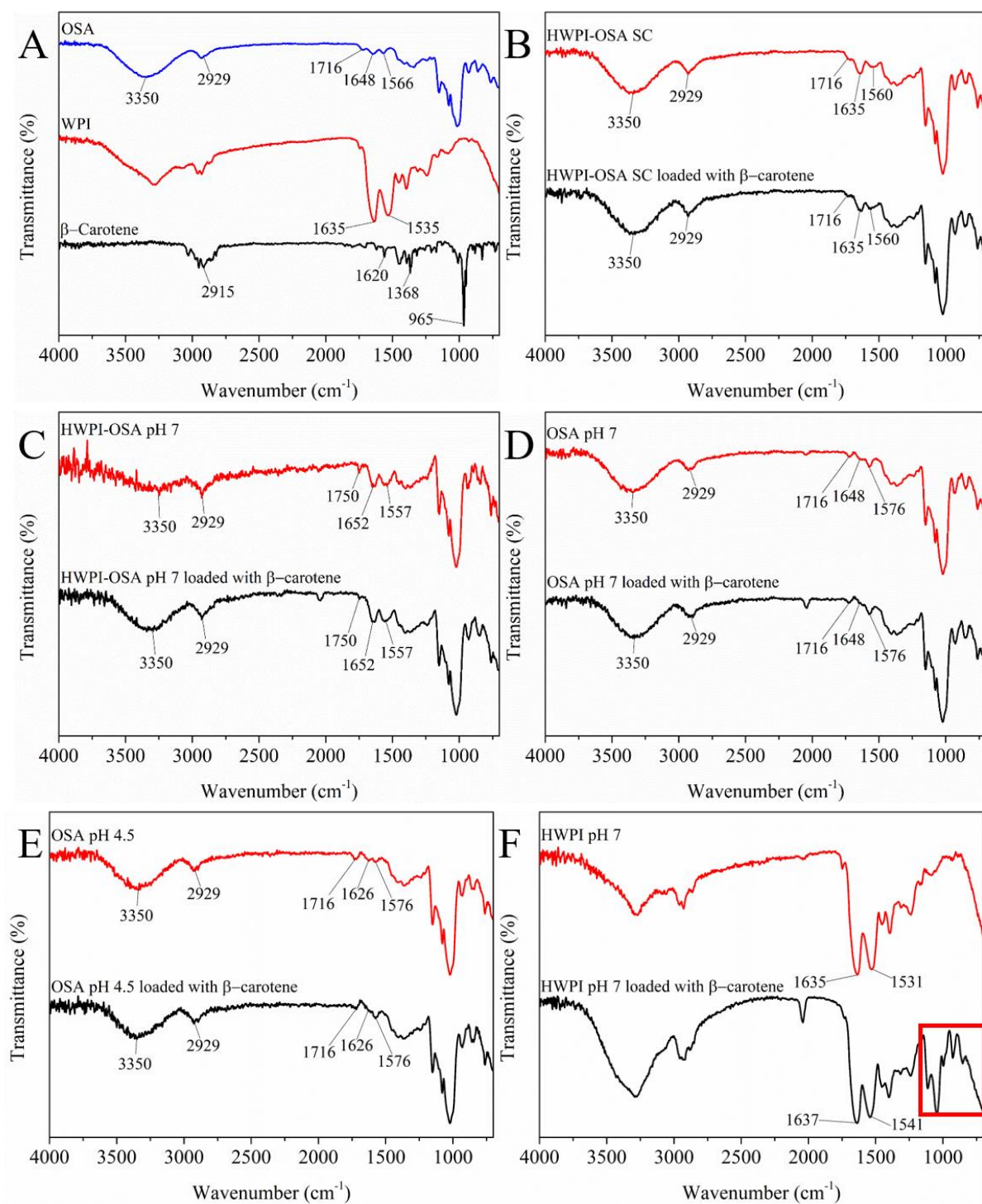


Figure 4. 6. FT-IR spectra of  $\beta$ -carotene, OSA-modified starch and WPI original powder (A); and different freeze-dried samples before and after encapsulation of  $\beta$ -carotene (B-F).



#### 4.5.6. X-ray diffraction

The physical state of  $\beta$ -carotene in different samples after encapsulation was determined by XRD, and the corresponding samples before encapsulation were also determined as control (Figure 4.7). The sharp peaks of the XRD spectrum of  $\beta$ -carotene (Figure 4.7B) showed its nature of highly crystalline (Yi et al., 2015). However, there were no differences observed between the spectra of each freeze-dried sample with or without encapsulation of  $\beta$ -carotene, which indicated that the  $\beta$ -carotene was in an amorphous form in all the samples after encapsulation (Peng et al., 2018). This result revealed that there were intermolecular interactions between the  $\beta$ -carotene and all the samples during the encapsulation process. In addition, the confinement of  $\beta$ -carotene in these samples could suppress its crystallization during freeze-drying (Dai et al., 2017; Peng et al., 2018). It is worth mentioning that the  $\beta$ -carotene was in an amorphous form in HWPI pH 7 determined by XRD. Based on the results of FT-IR for this sample, it could be confirmed that the particles observed under SEM in this sample might be the new complexes formed from HWPI and  $\beta$ -carotene during the freeze-drying process.



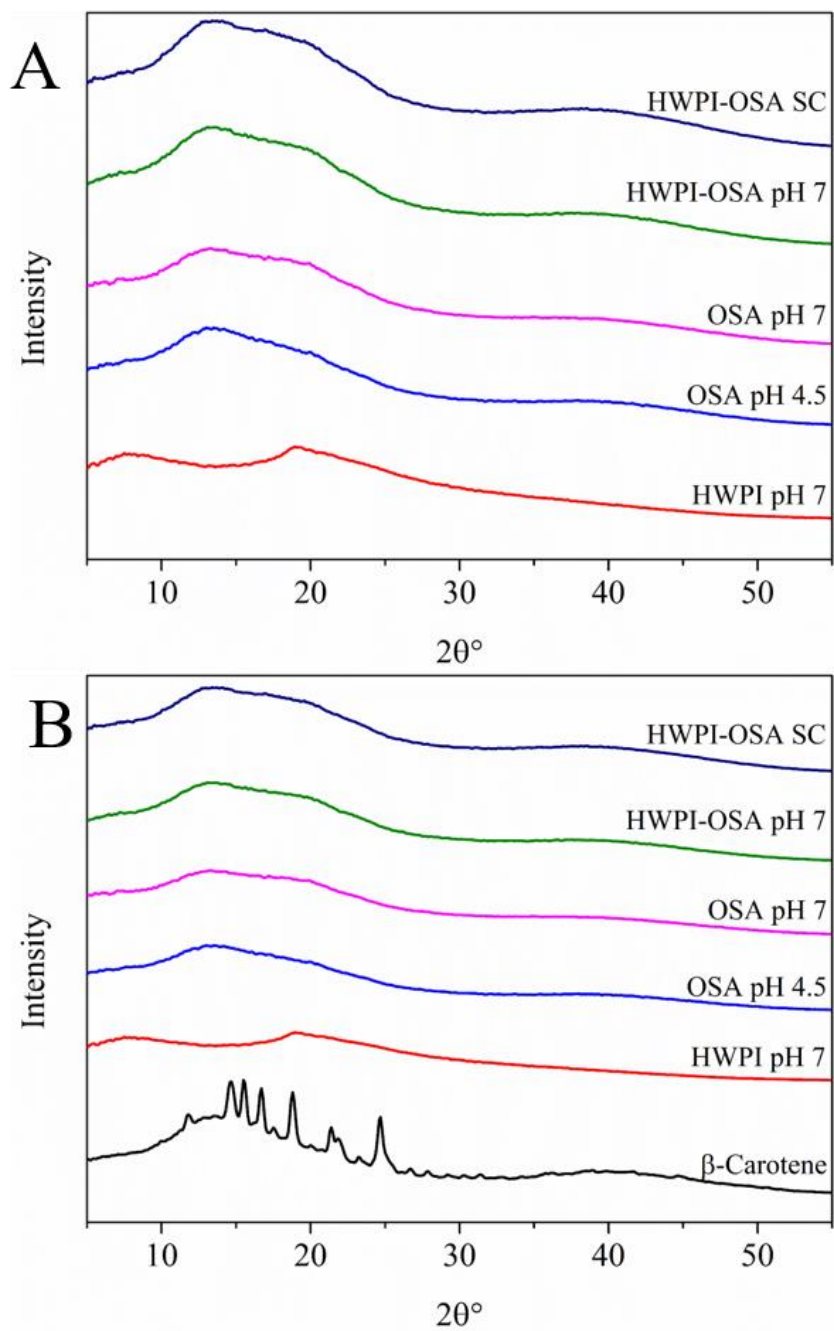


Figure 4. 7. XRD spectra of different freeze-dried samples before (A) and after (B) encapsulation of  $\beta$ -carotene.

#### 4.5.7. DSC

The thermal behaviour of all the samples before and after encapsulation of  $\beta$ -carotene was investigated by DSC, and the original powder of  $\beta$ -carotene, OSA-modified starch and WPI were also determined (Figure 4.8). It can be seen that there was a peak at 182.13 °C in the DSC thermogram of  $\beta$ -carotene, which corresponded to the melting point of crystalline  $\beta$ -carotene. However, there were no melting points at 182.13 °C observed in all the samples loaded with  $\beta$ -carotene, which indicated that the  $\beta$ -carotene was amorphous rather than crystalline in these samples. These results were in agreement with the results obtained by XRD.

The melting points of original OSA-modified starch and WPI were observed at 147.43 °C and 150.75 °C, whereas these melting points both increased after the gelatinization of OSA-modified starch and the denaturation of WPI, respectively. The melting points of the  $\beta$ -carotene-loaded samples increased when compared with the corresponding samples without encapsulation of  $\beta$ -carotene, except for the samples of pure OSA-modified starch, which decreased after encapsulation. In the samples containing HWPI, the melting points of these samples after encapsulation of  $\beta$ -carotene increased more than 10 °C. However, it seemed that the encapsulation of  $\beta$ -carotene in OSA-modified starch whether at pH 7 or 4.5 had less effect on their melting points, which decreased 1 and 8 °C, respectively. These results may be caused by the different encapsulation mechanism of these samples, and then leading to the formation of different structures.

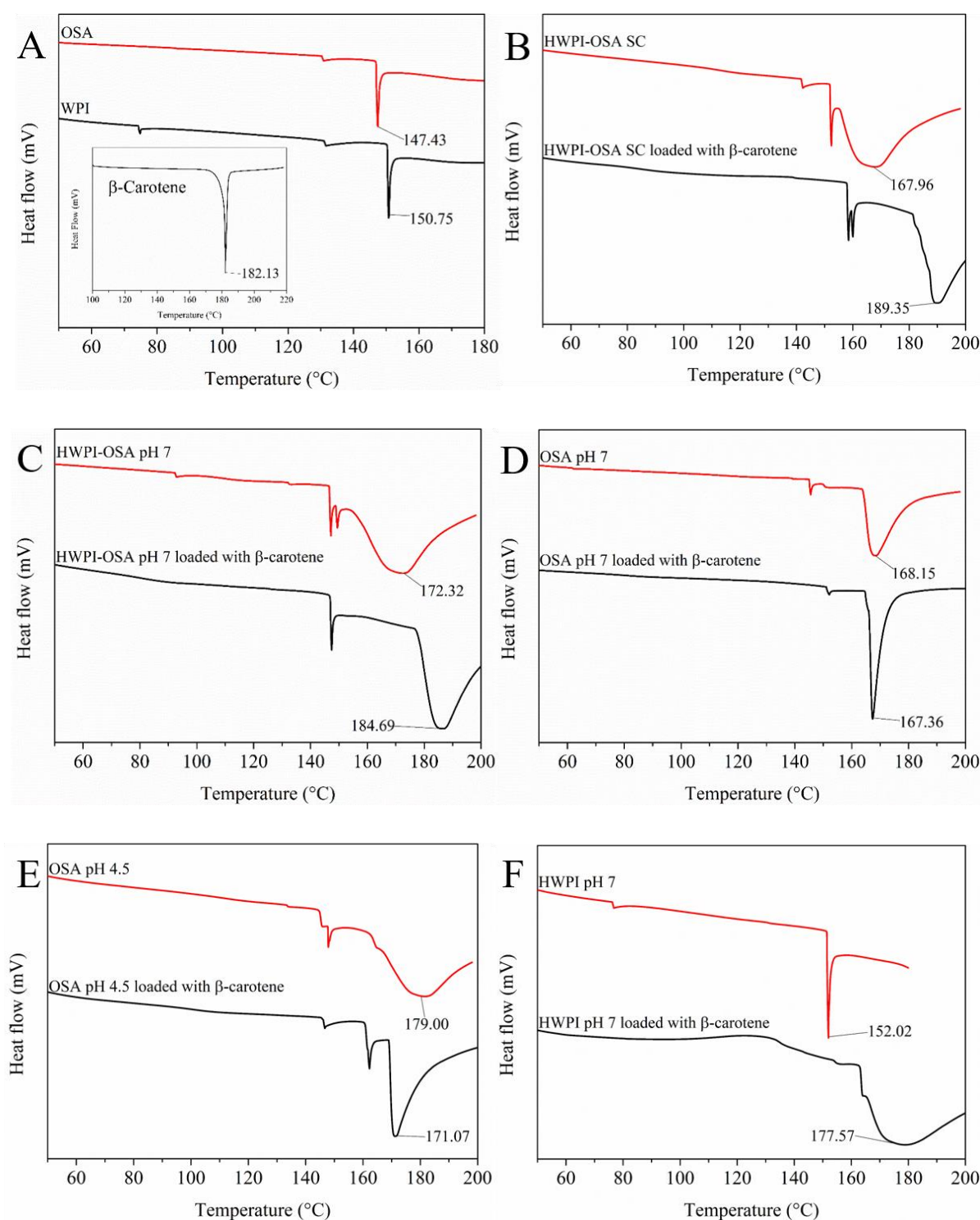


Figure 4. 8. DSC patterns of  $\beta$ -carotene, OSA-modified starch and WPI original powder (A); and different freeze-dried samples before and after encapsulation of  $\beta$ -carotene (B-F).

#### 4.5.8. Accelerated stability study

##### 4.5.8.1. Retention rate of $\beta$ -carotene bound with soluble complexes during storage

The  $\beta$ -carotene-loaded samples were stored under four 58 W fluorescent tubes with a distance of 20 cm for a period of 10 days at room temperature to evaluate the stability of the  $\beta$ -carotene-loaded samples during storage. The changes in the  $\beta$ -carotene retention rate in these samples were presented in Table 4.4. The degradation rate of the  $\beta$ -carotene bound with all these samples reduced with the increasing storage time. The concentration of the loaded  $\beta$ -carotene decreased sharply in all samples after 1 day of storage, which was more than 30%, whereas it decreased by more than 20% after 3 days of storage. HWPI-OSA SC showed the best protection for the  $\beta$ -carotene after 7 days of storage, which was significantly ( $p < 0.05$ ) higher than those of OSA pH 4.5 and HWPI pH 7. Although no significant difference ( $p > 0.05$ ) was observed in the loss of  $\beta$ -carotene among HWPI-OSA SC, HWPI-OSA pH 7 and OSA pH 7, the retention rate of  $\beta$ -carotene in HWPI-OSA SC was higher than those in the other two samples at pH 7, where it was expected to be significantly higher than the samples at pH 4.5. Xu et al. (2013) have investigated the influence of pH on the stability of  $\beta$ -carotene in the O/W emulsions during the 7-day storage at 55 °C in the dark. The results showed that the stability of  $\beta$ -carotene was improved with increasing pH values, and the highest loss of  $\beta$ -carotene was observed at pH 4. In the samples of pure OSA-modified starch, the loss of  $\beta$ -carotene at pH 4.5 was slightly higher than that at pH 7, which was in agreement with the previous study. However, higher retention rate of  $\beta$ -carotene in HWPI-OSA SC than that in HWPI-OSA pH 7 was observed. This phenomenon suggested that the encapsulation of  $\beta$ -carotene in the soluble complexes between HWPI and OSA-modified starch could effectively improve the chemical stability of  $\beta$ -carotene under low pH conditions during storage. It enabled the  $\beta$ -carotene show the best retention rate around the pH value where

it was expected to have a lower retention rate than other samples at pH 7. This result may be closely related to the encapsulation mechanism of the soluble complexes for  $\beta$ -carotene. The shells composed by the hydrophilic portion of OSA-modified starch and the protein aggregate cores of the soluble complexes could double protected the  $\beta$ -carotene during storage. This double protection thereby led to the higher retention rate of  $\beta$ -carotene at pH 4.5, especially after 7 days of storage, which indicated the potential of using the soluble complexes between HWPI and OSA-modified starch to protect lipophilic bioactive compounds for long-term storage under low pH conditions. The overall rapid reduction in the concentration of the loaded  $\beta$ -carotene in all the samples in the present study may be attributed to the acceleration conditions with synergistic effects of the high intensity of the lights and the short storage distance under the lights.

Table 4. 4.  $\beta$ -carotene retention in  $\beta$ -carotene-loaded samples during storage. Note: different lowercase letters indicate significant differences ( $p < 0.05$ ) in the  $\beta$ -carotene retention rate of these samples during storage.

Sample	$\beta$ -Carotene Retention (%)				
	0 day	1 day	3 day	7 day	10 day
HWPI-OSA SC	100	$65.65 \pm 3.86^{ab}$	$40.10 \pm 7.28^a$	$9.21 \pm 6.29^a$	$2.26 \pm 1.78^a$
HWPI-OSA pH 7	100	$61.32 \pm 5.27^b$	$35.50 \pm 7.23^a$	$6.24 \pm 3.29^a$	$0.85 \pm 0.25^{ab}$
OSA pH 7	100	$67.98 \pm 2.34^{ab}$	$42.24 \pm 3.88^a$	$7.61 \pm 2.95^a$	$0.63 \pm 0.54^{ab}$
OSA pH 4.5	100	$67.56 \pm 3.09^{ab}$	$41.14 \pm 3.31^a$	$5.50 \pm 2.22^a$	$0.44 \pm 0.32^b$
HWPI pH 7	100	$69.96 \pm 1.90^a$	$34.70 \pm 7.05^a$	$6.07 \pm 1.61^a$	$0.35 \pm 0.31^b$

#### 4.5.8.2. Changes in particle size of $\beta$ -carotene-loaded soluble complexes during storage

The changes in the mean particle diameter of the  $\beta$ -carotene-loaded samples during storage were also investigated in the present study, and the corresponding samples without encapsulation of  $\beta$ -carotene were measured as control (Figure 4.9). It can be seen that the particle size of all the samples before encapsulation of  $\beta$ -carotene did not change during storage. After encapsulation of  $\beta$ -carotene, all the samples showed a significant increase in particle size, which was in agreement with the results above. The particle size of the  $\beta$ -carotene-loaded HWPI-OSA SC and HWPI pH 7 gradually decreased during storage. For the  $\beta$ -carotene-loaded samples of the OSA-modified starch solution at pH 7 and pH 4.5, the particle size increased in the initial 7 days and then decreased. There were no obvious changes in the particle size of the  $\beta$ -carotene-loaded HWPI-OSA pH 7 during storage. The possible reason for the decrease in the particle size of the  $\beta$ -carotene-loaded soluble complexes seemed to be the synergistic effects of the degradation of  $\beta$ -carotene and the changes in its colour during storage on the particle size determination. Due to the light absorbing nature of  $\beta$ -carotene, lower  $\beta$ -carotene concentration in the soluble complexes with increasing storage time can lead to a brighter measuring environment. The changes in the scattering intensity caused by Brownian motion become more obvious, which led to the decreases in the reading of particle size during storage. The initial increase in the particle size of  $\beta$ -carotene-loaded OSA pH 7 and pH 4.5 may be attributed to the retrogradation of starch. After 7 days of storage, the effects of colour seemed to overcome those of the retrogradation of starch on the particle size determination of these two samples, which led to the further decrease in the reading of their particle size during the determination. The relatively constant particle size of the  $\beta$ -carotene-loaded HWPI-OSA pH 7 during storage could be attributed to the balance of the changes in particle size

of  $\beta$ -carotene-loaded HWPI and  $\beta$ -carotene-loaded OSA pH 7. The increase in the particle size during storage was not observed in the  $\beta$ -carotene-loaded soluble complexes, which suggested that the formation of the soluble complexes between HWPI and OSA-modified starch lead to the changes in the structure of OSA-modified starch micelles, thereby effectively preventing the retrogradation of the OSA-modified starch during long-term storage.

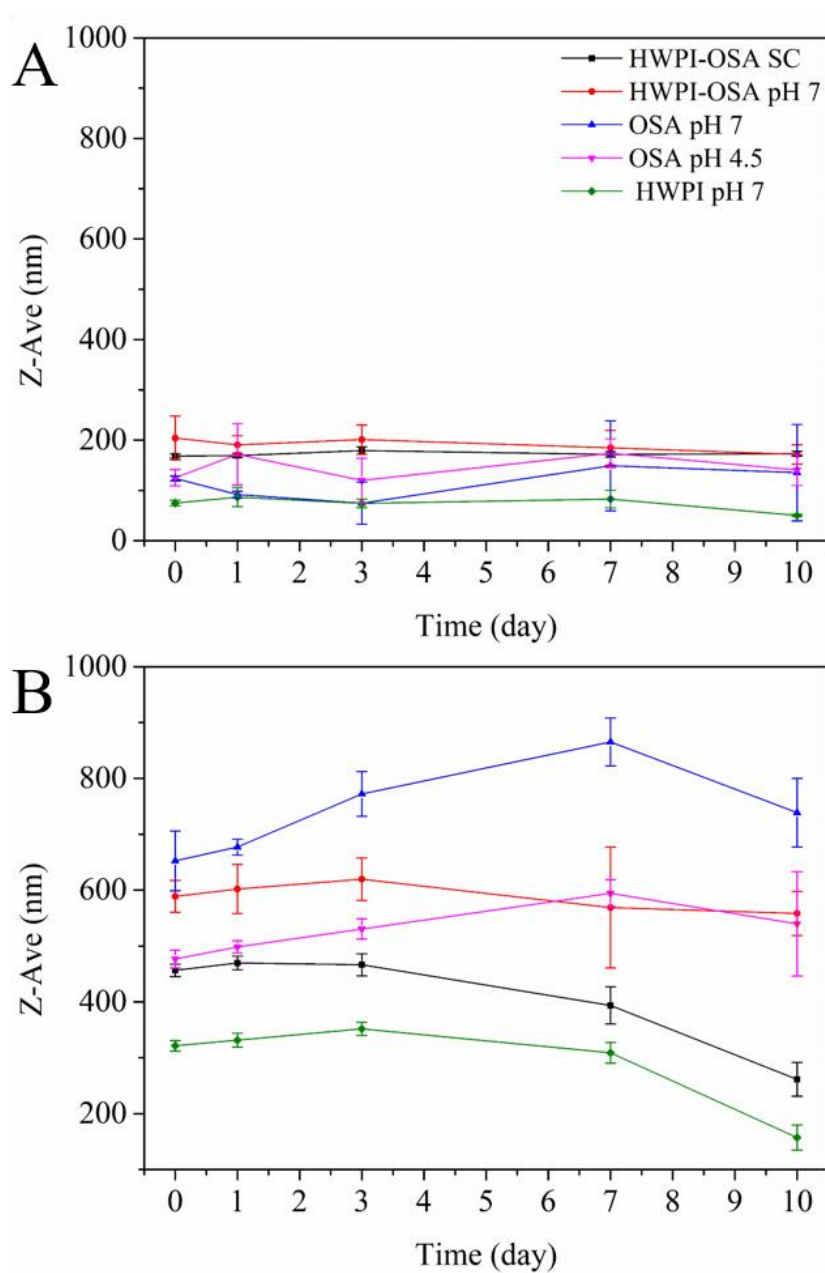


Figure 4. 9. Z-Ave of the samples before (A) and after (B) encapsulation of  $\beta$ -carotene as a function of storage time.



#### 4.5.9. Proposed encapsulation mechanism for $\beta$ -carotene of soluble complexes

Based on the results above in the present study, the possible conformations of all the samples before and after encapsulation of  $\beta$ -carotene are shown in Figure 4.10. Since the soluble complexes seemed to be formed by the strong hydrophobic interactions between the initial HWPI aggregates and the OSA groups of the OSA-modified starch, it could be inferred that the  $\beta$ -carotene may bind to the protein aggregate cores and the OSA groups attached to the cores of HWPI-OSA SC during the encapsulation process. In addition, the hydrophobic interactions between  $\beta$ -carotene and the protein aggregate cores should be increased with the increasing exposure of the hydrophobic groups at the pH value around the pI of WPI, thereby leading to their high encapsulation capacity. For the samples at pH 7 including OSA pH 7, HWPI pH 7 and their mixture, the OSA-modified starch molecules presented as nano-sized micelles in aqueous solution because of the hydrophobic bonding of OSA groups, and the HWPI molecules presented as filaments after heat treatment above their thermal denaturation temperature. The binding affinity of  $\beta$ -carotene to OSA pH 7 and HWPI pH 7 could be attributed to the hydrophobic cores of OSA-modified starch micelles and the small hydrophobic ligands bound on protein molecules, respectively. Since there was no complexation between HWPI and OSA-modified starch at pH 7, the HWPI and OSA-modified starch in the mixture at pH 7 may encapsulate  $\beta$ -carotene independently. As observed under TEM, the OSA-modified starch micelles tended to form aggregates at pH 4.5 due to the weakened electrostatic repulsive forces between them, which may lead to the increasing interactions between the hydrophobic groups of the OSA-modified starch micelles. The exposure of more hydrophobic groups may result in increasing hydrophobic interactions between the hydrophobic groups of OSA-modified starch micelles and  $\beta$ -carotene, therefore, the encapsulation capacity of OSA-modified starch at pH 4.5 was significantly higher than that at pH 7 (Figure 4.1A).



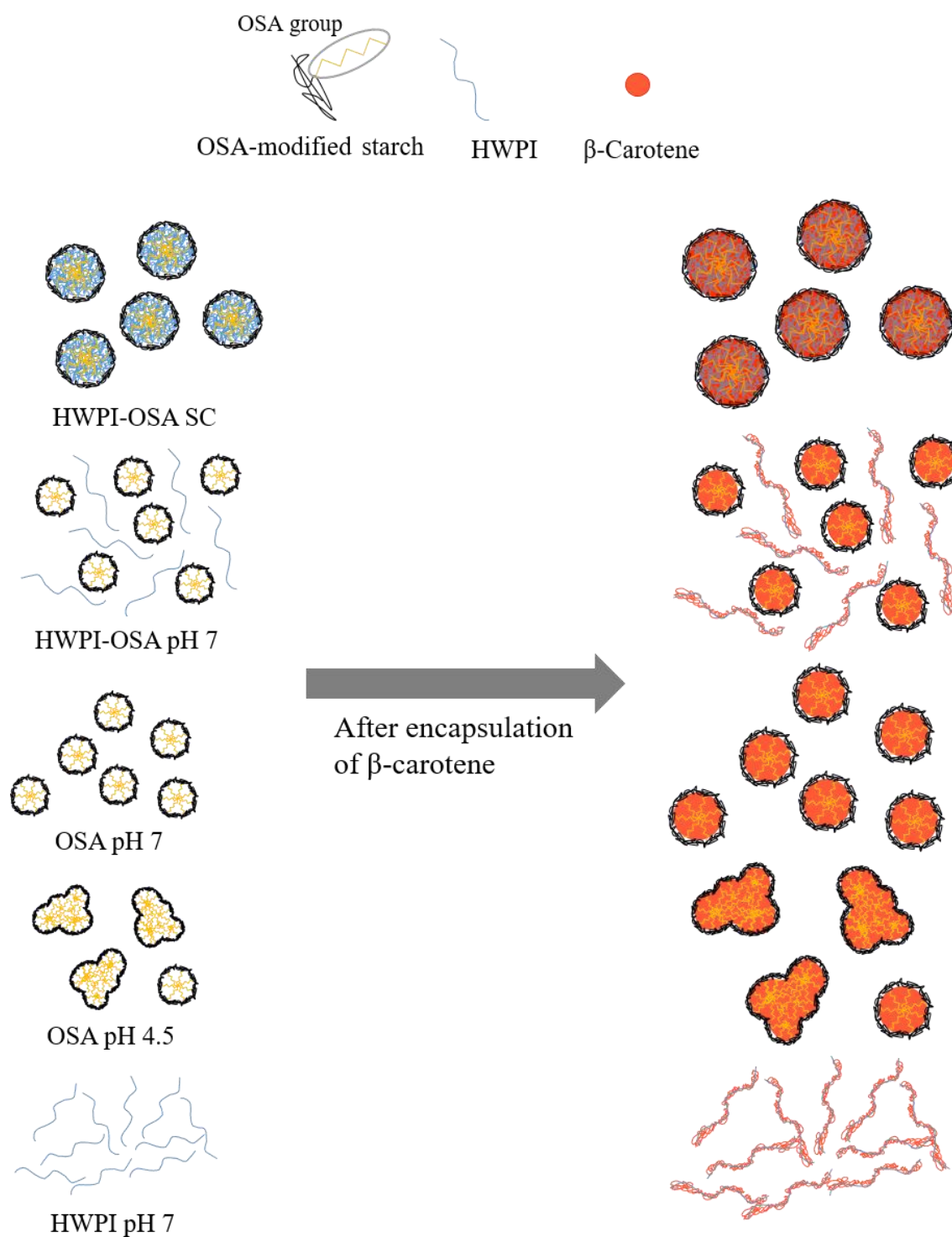


Figure 4. 10. Schematic representation of all the samples before and after encapsulation of  $\beta$ -carotene. Note: sizes are not proportional to the physical size of the molecules.

It can be seen that the  $\beta$ -carotene bound with HWPI-OSA SC could be double protected by the ‘shell’ composed by the hydrophilic portion of OSA-modified starch and the ‘core’ composed by the whey protein aggregates. This double protection thereby led to the significantly higher retention rate of  $\beta$ -carotene during storage under low pH conditions. The  $\beta$ -carotene bound with the OSA-modified starch micelles at pH 7 or their aggregates at pH 4.5 could be protected by a hydrophilic ‘shell’. However, the  $\beta$ -carotene bound with the HWPI soluble aggregates at pH 7 seemed to be only bound to the small hydrophobic ligands on protein molecules. This type of structure may not provide effective protection for the  $\beta$ -carotene, which led to the remarkable increase in particle size of the  $\beta$ -carotene-loaded HWPI-OSA pH 7 and HWPI pH 7 after redispersion and the significantly lower retention rate of  $\beta$ -carotene-loaded HWPI pH 7 during storage.

#### 4.6. Conclusion

In the present study, the soluble complexes between HWPI and OSA-modified starch formed at the protein to polysaccharide ratio of 1:10 and pH 4.5 were applied to encapsulate  $\beta$ -carotene. Their mixture at pH 7, the OSA-modified starch solution at pH 7 and 4.5, and the HWPI solution at pH 7 were also used to encapsulate  $\beta$ -carotene for further investigation of the encapsulation mechanism of the soluble complexes for lipophilic bioactive components. The apparent aqueous solubility of  $\beta$ -carotene was enormously improved ( $264.05 \pm 72.53 \mu\text{g/g}$ ) after encapsulation in the soluble complexes, which was significantly ( $p < 0.05$ ) higher than other samples. The  $\beta$ -carotene-loaded soluble complexes in a powdered form showed good redispersion behaviour with a high retention rate of the loaded  $\beta$ -carotene (89.75%). In addition, there were no changes in the particle size of the soluble complexes bound with  $\beta$ -carotene after redispersion. The loaded  $\beta$ -carotene was determined to be in an amorphous form inside the soluble

complexes by XRD and DSC, respectively. In combination with the results of FT-IR, the  $\beta$ -carotene seemed to be encapsulated by the soluble complexes via hydrophobic interactions. In the accelerated stability study, the soluble complexes between HWPI and OSA-modified starch showed the best protection for the loaded  $\beta$ -carotene after 7 days of storage, where it was expected to show significantly lower stability than the samples at pH 7 during storage. It indicated the potential of using the soluble complexes between HWPI and OSA-modified starch to protect lipophilic bioactive compounds for long-term storage at low pH conditions. The formation of the soluble complexes may lead to the changes in the original structure of the HWPI molecules and OSA-modified starch micelles, and the new structure could greatly improve the encapsulation capacity for  $\beta$ -carotene and its stability for long-term storage at low pH conditions. This study has developed the potential application of the soluble complexes between HWPI and OSA-modified starch for delivering lipophilic bioactive compounds in food industry.

## Chapter 5 Summary and Recommendations

This study illustrated the complexation process between WPI and OSA-modified starch and explored the application of their interactions in the encapsulation of lipophilic bioactive compounds.

### 5.1. Summary

The complex formation between WPI and OSA-modified starch was investigated during the acidification process from pH 7 to pH 3, which was greatly affected by the protein to polysaccharide ratios and the structural characteristics of WPI and OSA-modified starch. The OSA-modified starch was more likely to interact with heated-WPI rather than non-heated WPI. The optimum condition for the formation of insoluble coacervates between HWPI and OSA-modified starch was at ratio of 1:10 and pH 4.5, which was driven by both electrostatic and hydrophobic interactions. However, stable soluble complexes could be formed between HWPI and OSA-modified starch with higher DS values under the same condition, which may be attributed to the stronger steric hindrance of OSA-modified starch with higher DS values. The particle size of the soluble complexes decreased by the increasing DS values of OSA-modified starch involved in complexation. The complexation between HWPI and OSA-modified starch seemed to be firstly induced by electrostatic interactions. However, the structural properties of the complexes were most likely dominated by hydrophobic interactions rather than electrostatic interactions at pH 4.5. The soluble complexes may comprise a protein aggregate core and a ‘shell’ composed by the hydrophilic portion of OSA-modified starch, which could provide

enough steric stabilization for the complexes, thereby preventing them from further aggregation.

These soluble complexes were applied to encapsulate  $\beta$ -carotene, which was used as a model of lipophilic bioactive compounds in this study. The apparent aqueous solubility of  $\beta$ -carotene was enormously improved ( $264.05 \pm 72.53 \mu\text{g/g}$ ) after encapsulation in the soluble complexes. The  $\beta$ -carotene-loaded soluble complexes could be successfully converted into a powdered form with good redispersion behaviour and a high retention rate of the loaded  $\beta$ -carotene (89.75%). The  $\beta$ -carotene was in an amorphous form loaded inside the soluble complexes determined by XRD and DSC, and the results of FT-IR indicated the  $\beta$ -carotene was encapsulated by the soluble complexes via hydrophobic interactions. In the accelerated stability study, it was determined that the soluble complexes between HWPI and OSA-modified starch could effectively protect the  $\beta$ -carotene at pH 4.5 after 7 days of storage, which revealed the potential of using these soluble complexes in the protection of lipophilic bioactive compounds for long-term storage at low pH conditions.

In conclusion, the formation of the soluble complexes between HWPI and OSA-modified starch with high DS values could effectively prevent the HWPI molecules from extensive aggregation at pH 4.5. These soluble complexes could significantly improve the apparent aqueous solubility of  $\beta$ -carotene and its stability for long-term storage at low pH conditions. This study may be beneficial for the utilization of the soluble complexes between HWPI and OSA-modified starch for delivering lipophilic bioactive compounds in food industry.

## 5.2. Recommendations for future work

$\beta$ -Carotene is one of the typical hydrophobic nutraceuticals, but its poor water-solubility, instability and low bioavailability have limited its use in functional foods. Therefore, different types of colloidal delivery systems have been developed to encapsulate these compounds in order to overcome these challenges. Micelle and emulsion are the most popular delivery systems because of their relatively simple preparation process.

Our work has already successfully applied the stable complexes formed from HWPI and OSA-modified starch at pH 4.5 to encapsulate  $\beta$ -carotene, which could significantly improve the apparent aqueous solubility and the chemical stability of  $\beta$ -carotene during long-term storage under low pH conditions. Based on these findings, there are some recommendations for future work:

1. Tailoring the particle size of the soluble complexes between HWPI and OSA-modified starch.

The particle size of the soluble complexes could be tailored by modification of the molecular characteristics of the OSA-modified starch and the biopolymer ratios. Soluble complexes with different particle size could be used in different food applications in future.

2. Studying the bioavailability of  $\beta$ -carotene in the soluble complexes.

The gastrointestinal fate of the  $\beta$ -carotene-loaded soluble complexes could be established using a simulated gastrointestinal tract. The bioaccessibility of  $\beta$ -carotene could be evaluated by an *in vitro* digestion model. Further studies on the bioavailability of the  $\beta$ -carotene in these soluble complexes could be investigated

by cell or animal models. The results may lead to novel colloidal delivery systems, which can be used to incorporate  $\beta$ -carotene into food products.

3. Application of the soluble complexes loaded with  $\beta$ -carotene in the functional beverage systems.

In the present study, the  $\beta$ -carotene-loaded soluble complexes could be used as a novel food ingredient in the functional beverage systems because of their improved functional properties. The loaded lipophilic bioactive compounds in the soluble complexes are not limited to  $\beta$ -carotene.

4. Investigating the emulsifying capacity of the soluble complexes between HWPI and OSA-modified starch.

The emulsions stabilised by these soluble complexes could also be used to encapsulate different lipophilic bioactive compounds. Consequently, further studies could be carried out to evaluate the bioavailability of these lipophilic bioactive compounds in the emulsions stabilised by the soluble complexes.

## References

- Aloys, H., Korma, S. A., Alice, T. M., Chantal, N., Ali, A. H., Abed, S. M., & Ildephonse, H. (2016). Microencapsulation by complex coacervation: Methods, techniques, benefits, and applications-A review. *American Journal of Food Science and Nutrition Research*, 3(6), 188-192.
- Anal, A. K., Tobiassen, A., Flanagan, J., & Singh, H. (2008). Preparation and characterization of nanoparticles formed by chitosan–caseinate interactions. *Colloids and Surfaces B: Biointerfaces*, 64(1), 104-110.
- Azarikia, F., & Abbasi, S. (2016). Mechanism of soluble complex formation of milk proteins with native gums (tragacanth and Persian gum). *Food hydrocolloids*, 59, 35-44.
- Bédié, G. K., Turgeon, S. L., & Makhoulf, J. (2008). Formation of native whey protein isolate–low methoxyl pectin complexes as a matrix for hydro-soluble food ingredient entrapment in acidic foods. *Food hydrocolloids*, 22(5), 836-844.
- Bertoft, E. (2004). Analysing starch structure. *Starch in food: Structure, function and applications*, 57-96.
- Blennow, A. (2004). Starch bioengineering. In *Starch in food: Structure, function and applications*: CRC Press LLC.
- Boon, C. S., McClements, D. J., Weiss, J., & Decker, E. A. (2010). Factors influencing the chemical stability of carotenoids in foods. *Critical reviews in food science and nutrition*, 50(6), 515-532.
- Bosnea, L. A., Moschakis, T., & Biliaderis, C. G. (2014). Complex coacervation as a novel microencapsulation technique to improve viability of probiotics under different stresses. *Food and bioprocess technology*, 7(10), 2767-2781.



- Bryant, C., & McClements, D. (2000). Influence of xanthan gum on physical characteristics of heat-denatured whey protein solutions and gels. *Food hydrocolloids*, 14(4), 383-390.
- Caldwell, C. G., & Wurzburg, O. B. (1953). Polysaccharide derivatives of substituted dicarboxylic acids. In: Google Patents.
- Chen, Y.-F., Kaur, L., & Singh, J. (2018). Chapter 7 - Chemical Modification of Starch. In M. Sjöö & L. Nilsson (Eds.), *Starch in Food (Second Edition)* (pp. 283-321): Woodhead Publishing.
- Chun, J.-Y., Hong, G.-P., Surassmo, S., Weiss, J., Min, S.-G., & Choi, M.-J. (2014). Study of the phase separation behaviour of native or preheated WPI with polysaccharides. *Polymer*, 55(16), 4379-4384.
- Cuevas-Bernardino, J. C., Leyva-Gutierrez, F. M., Vernon-Carter, E. J., Lobato-Calleros, C., Román-Guerrero, A., & Davidov-Pardo, G. (2018). Formation of biopolymer complexes composed of pea protein and mesquite gum—Impact of quercetin addition on their physical and chemical stability. *Food hydrocolloids*, 77, 736-745.
- Dai, L., Sun, C., Li, R., Mao, L., Liu, F., & Gao, Y. (2017). Structural characterization, formation mechanism and stability of curcumin in zein-lecithin composite nanoparticles fabricated by antisolvent co-precipitation. *Food Chemistry*, 237, 1163-1171.
- de Kruif, C. (1999). Casein micelle interactions. *International Dairy Journal*, 9(3-6), 183-188.
- de Kruif, C. G., & Tuinier, R. (2001). Polysaccharide protein interactions. *Food hydrocolloids*, 15(4-6), 555-563.

- de Kruif, C. G., Weinbreck, F., & de Vries, R. (2004). Complex coacervation of proteins and anionic polysaccharides. *Current opinion in colloid & interface science*, 9(5), 340-349.
- de Wit, J. N. (1990). Thermal stability and functionality of whey proteins. *Journal of Dairy Science*, 73(12), 3602-3612.
- Deng, X. X., Zhang, N., & Tang, C. H. (2017). Soy protein isolate as a nanocarrier for enhanced water dispersibility, stability and bioaccessibility of  $\beta$  - carotene. *Journal of the Science of Food and Agriculture*, 97(7), 2230-2237.
- Devi, N., Sarmah, M., Khatun, B., & Maji, T. K. (2017). Encapsulation of active ingredients in polysaccharide–protein complex coacervates. *Advances in colloid and interface science*, 239, 136-145.
- Dickinson, E. (1998). Stability and rheological implications of electrostatic milk protein–polysaccharide interactions. *Trends in Food Science & Technology*, 9(10), 347-354.
- Dickinson, E. (2008). Interfacial structure and stability of food emulsions as affected by protein–polysaccharide interactions. *Soft Matter*, 4(5), 932-942.
- Doublier, J.-L., Garnier, C., Renard, D., & Sanchez, C. (2000). Protein–polysaccharide interactions. *Current opinion in colloid & interface science*, 5(3-4), 202-214.
- Eghbal, N., & Choudhary, R. (2017). Complex coacervation: Encapsulation and controlled release of active agents in food systems. *LWT-Food Science and Technology*.
- Eratte, D., Dowling, K., Barrow, C. J., & Adhikari, B. P. (2017). In-vitro digestion of probiotic bacteria and omega-3 oil co-microencapsulated in whey protein isolate-gum Arabic complex coacervates. *Food Chemistry*, 227, 129-136.

- Eratte, D., McKnight, S., Gengenbach, T. R., Dowling, K., Barrow, C. J., & Adhikari, B. P. (2015). Co-encapsulation and characterisation of omega-3 fatty acids and probiotic bacteria in whey protein isolate–gum Arabic complex coacervates. *Journal of Functional Foods*, 19, 882-892.
- Eratte, D., Wang, B., Dowling, K., Barrow, C. J., & Adhikari, B. P. (2014). Complex coacervation with whey protein isolate and gum arabic for the microencapsulation of omega-3 rich tuna oil. *Food & Function*, 5(11), 2743-2750.
- Evans, M., Ratcliffe, I., & Williams, P. A. (2013). Emulsion stabilisation using polysaccharide–protein complexes. *Current opinion in colloid & interface science*, 18(4), 272-282.
- Fioramonti, S. A., Perez, A. A., Aríngoli, E. E., Rubiolo, A. C., & Santiago, L. G. (2014). Design and characterization of soluble biopolymer complexes produced by electrostatic self-assembly of a whey protein isolate and sodium alginate. *Food hydrocolloids*, 35, 129-136.
- Fox, P. F. (2003). Milk proteins: general and historical aspects. In *Advanced Dairy Chemistry—I Proteins* (pp. 1-48): Springer.
- Fox, P. F. (2009). Milk: an overview. In *Milk Proteins* (pp. 1-54): Elsevier.
- Fox, P. F., McSweeney, & Paul, L. H. (1998). *Dairy chemistry and biochemistry*. Retrieved from
- Goh, K. K., Sarkar, A., & Singh, H. (2014). Milk protein–polysaccharide interactions. In *Milk Proteins (Second Edition)* (pp. 387-419): Elsevier.
- Gomez-Estaca, J., Comunian, T., Montero, P., Ferro-Furtado, R., & Favaro-Trindade, C. (2016). Encapsulation of an astaxanthin-containing lipid extract from shrimp waste by complex coacervation using a novel gelatin–cashew gum complex. *Food hydrocolloids*, 61, 155-162.

- Grinberg, V. Y., & Tolstoguzov, V. (1997). Thermodynamic incompatibility of proteins and polysaccharides in solutions. *Food hydrocolloids*, 11(2), 145-158.
- Hernández-Rodríguez, L., Lobato-Calleros, C., Pimentel-González, D. J., & Vernon-Carter, E. J. (2014). Lactobacillus plantarum protection by entrapment in whey protein isolate:  $\kappa$ -carrageenan complex coacervates. *Food hydrocolloids*, 36, 181-188.
- Hong, Y., Li, Z., Gu, Z., Wang, Y., & Pang, Y. (2017). Structure and emulsification properties of octenyl succinic anhydride starch using acid-hydrolyzed method. *Starch-Stärke*, 69(1-2), 1600039.
- Hosseini, S. M. H., Emam-Djomeh, Z., Sabatino, P., & Van der Meeren, P. (2015). Nanocomplexes arising from protein-polysaccharide electrostatic interaction as a promising carrier for nutraceutical compounds. *Food hydrocolloids*, 50, 16-26.
- Hu, K., Huang, X., Gao, Y., Huang, X., Xiao, H., & McClements, D. J. (2015). Core-shell biopolymer nanoparticle delivery systems: synthesis and characterization of curcumin fortified zein-pectin nanoparticles. *Food Chemistry*, 182, 275-281.
- Ilyasoglu, H., & El, S. N. (2014). Nanoencapsulation of EPA/DHA with sodium caseinate-gum arabic complex and its usage in the enrichment of fruit juice. *LWT-Food Science and Technology*, 56(2), 461-468.
- Jain, A., Thakur, D., Ghoshal, G., Katare, O., & Shivhare, U. (2015). Microencapsulation by complex coacervation using whey protein isolates and gum acacia: an approach to preserve the functionality and controlled release of  $\beta$ -carotene. *Food and bioprocess technology*, 8(8), 1635-1644.
- Jain, A., Thakur, D., Ghoshal, G., Katare, O., & Shivhare, U. (2016). Characterization of microcapsulated  $\beta$ -carotene formed by complex coacervation using casein and gum tragacanth. *International journal of biological macromolecules*, 87, 101-113.

- Jones, O., Decker, E. A., & McClements, D. J. (2010). Thermal analysis of  $\beta$ -lactoglobulin complexes with pectins or carrageenan for production of stable biopolymer particles. *Food hydrocolloids*, 24(2-3), 239-248.
- Jones, O. G., Decker, E. A., & McClements, D. J. (2009). Formation of biopolymer particles by thermal treatment of  $\beta$ -lactoglobulin–pectin complexes. *Food hydrocolloids*, 23(5), 1312-1321.
- Jones, O. G., & McClements, D. J. (2010). Biopolymer Nanoparticles from Heat-Treated Electrostatic Protein – Polysaccharide Complexes: Factors Affecting Particle Characteristics. *Journal of food science*, 75(2), N36-N43.
- Jones, O. G., & McClements, D. J. (2011). Recent progress in biopolymer nanoparticle and microparticle formation by heat-treating electrostatic protein–polysaccharide complexes. *Advances in colloid and interface science*, 167(1-2), 49-62.
- Jun-xia, X., Hai-yan, Y., & Jian, Y. (2011). Microencapsulation of sweet orange oil by complex coacervation with soybean protein isolate/gum Arabic. *Food Chemistry*, 125(4), 1267-1272.
- Kaushik, P., Dowling, K., Barrow, C. J., & Adhikari, B. (2015). Complex coacervation between flaxseed protein isolate and flaxseed gum. *Food Research International*, 72, 91-97.
- Khalesi, H., Emadzadeh, B., Kadkhodaei, R., & Fang, Y. (2017). Effects of biopolymer ratio and heat treatment on the complex formation between whey protein isolate and soluble fraction of Persian gum. *Journal of Dispersion Science and Technology*, 38(9), 1234-1241.
- Kim, H.-J., Decker, E. A., & McClements, D. J. (2006). Preparation of multiple emulsions based on thermodynamic incompatibility of heat-denatured whey protein and pectin solutions. *Food hydrocolloids*, 20(5), 586-595.

- Klassen, D. R., Elmer, C. M., & Nickerson, M. T. (2011). Associative phase separation involving canola protein isolate with both sulphated and carboxylated polysaccharides. *Food Chemistry*, 126(3), 1094-1101.
- Kontopidis, G., Holt, C., & Sawyer, L. (2004). Invited review:  $\beta$ -lactoglobulin: binding properties, structure, and function. *Journal of Dairy Science*, 87(4), 785-796.
- Koupantsis, T., Pavlidou, E., & Paraskevopoulou, A. (2014). Flavour encapsulation in milk proteins–CMC coacervate-type complexes. *Food hydrocolloids*, 37, 134-142.
- Langton, M., & Hermansson, A.-M. (1992). Fine-stranded and particulate gels of  $\beta$ -lactoglobulin and whey protein at varying pH. *Food hydrocolloids*, 5(6), 523-539.
- Li, X., Zhang, P., Chen, L., Xie, F., Li, L., & Li, B. (2012). Structure and colon-targeted releasing property of resistant octenyl succinate starch. *Food Research International*, 47(2), 246-252.
- Lin, Q., Liang, R., Zhong, F., Ye, A., & Singh, H. (2018a). Effect of degree of octenyl succinic anhydride (OSA) substitution on the digestion of emulsions and the bioaccessibility of  $\beta$ -carotene in OSA-modified-starch-stabilized-emulsions. *Food hydrocolloids*.
- Lin, Q., Liang, R., Zhong, F., Ye, A., & Singh, H. (2018b). Interactions between octenyl-succinic-anhydride-modified starches and calcium in oil-in-water emulsions. *Food hydrocolloids*, 77, 30-39.
- Lin, Q., Liang, R., Zhong, F., Ye, A., & Singh, H. (2018c). Physical properties and biological fate of OSA-modified-starch-stabilized emulsions containing  $\beta$ -carotene: Effect of calcium and pH. *Food hydrocolloids*, 77, 549-556.
- Liu, Q.-R., Qi, J.-R., Yin, S.-W., Wang, J.-M., Guo, J., Feng, J.-L., . . . Yang, X.-Q. (2016). The influence of heat treatment on acid-tolerant emulsions prepared from acid

- soluble soy protein and soy soluble polysaccharide complexes. *Food Research International*, 89, 211-218.
- Liu, Q.-R., Wang, W., Qi, J., Huang, Q., & Xiao, J. (2018). Oregano essential oil loaded soybean polysaccharide films: Effect of Pickering type immobilization on physical and antimicrobial properties. *Food hydrocolloids*.
- Liu, W., Chen, X. D., Cheng, Z., & Selomulya, C. (2016). On enhancing the solubility of curcumin by microencapsulation in whey protein isolate via spray drying. *Journal of Food Engineering*, 169, 189-195.
- Luallen, T. (2004). Utilizing starches in product development. In *Starch in food* (pp. 393-424): Elsevier.
- Magnusson, E., & Nilsson, L. (2011). Interactions between hydrophobically modified starch and egg yolk proteins in solution and emulsions. *Food hydrocolloids*, 25(4), 764-772.
- Marozienne, A., & de Kruif, C. (2000). Interaction of pectin and casein micelles. *Food hydrocolloids*, 14(4), 391-394.
- McClements, D., Decker, E., & Weiss, J. (2007). Emulsion-based delivery systems for lipophilic bioactive components. *Journal of food science*, 72(8), R109-R124.
- McClements, D. J. (2012). Crystals and crystallization in oil-in-water emulsions: Implications for emulsion-based delivery systems. *Advances in colloid and interface science*, 174, 1-30.
- Mensi, A., Choiset, Y., Haertlé, T., Reboul, E., Borel, P., Guyon, C., . . . Chobert, J.-M. (2013). Interlocking of  $\beta$ -carotene in beta-lactoglobulin aggregates produced under high pressure. *Food Chemistry*, 139(1-4), 253-260.

- Mirpoor, S. F., Hosseini, S. M. H., & Yousefi, G. H. (2017). Mixed biopolymer nanocomplexes conferred physicochemical stability and sustained release behavior to introduced curcumin. *Food hydrocolloids*, 71, 216-224.
- Nilsson, L., & Bergenståhl, B. (2007). Adsorption of hydrophobically modified anionic starch at oppositely charged oil/water interfaces. *Journal of Colloid and Interface Science*, 308(2), 508-513.
- Patino, J. M. R., & Pilosof, A. M. (2011). Protein–polysaccharide interactions at fluid interfaces. *Food hydrocolloids*, 25(8), 1925-1937.
- Peng, S., Li, Z., Zou, L., Liu, W., Liu, C., & McClements, D. J. (2018). Improving curcumin solubility and bioavailability by encapsulation in saponin-coated curcumin nanoparticles prepared using a simple pH-driven loading method. *Food & Function*, 9(3), 1829-1839.
- Perez, A. A., Carrara, C. R., Sánchez, C. C., Patino, J. M. R., & Santiago, L. G. (2009). Interactions between milk whey protein and polysaccharide in solution. *Food Chemistry*, 116(1), 104-113.
- Peris-Tortajada, M. (2004). Measuring starch in food. *Starch in Food*. CRC Press, Woodhead Publishing Limited, England, 185-207.
- Protte, K., Ruf, T., Atamer, Z., Sonne, A., Weiss, J., & Hinrichs, J. (2017). Influence of shear stress, pectin type and calcium chloride on the process stability of thermally stabilised whey protein–pectin complexes. *Food Structure*, 14, 76-84.
- Puerta-Gomez, A., & Castell-Perez, M. (2017). Visual spectroscopy method to evaluate entrapment efficiency of electrostatically precipitated proteins in combination with octenyl succinic anhydride (OSA)-modified polysaccharides. *Food hydrocolloids*, 63, 160-169.



- Puerta - Gomez, A. F., & Castell - Perez, M. E. (2016). Studies on self - assembly interactions of proteins and octenyl succinic anhydride (OSA) - modified depolymerized waxy rice starch using rheological principles. *Journal of Applied Polymer Science*, 133(27).
- Qi, P. X., & Onwulata, C. I. (2011). Physical properties, molecular structures, and protein quality of texturized whey protein isolate: Effect of extrusion temperature. *Journal of agricultural and food chemistry*, 59(9), 4668-4675.
- Ron, N., Zimet, P., Bargarum, J., & Livney, Y. D. (2010). Beta-lactoglobulin-polysaccharide complexes as nanovehicles for hydrophobic nutraceuticals in non-fat foods and clear beverages. *International Dairy Journal*, 20(10), 686-693.
- Ryan, K., Vardhanabhuti, B., Jaramillo, D., Van Zanten, J., Coupland, J., & Foegeding, E. (2012). Stability and mechanism of whey protein soluble aggregates thermally treated with salts. *Food hydrocolloids*, 27(2), 411-420.
- Saha, N., Samanta, A. K., Chaudhuri, S., & Dutta, D. (2015). Characterization and antioxidant potential of a carotenoid from a newly isolated yeast. *Food Science and Biotechnology*, 24(1), 117-124.
- Salminen, H., & Weiss, J. (2014). Effect of pectin type on association and pH stability of whey protein—pectin complexes. *Food biophysics*, 9(1), 29-38.
- Santipanichwong, R., Supphantharika, M., Weiss, J., & McClements, D. (2008). Core-shell biopolymer nanoparticles produced by electrostatic deposition of beet pectin onto heat-denatured  $\beta$ -lactoglobulin aggregates. *Journal of food science*, 73(6), N23-N30.
- Schmitt, C., Bovay, C., Rouvet, M., Shojaei-Rami, S., & Kolodziejczyk, E. (2007). Whey protein soluble aggregates from heating with NaCl: physicochemical, interfacial, and foaming properties. *Langmuir*, 23(8), 4155-4166.

- Schmitt, C., Bovay, C., Vuilliamenot, A.-M., Rouvet, M., Bovetto, L., Barbar, R., & Sanchez, C. (2009). Multiscale characterization of individualized  $\beta$ -lactoglobulin microgels formed upon heat treatment under narrow pH range conditions. *Langmuir*, 25(14), 7899-7909.
- Schmitt, C., Sanchez, C., Desobry-Banon, S., & Hardy, J. (1998). Structure and technofunctional properties of protein-polysaccharide complexes: a review. *Critical reviews in food science and nutrition*, 38(8), 689-753.
- Schmitt, C., & Turgeon, S. L. (2011). Protein/polysaccharide complexes and coacervates in food systems. *Advances in colloid and interface science*, 167(1-2), 63-70.
- Singh, H., & Havea, P. (2003). Thermal denaturation, aggregation and gelation of whey proteins. In *Advanced Dairy Chemistry—I Proteins* (pp. 1261-1287): Springer.
- Sneharani, A. H., Karakkat, J. V., Singh, S. A., & Rao, A. A. (2010). Interaction of curcumin with  $\beta$ -lactoglobulin stability, spectroscopic analysis, and molecular modeling of the complex. *Journal of agricultural and food chemistry*, 58(20), 11130-11139.
- Soukoulis, C., & Bohn, T. (2018). A comprehensive overview on the micro-and nano-technological encapsulation advances for enhancing the chemical stability and bioavailability of carotenoids. *Critical reviews in food science and nutrition*, 58(1), 1-36.
- Sun, N.-x., Liang, Y., Yu, B., Tan, C.-p., & Cui, B. (2016). Interaction of starch and casein. *Food hydrocolloids*, 60, 572-579.
- Sweedman, M. C., Tizzotti, M. J., Schäfer, C., & Gilbert, R. G. (2013). Structure and physicochemical properties of octenyl succinic anhydride modified starches: A review. *Carbohydrate polymers*, 92(1), 905-920.

- Taggart, P. (2004). Starch as an ingredient: manufacture and applications. In *Starch in food* (pp. 363-392): Elsevier.
- Tan, C. P., & Nakajima, M. (2005).  $\beta$ -Carotene nanodispersions: preparation, characterization and stability evaluation. *Food Chemistry*, 92(4), 661-671.
- Tesch, S., Gerhards, C., & Schubert, H. (2002). Stabilization of emulsions by OSA starches. *Journal of Food Engineering*, 54(2), 167-174.
- Thakur, D., Jain, A., Ghoshal, G., Shivhare, U., & Katare, O. (2017). Microencapsulation of  $\beta$ -carotene based on casein/guar gum blend using zeta potential-yield stress phenomenon: An approach to enhance photo-stability and retention of functionality. *AAPS PharmSciTech*, 18(5), 1447-1459.
- Tiebackx, F. (1911). Gleichzeitige ausflockung zweier kolloide. *Zeitschrift für Chemie und Industrie der Kolloide*, 8(4), 198-201.
- Tolstoguzov, V. (1991). Functional properties of food proteins and role of protein-polysaccharide interaction. *Food hydrocolloids*, 4(6), 429-468.
- Tolstoguzov, V. (1998). Functional properties of protein-polysaccharide. *Functional properties of food macromolecules*(1), 252.
- Tolstoguzov, V. B. (1997). Protein-polysaccharide interactions. In *Food proteins and their applications* (pp. 171-198). New York: Marcel Dekker, Inc.
- Turgeon, S., Schmitt, C., & Sanchez, C. (2007). Protein-polysaccharide complexes and coacervates. *Current opinion in colloid & interface science*, 12(4-5), 166-178.
- Wang, B., Akanbi, T. O., Agyei, D., Holland, B. J., & Barrow, C. J. (2018). Coacervation Technique as an Encapsulation and Delivery Tool for Hydrophobic Biofunctional Compounds. In *Role of Materials Science in Food Bioengineering* (pp. 235-261): Elsevier.

- Wang, X., Lee, J., Wang, Y.-W., & Huang, Q. (2007). Composition and rheological properties of  $\beta$ -lactoglobulin/pectin coacervates: effects of salt concentration and initial protein/polysaccharide ratio. *Biomacromolecules*, 8(3), 992-997.
- Weinbreck, F., de Vries, R., Schrooyen, P., & de Kruif, C. (2003). Complex coacervation of whey proteins and gum arabic. *Biomacromolecules*, 4(2), 293-303.
- Weinbreck, F., Tromp, R., & De Kruif, C. (2004). Composition and structure of whey protein/gum arabic coacervates. *Biomacromolecules*, 5(4), 1437-1445.
- Wu, B.-c., & McClements, D. J. (2015). Microgels formed by electrostatic complexation of gelatin and OSA starch: Potential fat or starch mimetics. *Food hydrocolloids*, 47, 87-93.
- Wurzburg, O. B. (1986). *Modified starches: properties and uses*.
- Xia, J., & Dubin, P. L. (1994). Protein-polyelectrolyte complexes. In *Macromolecular complexes in chemistry and biology* (pp. 247-271): Springer.
- Xu, D., Wang, X., Jiang, J., Yuan, F., Decker, E. A., & Gao, Y. (2013). Influence of pH, EDTA,  $\alpha$ -tocopherol, and WPI oxidation on the degradation of  $\beta$ -carotene in WPI-stabilized oil-in-water emulsions. *LWT-Food Science and Technology*, 54(1), 236-241.
- Ye, A. (2008). Complexation between milk proteins and polysaccharides via electrostatic interaction: principles and applications—a review. *International journal of food science & technology*, 43(3), 406-415.
- Ye, A., Flanagan, J., & Singh, H. (2006). Formation of stable nanoparticles via electrostatic complexation between sodium caseinate and gum arabic. *Biopolymers: Original Research on Biomolecules*, 82(2), 121-133.

- Yi, J., Lam, T. I., Yokoyama, W., Cheng, L. W., & Zhong, F. (2015). Beta-carotene encapsulated in food protein nanoparticles reduces peroxyl radical oxidation in Caco-2 cells. *Food hydrocolloids*, 43, 31-40.
- Zeeb, B., Mi-Yeon, L., Gibis, M., & Weiss, J. (2018). Growth phenomena in biopolymer complexes composed of heated WPI and pectin. *Food hydrocolloids*, 74, 53-61.
- Zhang, B., Huang, Q., Luo, F.-x., Fu, X., Jiang, H., & Jane, J.-l. (2011). Effects of octenylsuccinylation on the structure and properties of high-amylose maize starch. *Carbohydrate polymers*, 84(4), 1276-1281.
- Zhao, Y., Khalid, N., Shu, G., Neves, M. A., Kobayashi, I., & Nakajima, M. (2018). Complex coacervates from gelatin and octenyl succinic anhydride modified kudzu starch: Insights of formulation and characterization. *Food hydrocolloids*.
- Zhu, J., Li, L., Chen, L., & Li, X. (2013). Nano-structure of octenyl succinic anhydride modified starch micelle. *Food hydrocolloids*, 32(1), 1-8.
- Zimet, P., & Livney, Y. D. (2009). Beta-lactoglobulin and its nanocomplexes with pectin as vehicles for  $\omega$ -3 polyunsaturated fatty acids. *Food hydrocolloids*, 23(4), 1120-1126.

## Appendices

Permission from Elsevier for reprinting Figure 2.4.

### ELSEVIER LICENSE TERMS AND CONDITIONS

Nov 06, 2018

This Agreement between Dan Wu ("You") and Elsevier ("Elsevier") consists of your license details and the terms and conditions provided by Elsevier and Copyright Clearance Center.

License Number	4463440507706
License date	Nov 06, 2018
Licensed Content Publisher	Elsevier
Licensed Content Publication	Current Opinion in Colloid & Interface Science
Licensed Content Title	Complex coacervation of proteins and anionic polysaccharides
Licensed Content Author	Cornelus G. de Kruif, Fanny Weinbreck, Renko de Vries
Licensed Content Date	Dec 1, 2004
Licensed Content Volume	9
Licensed Content Issue	5
Licensed Content Pages	10
Start Page	340
End Page	349
Type of Use	reuse in a thesis/dissertation
Portion	figures/tables/illustrations
Number of figures/tables/illustrations	1
Format	both print and electronic
Are you the author of this Elsevier article?	No
Will you be translating?	No
Original figure numbers	Fig. 4
Title of your thesis/dissertation	Complexation between whey protein and octenyl succinic anhydride modified starch: a novel approach for encapsulation of lipophilic bioactive compounds
Expected completion date	Dec 2018
Estimated size (number of pages)	120
Requestor Location	Dan Wu 270A Grey st  Palmerston North, New Zealand 4414 New Zealand Attn: Dan Wu
Publisher Tax ID	GB 494 6272 12
Total	0.00 USD
Terms and Conditions	

Permission from John Wiley and Sons for reprinting Figure 2.6.

**JOHN WILEY AND SONS LICENSE  
TERMS AND CONDITIONS**

Nov 07, 2018

This Agreement between Dan Wu ("You") and John Wiley and Sons ("John Wiley and Sons") consists of your license details and the terms and conditions provided by John Wiley and Sons and Copyright Clearance Center.

License Number	4463450503238
License date	Nov 07, 2018
Licensed Content Publisher	John Wiley and Sons
Licensed Content Publication	Biopolymers
Licensed Content Title	Formation of stable nanoparticles via electrostatic complexation between sodium caseinate and gum arabic
Licensed Content Author	Aiqian Ye, John Flanagan, Harjinder Singh
Licensed Content Date	Feb 1, 2006
Licensed Content Volume	82
Licensed Content Issue	2
Licensed Content Pages	13
Type of use	Dissertation/Thesis
Requestor type	University/Academic
Format	Print and electronic
Portion	Figure/table
Number of figures/tables	1
Original Wiley figure/table number(s)	Figure 4
Will you be translating?	No
Title of your thesis / dissertation	Complexation between whey protein and octenyl succinic anhydride modified starch: a novel approach for encapsulation of lipophilic bioactive compounds
Expected completion date	Dec 2018
Expected size (number of pages)	120
Requestor Location	Dan Wu 270A Grey st  Palmerston North, New Zealand 4414 New Zealand Attn: Dan Wu
Publisher Tax ID	EU826007151
Total	0.00 USD
Terms and Conditions	

Permission from Elsevier for reprinting Figure 2.8 and Figure 2.9.

# ELSEVIER LICENSE TERMS AND CONDITIONS

Nov 07, 2018

This Agreement between Dan Wu ("You") and Elsevier ("Elsevier") consists of your license details and the terms and conditions provided by Elsevier and Copyright Clearance Center.

License Number	4463450863780
License date	Nov 07, 2018
Licensed Content Publisher	Elsevier
Licensed Content Publication	Food Hydrocolloids
Licensed Content Title	Nanocomplexes arising from protein-polysaccharide electrostatic interaction as a promising carrier for nutraceutical compounds
Licensed Content Author	Seyed Mohammad Hashem Hosseini,Zahra Emam-Djomeh,Paolo Sabatino,Paul Van der Meer
Licensed Content Date	Aug 1, 2015
Licensed Content Volume	50
Licensed Content Issue	n/a
Licensed Content Pages	11
Start Page	16
End Page	26
Type of Use	reuse in a thesis/dissertation
Intended publisher of new work	other
Portion	figures/tables/illustrations
Number of figures/tables/illustrations	2
Format	both print and electronic
Are you the author of this Elsevier article?	No
Will you be translating?	No
Original figure numbers	Graphical abstract and Fig 6
Title of your thesis/dissertation	Complexation between whey protein and octenyl succinic anhydride modified starch: a novel approach for encapsulation of lipophilic bioactive compounds
Expected completion date	Dec 2018
Requestor Location	Dan Wu 270A Grey st  Palmerston North, New Zealand 4414 New Zealand Attn: Dan Wu
Publisher Tax ID	GB 494 6272 12



Permission from Elsevier for reprinting Figure 2.10.

**ELSEVIER LICENSE  
TERMS AND CONDITIONS**

Nov 07, 2018

This Agreement between Dan Wu ("You") and Elsevier ("Elsevier") consists of your license details and the terms and conditions provided by Elsevier and Copyright Clearance Center.

License Number	4463451312297
License date	Nov 07, 2018
Licensed Content Publisher	Elsevier
Licensed Content Publication	Food Hydrocolloids
Licensed Content Title	Oregano essential oil loaded soybean polysaccharide films: Effect of Pickering type immobilization on physical and antimicrobial properties
Licensed Content Author	Qian-Ru Liu, Wenbo Wang, Junru Qi, Qingrong Huang, Jie Xiao
Licensed Content Date	Feb 1, 2019
Licensed Content Volume	87
Licensed Content Issue	n/a
Licensed Content Pages	8
Start Page	165
End Page	172
Type of Use	reuse in a thesis/dissertation
Intended publisher of new work	other
Portion	figures/tables/illustrations
Number of figures/tables/illustrations	1
Format	both print and electronic
Are you the author of this Elsevier article?	No
Will you be translating?	No
Original figure numbers	Graphical abstract
Title of your thesis/dissertation	Complexation between whey protein and octenyl succinic anhydride modified starch: a novel approach for encapsulation of lipophilic bioactive compounds
Expected completion date	Dec 2018
Requestor Location	Dan Wu 270A Grey st  Palmerston North, New Zealand 4414 New Zealand Attn: Dan Wu
Publisher Tax ID	GB 494 6272 12

Permission from Elsevier for reprinting Figure 2.11.

**SPRINGER NATURE LICENSE  
TERMS AND CONDITIONS**

Nov 07, 2018

This Agreement between Dan Wu ("You") and Springer Nature ("Springer Nature") consists of your license details and the terms and conditions provided by Springer Nature and Copyright Clearance Center.

License Number	4463460027545
License date	Nov 07, 2018
Licensed Content Publisher	Springer Nature
Licensed Content Publication	Food and Bioprocess Technology
Licensed Content Title	Microencapsulation by Complex Coacervation Using Whey Protein Isolates and Gum Acacia: An Approach to Preserve the Functionality and Controlled Release of $\beta$ -Carotene
Licensed Content Author	Ashay Jain, Deepika Thakur, Gargi Ghoshal et al
Licensed Content Date	Jan 1, 2015
Licensed Content Volume	8
Licensed Content Issue	8
Type of Use	Thesis/Dissertation
Requestor type	academic/university or research institute
Format	print and electronic
Portion	figures/tables/illustrations
Number of figures/tables/illustrations	1
Will you be translating?	no
Circulation/distribution	<501
Author of this Springer Nature content	no
Title	Complexation between whey protein and octenyl succinic anhydride modified starch: a novel approach for encapsulation of lipophilic bioactive compounds
Institution name	n/a
Expected presentation date	Dec 2018
Portions	Fig. 1
Requestor Location	Dan Wu 270A Grey st  Palmerston North, New Zealand 4414 New Zealand Attn: Dan Wu
Billing Type	Invoice
Billing Address	Dan Wu 270A Grey st

Permission from Elsevier for reprinting Figure 2.12.

**ELSEVIER LICENSE  
TERMS AND CONDITIONS**

Nov 07, 2018

This Agreement between Dan Wu ("You") and Elsevier ("Elsevier") consists of your license details and the terms and conditions provided by Elsevier and Copyright Clearance Center.

License Number	4463460230845
License date	Nov 07, 2018
Licensed Content Publisher	Elsevier
Licensed Content Publication	International Journal of Biological Macromolecules
Licensed Content Title	Characterization of microcapsulated $\beta$ -carotene formed by complex coacervation using casein and gum tragacanth
Licensed Content Author	Ashay Jain, Deepika Thakur, Gargi Ghoshal, O.P. Katare, U.S. Shivhare
Licensed Content Date	Jun 1, 2016
Licensed Content Volume	87
Licensed Content Issue	n/a
Licensed Content Pages	13
Start Page	101
End Page	113
Type of Use	reuse in a thesis/dissertation
Intended publisher of new work	other
Portion	figures/tables/illustrations
Number of figures/tables/illustrations	1
Format	both print and electronic
Are you the author of this Elsevier article?	No
Will you be translating?	No
Original figure numbers	Scheme 1
Title of your thesis/dissertation	Complexation between whey protein and octenyl succinic anhydride modified starch: a novel approach for encapsulation of lipophilic bioactive compounds
Expected completion date	Dec 2018
Requestor Location	Dan Wu 270A Grey st  Palmerston North, New Zealand 4414 New Zealand Attn: Dan Wu
Publisher Tax ID	GB 494 6272 12
Total	0.00 USD

Permission from Elsevier for reprinting Figure 2.13.

**ELSEVIER LICENSE  
TERMS AND CONDITIONS**

Nov 07, 2018

This Agreement between Dan Wu ("You") and Elsevier ("Elsevier") consists of your license details and the terms and conditions provided by Elsevier and Copyright Clearance Center.

License Number	4463460379516
License date	Nov 07, 2018
Licensed Content Publisher	Elsevier
Licensed Content Publication	Food Hydrocolloids
Licensed Content Title	Encapsulation of an astaxanthin-containing lipid extract from shrimp waste by complex coacervation using a novel gelatin-cashew gum complex
Licensed Content Author	J. Gomez-Estaca,T.A. Comunian,P. Montero,R. Ferro-Furtado,C.S. Favaro-Trindade
Licensed Content Date	Dec 1, 2016
Licensed Content Volume	61
Licensed Content Issue	n/a
Licensed Content Pages	8
Start Page	155
End Page	162
Type of Use	reuse in a thesis/dissertation
Intended publisher of new work	other
Portion	figures/tables/illustrations
Number of figures/tables/illustrations	1
Format	both print and electronic
Are you the author of this Elsevier article?	No
Will you be translating?	No
Original figure numbers	Graphical abstract
Title of your thesis/dissertation	Complexation between whey protein and octenyl succinic anhydride modified starch: a novel approach for encapsulation of lipophilic bioactive compounds
Expected completion date	Dec 2018
Requestor Location	Dan Wu 270A Grey st  Palmerston North, New Zealand 4414 New Zealand Attn: Dan Wu
Publisher Tax ID	GB 494 6272 12